
SOLAR ORBITER

PAYLOAD DEFINITION DOCUMENT

DOCUMENT MARKED UP BY D. MCCOY FOR ISSUE WITH CALL FOR LETTERS OF INTENT

prepared by/ <i>préparé par</i>	Solar Orbiter assessment team
reference/ <i>référence</i>	SCI-A/2004/175/AO
issue/ <i>édition</i>	5
revision/ <i>révision</i>	0
date of issue/ <i>date d'édition</i>	31/03/2006
status/ <i>état</i>	Final
Document type/ <i>type de document</i>	Technical Note
Distribution/ <i>distribution</i>	Public document

A P P R O V A L

Title <i>titre</i>	issue 5 <i>issue</i>	revision 0 <i>revision</i>
-----------------------	-------------------------	-------------------------------

author <i>auteur</i>	date <i>date</i>
-------------------------	---------------------

approved by <i>approuvé by</i>	date <i>date</i>
-----------------------------------	---------------------

C H A N G E L O G

<i>reason for change /raison du changement</i>	<i>issue/issue</i>	<i>revision/revision</i>	<i>date/date</i>
First release	1	0	19/12/2002
Including SDT recommendations and overall update	2	0	1/12/2003
Overall update	2	4	9/1/2004
Major revision – based on results of Astrium’s ISP study	3	0	11/08/2004
Revision based on payload working group and instrument experts inputs	4	0	31/3/2005
Updated values and corrections	4	1	23/8/2005
Final release with LOI	5	0	31/03/2006

C H A N G E R E C O R D

Issue: 5 Revision: 0

<i>reason for change/raison du changement</i>	<i>page(s)/page(s)</i>	<i>paragraph(s)/paragraph(s)</i>

T A B L E O F C O N T E N T S

PART 1	PREFACE	7
1	List of acronyms	8
2	Reference list	10
3	Spacecraft Reference coordinate system.....	11
4	Introduction.....	12
4.1	Changes since PDD v4.....	12
5	Contact persons	13
6	Payload procurement – Announcement of Opportunity.....	Error! Bookmark not defined.
6.1	Key events and preliminary dates leading to the payload AO..	Error! Bookmark not defined.
7	Payload overview.....	14
7.1	Core payload complement.....	14
7.2	High priority augmentation	14
PART 2	DESCRIPTION OF THE INSTRUMENTS	18
1	Introduction.....	19
2	Payload support elements (PSE).....	20
3	Remote-sensing Units.....	21
3.1	Visible-Light Imager and Magnetograph (VIM).....	21
3.1.1	Scientific Goals	21
3.1.2	Instrument concept	22
3.1.3	Orbit, Operations and Pointing Requirements.....	29
3.1.4	Calibration	29
3.1.5	Accommodation	29
3.1.6	Interface and Physical Resource Requirements.....	30
3.1.7	Cleanliness, Ground Operations and Other Requirements.....	33
3.1.8	Open Points and Critical Issues.....	33
3.2	EUV Spectrometer (EUS)	35
3.2.1	Scientific Goals	35
3.2.2	Instrument concept	35
3.2.2.1	Optical configuration	36
3.2.2.2	Thermal design	38
3.2.2.3	Resolution/detector	38
3.2.3	Orbit, Operations and Pointing Requirements.....	40
3.2.4	Calibration.....	40
3.2.5	Accommodation	40
3.2.6	Interface and Physical Resource Requirements.....	41
3.2.7	Cleanliness, Ground Operations and Other Requirements.....	43
3.2.8	Open Points and Critical Issues.....	43
3.3	EUV Imager (EUI).....	44
3.3.1	Scientific Goals	44

3.3.2	Instrument Concept	44
3.3.3	Orbit, Operations and Pointing Requirements.....	48
3.3.4	Calibration	48
3.3.5	Accommodation	48
3.3.6	Interface and Physical Resource Requirements.....	48
3.3.7	Cleanliness, Ground Operations and Other Requirements.....	50
3.3.8	Open Points and Critical Issues.....	50
3.4	Coronagraph (COR).....	51
3.4.1	Scientific Goals	51
3.4.2	Instrument concept	52
3.4.3	Orbit, Operations and Pointing Requirements.....	56
3.4.4	Accommodation	56
3.4.5	Interface and Physical Resource Requirements.....	57
3.4.6	Cleanliness, Ground Operations and Other Requirements.....	58
3.4.7	Open Points and Critical Issues.....	58
3.5	Spectrometer/Telescope for Imaging X-rays (STIX).....	59
3.5.1	Scientific Goals	59
3.5.2	Instrument Concept	59
3.5.3	Orbit, Operations and Pointing Requirements.....	60
3.5.4	Calibration	61
3.5.5	Accommodation	61
3.5.6	Interface and Physical Resource Requirements.....	62
3.5.7	Cleanliness, Ground Operations and Other Requirements.....	63
3.5.8	Open Points and Critical Issues.....	63
3.6	Remote-sensing Instruments: Open Issues & Critical Items	64
3.6.1	APS Detectors	64
3.6.2	Cleanliness requirements.....	64
3.6.3	Thermal Control	66
3.6.3.1	VIM thermal architecture concept (on-axis design)	66
3.6.3.2	VIM thermal architecture concept (off-axis design).....	67
3.6.3.3	EUS thermal architecture concept	67
3.6.3.4	EUI thermal architecture concept	68
3.6.3.5	COR thermal control concept	69
3.6.3.6	STIX thermal control concept	70
3.6.4	Instrument doors.....	70
3.6.5	Data Rates.....	70
4	In-situ Units	72
4.1	Solar Wind Plasma Analyser (SWA)	72
4.1.1	Science Goals	72
4.1.2	Instrument concept	72
4.1.3	Sensors	73
4.1.3.1	Proton and Alpha Particle Sensor (SW-PAS).....	73
4.1.3.2	Solar Wind Heavy Ion Sensor (SW-HIS).....	75
4.1.3.3	Electron Analyser Sensor (SW-EAS).....	78
4.2	Radio and Plasma Wave Analyser (RPW)	80
4.2.1	Science goals	80
4.2.2	Instrument concept	80
4.2.3	Sensors	83
4.2.3.1	Thermal Noise Receiver (TNR).....	83

4.2.3.2	Low Frequency Receiver (LFR).....	83
4.2.3.3	High Frequency Receiver (HFR).....	84
4.2.3.4	Antennas	84
4.2.3.5	Search Coil Magnetometer	86
4.2.3.6	Loop Magnetometer.....	86
4.3	Magnetometer	88
4.3.1	Scientific goals	88
4.3.2	Instrument concept	88
4.4	Energetic Particle Detector (EPD)	93
4.4.1	Scientific goals	93
4.4.2	Instrument concept	93
4.4.3	Open points and critical issues	94
4.4.4	Sensors	94
4.4.4.1	Supra Thermal Electron Detector (STE)	94
4.4.4.2	Electron and Proton Telescope (EPT)	95
4.4.4.3	Supra-thermal Ion Spectrograph (SIS)	96
4.4.4.4	Low Energy Telescope (LET)	98
4.4.4.5	High Energy Telescope with Neutron Detection (HETn).....	100
4.5	Dust Particle Detector (DPD).....	102
4.5.1	Scientific goals	102
4.5.2	Instrument concept	102
4.5.3	Dust sensor	103
4.6	Neutron and Gamma-Ray Detector (NGD).....	105
4.6.1	Scientific Goals	105
4.6.2	Instrument Concept	105
4.6.3	Accommodation	107
4.6.4	Orbit, Operations and Pointing Requirements.....	107
4.6.5	Cleanliness, Ground Operations and Other Requirements	108
4.6.6	Open Points, Critical Issues and technology development activities	108
5	High Priority Augmentation Units	109

PART 3 ANNEXES 110

ANNEX I	High priority augmentations to baseline mission.....	111
1	High Priority augmentation instruments.....	114
1.1	Neutral Particle Detector (NPD)	114
1.1.1	Instrument Description	114
1.1.2	Scientific drivers.....	114
1.1.3	Instrument concept	115
1.1.4	Orbit, Operations and Pointing Requirements.....	116
1.1.5	Accommodation	116
1.1.6	Interface and Physical Resource Requirements.....	117
1.1.7	Cleanliness, Ground Operations and Other Requirements	117
1.1.8	Open Points and Critical Issues	117
1.2	Coronal Radio Sounding (CRS)	118
1.2.1	Scientific goals	118
1.2.2	Instrument concept	118
1.3	Dust Composition Analyser (DCA)	120

1.3.1	Scientific goals	120
1.3.2	Instrument concept	120
1.3.3	Dust composition sensor	121

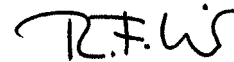
Part 1 Preface

The content of this Payload Definition Document (PDD) has been agreed by the contributors listed below.

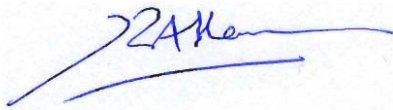
The PDD describes a reference payload that a) satisfies the measurement requirements given in the Solar Orbiter Science Requirements Document, and b) can be implemented within the resource envelope as specified in the document.

While not precluding other design solutions (provided they meet the measurement requirements and are compatible with the resource envelope), this reference payload has been used to establish the overall system design and corresponding cost, and in its final version will be part of the reference documentation for the Announcement of Opportunity (AO).

R. Wimmer-Schweingruber (on behalf of the In-Situ Payload Working Group)



R.A. Harrison



J.M. Defise



V. Martinez



S. Fineschi



NOTE: THE SIGNATORIES ABOVE HAVE NOT REVIEWED THE DELETIONS IN THIS VERSION OF THE DOCUMENT

LIST OF ACRONYMS

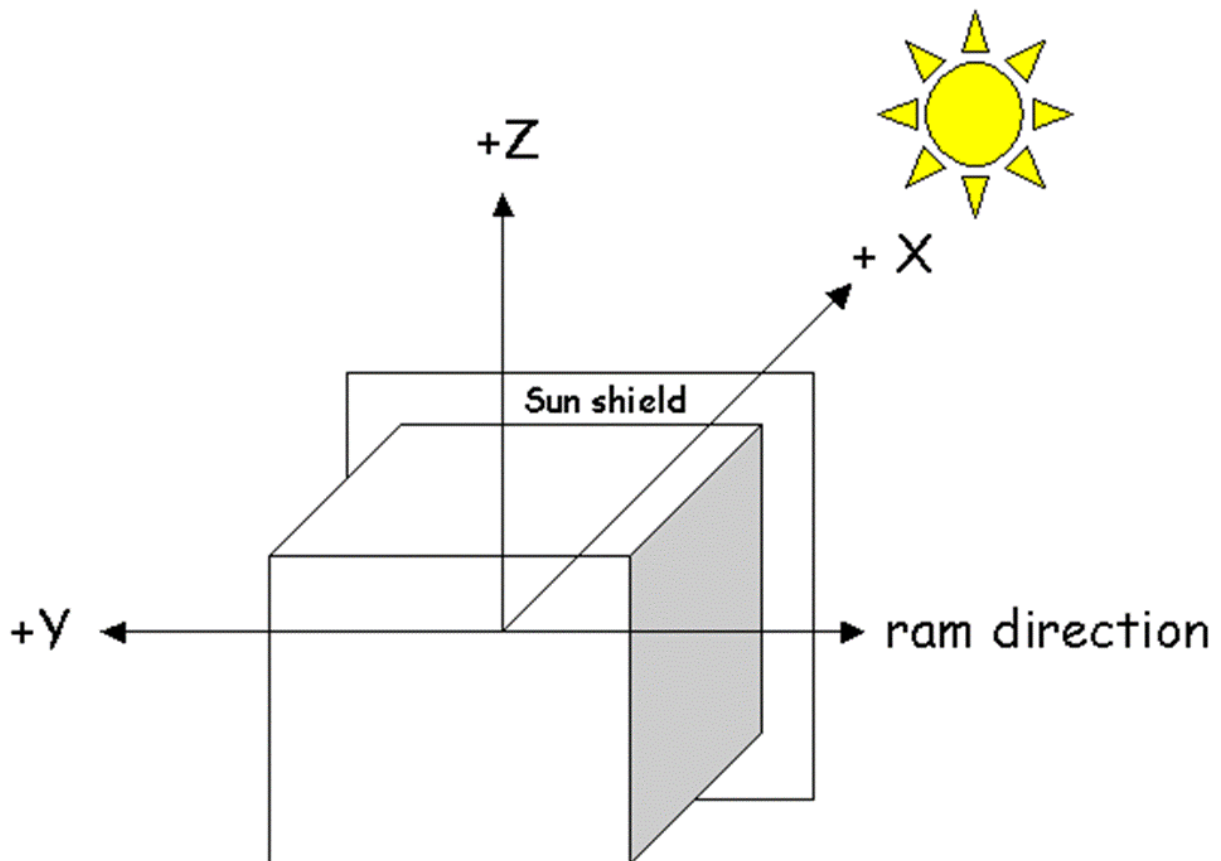
AC	Alternating Current
ACT/CAPS	Actuator/Cassini Plasma Spectrometer
ADC	Analog to Digital Converter
AIV	Assembly, Integration and Verification
AO	Announcement of Opportunity
AOCS	Attitude and Orbit Control System
ASIC	Application Specific Integrated Circuit
BMI	Boom Mounted Instruments
BOL	Beginning of Life
CAN	Controller Area Network
COR	Coronagraph
CPPS	Centralized Payload Power Supply
CRB	Contamination Review Board
CRS	Coronal Radio Sounding
CSA	Charge Sensitive Amplifier
DAC	Digital to Analog Converter
DC	Direct Current
DCA	Dust Composition Analyser
DPD	Dust Particle Detector
DPU	Digital Processing Unit
DSP	Digital Signal Processor
EAS	Electron Analyzer Sensor
EMC	Electromagnetic Cleanliness/compatibility
EMCB	Electromagnetic Cleanliness Board
EMI	Electromagnetic Interference
EOL	End of Life
EPD	Energetic Particle Detector
EPT	Electron and Proton Telescope
EUI	Extreme Ultraviolet Imager
EUS	Extreme Ultraviolet Spectrometer
EUV	Extreme Ultra-Violet
FFT	Fast Fourier Transform
FDT	Full Disc Telescope
FEE	Front End Electronics
FIFO	First In First Out
FPGA	Field Programmable Array
HETn	High Energy Telescope with <u>n</u> neutron detection
HFR	High Frequency Receiver
HGA	High Gain Antenna
HIS	Heavy Ion Sensor
HRT	High Resolution Telescope
HTHGA	High Temperature High Gain Antenna
H/W	Hardware
ICU	Instrument Control Unit
I/O	Input/Output
IR	Infra Red
LEMMS	Low Energy Magnetospheric Measurement Subsystem
LEOP	Launch and Early Orbit Phase
ISS	Internal Stabilisation System (VIM)
LCPM	liquid crystal polarisation module
LET	Low Energy Telescope

LFR	Low Frequency Receiver
LOS	Line Of Sight
MAG	Magnetometer
MCGA	Multicolor Graphics Array
MCP	Micro Channel Plate
MIMI	Magnetospheric Imaging Instrument
MLI	Multi Layer Insulation
NGD	Neutron and Gamma-ray Detector
NIS	Normal Incidence Spectrometer
PA	Product Assurance
PAS	Proton and Alpha particle Sensor
PDD	Payload Definition Document
PDMU	Payload Data Management Unit
PHA	Pulse Height Analysis
PIPS	Passivated Implanted Silicon
PMT	Photo Multiplier Tube
PZT	Piezo-Electric Transducer
QCM	Quartz Crystal Microbalance
RAD	Radiometer
RAM	Random Access Memory
RPE	Relative Pointing Error
RPW	Radio and Plasma Wave analyser
RTC	Remote Terminal Controller
S/C	Spacecraft
SciRD	Scientific Requirements Document
SDT	Solar Orbiter Science Definition Team
SEPM	Solar Electric Propulsion Module
SIS	Supra-thermal Ion Spectrograph
Solo	Solar Orbiter
SPS	Sun Pointing Suite
SpW	Space Wire
SS	Solid state
SSMM	Solid State Mass Memory
STE	Supra-Thermal Electron detector
STIX	Spectrometer Telescope Imaging X-rays
SWA	Solar Wind Analyser
SWT	Science Working Team
TBC	To Be Confirmed
TBD	To Be Determined
TC/TM	Tele-command / Telemetry
TDA	Technology Development Activity
TDP	Technology Development Plan
TNR	Thermal Noise receiver
TOF	Time-Of-Flight
UART	Universal Asynchronous Receiver/Transmitter
USO	Ultra Stable Oscillator
UV	Ultra-Violet
VIM	Visual-light Imaging Magnetograph
VLS	Variable Line Spacing
VTT	Technical Research Center of Finland (Valtion Teknillinen Tutkimuskeskus)

1 REFERENCE LIST

- [RD1] Solar Orbiter Science Requirements Document - R.Marsden, E.Marsch - iss 1, rev 2, 31 March 2005
- [RD2] Solar Orbiter Payload Definition Document – issue 2, revision 4.1 – ref. SCI-A/TA/2004 – January 2004.
- [RD3] In-Situ Payload Working Group - Final Report - ref. ISPWG/rgm/rw-s/16.05.2003
- [RD4] Remote-Sensing Payload Working Group - Final Report - May 14, 2003
- [RD5] Integrated Science Payload for the Solar Orbiter mission - Final review - Estec 29/6/2004 - ref SOP-HO-ASF-023
- [RD6] Payload Suite Interface Control Document - Astrium ref. SOP-ASF-RS-008, issue 2, rev 0, dated 20/6/2004
- [RD7] Solar Orbiter Phase A Mission Analysis Input - MAO WP 481 - issue 1, rev 1- March 2005
- [RD8] Solar Orbiter 2 - Composite option - pre-assessment. Ref. CDF-25(A), April 2004
- [RD9] Mission Requirements Document for Solar orbiter - issue 2, rev 0 - 22 - ref. Sci-A/2004-024/AJ - April 2004
- [RD10] ECSS-Q-70-01A, Space Product Assurance, Cleanliness and contamination control
- [RD11] ASTM E1559-3, Standard Test Method for Contamination out-gassing characteristics of Spacecraft Materials

2 SPACECRAFT REFERENCE COORDINATE SYSTEM



Note:

The correspondence of the $-Y$ axis with RAM (velocity) direction is only appropriate when the spacecraft is orbiting at the minimum and maximum heliocentric radii (and in absence of any de-pointing with respect to the Sun center). During science operations the $+X$ -axis may be off-pointed from the Sun center by up to $\pm 1.25^\circ$. This implies S/C slewing to ensure that offset pointing is maintained during offset observations.

It should be noted that the Z axis remains perpendicular to the orbital plane (and not to the ecliptic plane) throughout the mission (science phase).

3 INTRODUCTION

This Payload Definition Document (PDD) is a compilation of the Solar Orbiter reference payload requirements and of their related reference design. The PDD plays a key role in defining the resources required by the Solar Orbiter instruments and in providing the information necessary to conduct the mission assessment study and the preliminary spacecraft design.

The reference payload described in this document originates from the scientific objectives of the Solar Orbiter mission as spelled out in the associated Scientific Requirements Document [RD1]. In fact, each instrument addresses a part of the scientific goals of the mission with associated performance requirements (see sections 2 and 3 of RD1).

Information on the reference payload has been provided by selected experts of the Remote-sensing (RS) and In-Situ (IS) Payload Working Groups (PLWG) under the lead of the respective chairmen (Prof. Richard Harrison for the Remote-sensing units and Prof. Robert Wimmer-Schweingruber for the In-Situ units). The input provided by the 2 working groups has led to the compilation of previous versions of the PDD (in particular version 4.1 [RD2], issued on August 23rd, 2005) as well as to two individual reports containing a number of recommendations for technology development activities as well as addressing more specific technical issues [RD3, RD4].

The information contained in earlier versions of the PDD has been reviewed by *EADS-Astrium* in the context of the *Study of an integrated science payload for the Solar Orbiter* (ESA contract, AO/1-4408/03/NL/HB). This study (January-June 2004) has revisited the instrument design architectures, the associated resource budgets, and the P/L accommodation aspects in order to consolidate further the maturity of the reference payload [5, 6]. In the course of the study a number of interactions with the external community have taken place, triggering further work on the instrument design.

The study showed that the previously identified payload resources were largely under-estimated and that it was necessary to adopt a '*resource effective payload architecture*' in order to make the mission feasible [RD5]. Thermal issues were also found to have a major impact on system resources and spacecraft design, and had not been adequately researched. Such a payload architecture implies remote-sensing instruments having a maximum size of order 1 m and a typical diffraction limited resolution of 1 arcsec in the visible (corresponding to a spatial resolution of 150 km at perihelion). Such a design choice is in fact enabling the adoption of a fast cruise scenario at mission level, with the possibility to deliver key scientific data 1.5 years after launch.

3.1 Changes since PDD v4

Following the distribution of PDD v4.1 and the completion of the Solar Orbiter Assessment Phase, PDD v5 is a key reference document in support of the call for the Letters Of Intent to propose instrumentation for Solar Orbiter. This last version retains detailed information on the reference instruments but no longer contains specific interface information, which has been transferred to the Experiment Interface Document - part A. Version 5 is the last envisaged version of the Payload Definition Document, which will be superseded by the information provided in the proposals and the resulting EID-B.

4 CONTACT PERSONS

Instrument	Acronym	Name	Address	Telephone	Fax	E-mail
Solar Wind Analyzer	SWA	D.McComas	Southwest Research Institute, P.O. Drawer 28510, San Antonio, TX 78228-0510	+1-210-522-5983	+1-210-520-9935	dmccomas@swri.edu
Radio and Plasma Wave Analyzer	RPW	S.Bale	Space Sciences Laboratory, University of California, Berkeley, CA 94720-7450	+1-510-643-3324	+1-510-643-8302	bale@ssl.berkeley.edu
Magnetometer	MAG	C.Carr	Imperial College London, South Kensington campus, London SW7 2AZ, UK	+44-20-7594-7765	+44 20 75947772	c.m.carr@ic.ac.uk
Energetic Particle Detector	EPD	R. Müller-Mellin	Institut für Experimentelle und Angewandte Physik Christian-Albrechts-Universitaet zu Kiel Leibnizstrasse 11, D - 24118 Kiel, Germany	+49-431-880-3227	+49-431- 88-85660	mueller-mellin@physik.uni-kiel.de
Dust Particle Detector	DPD	I. Mann	Institut fuer Planetologie, Westfaelische Wilhelms – Universitaet, Wilhelm - Klemm - Str. 10, 48149 Muenster, Germany	+49-251-83-39081	+49-251-83-36301	imann@uni-muenster.de
Neutral Particle Detector	NPD	M.Hilchenbach	Max-Planck-Institut für Aeronomie, Max-Planck-Straße 2, 37191 Katlenburg-Lindau, Germany	+49-5556-979-162	+49-5556-979-240	hilchenbach@linmpi.mpg.de
Neutron Gamma Ray Detector	NGD	B.Barraclough	Los Alamos National Laboratory, P.O. Box 1663 Los Alamos, NM 87545	+1-505-667-8244	+1-505-665-7395	bbarraclough@lanl.gov
Visible Imager	VIM	V.Martinez	Instituto de Astrofisica de Canarias, c/ Via Lactea s/n, La Laguna, 38200, Tenerife, Spain	+34-922-605237	+34-922-605210	vmp@ll.iac.es
EUV Imager	EUI	J.M.Defise	Centre Spatial de Liège, Université de Liège, Parc Scientifique du Sart Tilman, Avenue du Pré-Aily, B-4031, Angleur-Liège, Belgium	+32-43-676668	+32-43-675613	jmdefise@ulg.ac.be
EUV Spectrometer	EUS	R.Harrison	Rutherford Appleton Laboratory, Chilton Didcot, Oxfordshire, OX11 0QX, UK	+44-1235-446884	+44-1235-445848	R.A.Harrison@rl.ac.uk
VIS-EUV Coronagraph	COR	S.Fineschi	Osservatorio Astronomico di Torino, 20 Strada Osservatorio, 10025 Pino Torinese, Italy	+39-011-810-1919	+39-011-810-1930	fineschi@to.astro.it
Spectrometer Telescope Imaging X-ray	STIX	G.Hurford	Space Sciences Laboratory, University of California, Berkeley, CA 94720-7450	+1-510-643-9653	+1-510-6438302	ghurford@ssl.berkeley.edu

5 SECTION DELETED FOR THE CALL FOR LETTERS OF INTENT

TEXT DELETED WAS OUT OF DATE

6 PAYLOAD OVERVIEW

Tables 6.1, 6.2 and 6.3 provide an overview of the payload characteristics. Two instrument groups are identified: the so-called *in-situ* (IS) instruments and the so-called *remote-sensing* (RS) units. All instrument requirements are compatible with the science goals described in the *Scientific Requirement Document* (SciRD) of the Solar Orbiter Mission [RD1].

The Solar Orbiter Science Definition Team (SDT) has identified a Baseline Mission (with an associated *Core payload complement*) as well as a *High Priority Augmentation payload complement* and a *Minimum payload complement*. The Baseline Mission represents first-class science, while still being compatible with the constraints imposed by the resources - both technical and financial - that are likely to be available for implementation of the mission. Finally, it should be noted that while the reference payload described in this document demonstrates that the science requirements can be achieved within the resource constraints of the mission, it is not meant to preclude alternative concepts that could meet and improve on both the science return and the use of resources.

6.1 Core payload complement

The Baseline Mission could be accomplished by an instrument complement comprising the following generic types [RD1]:

- Field Package
- Particle Package (including neutrons, γ -rays and dust speed, mass and velocity measurement, but without directionality and elemental composition information)
- Plasma Package
- Remote-Sensing Package comprising
 - Coronagraph (white-light and UV)
 - EUV imager
 - EUV spectrometer
 - Visible light imager & magnetograph
 - X-ray spectrometer/imager

6.2 High priority augmentation

In the event that additional resources become available, the SDT recommended a number of so-called High Priority Augmentations to the Solar Orbiter Baseline Mission, described in Appendix I.

Table 7.1 – Core payload complement: summary of main characteristics

Instrument	Acronym	Science goals	Spectral band – Particle range	Nom. Mass (1) [kg]	Mass margin (%)	Total Mass [kg]	Physical size of main units [cm]	Power (2) [W]	TM (3) [kbps]
In-Situ Instruments									
Solar Wind Plasma Analyzer	SWA	Investigation of kinetic properties and composition (mass and charge states) of solar wind plasma	e-: 0.001 – 5 keV/q p+, α : 0.2 – 20 keV/q ions: 0.5 – 100 keV/q	15	10	16.5	HIS: 40 × 40 × 30 PAS: 40 × 30 × 20 EAS (2×): 15 × 15 × 15	15.5	7
Radio and Plasma Wave Analyzer	RPW	Investigation of radio and plasma waves including coronal and interplanetary emissions	1 Hz to 10 MHz	11.8	10	13.0	Ant.: 500-600 Loop: 20 Coils: 20	7.0	5
Magnetometer	MAG	Investigation of the solar wind magnetic field	Time resolution: 16 samples / sec normal ops Absolute precision: 1 nT	1.9	10	2.1	Sensor: 11 × 7 × 5 Elect: 15 × 14 × 10	1.5	0.8
Energetic Particle Detector	EPD	Investigation of the origin, acceleration and propagation of solar energetic particles	0.002–100 MeV/nucleon in 5 units (e-/+, p+, ions)	13.7	10	15.1	10 units, typical size: 15 × 15 × 10	14.5	3.1
Dust Particle Detector	DPD	Investigation of the flux, mass and major elemental composition of near-Sun dust	10 ⁻¹⁵ - 10 ⁻⁶ gr	1.6	10	1.8	20 × 15 × 15 (2 units)	6	0.1
Neutron Gamma ray Detector	NGD	Investigation of the characteristics of low-energy solar neutrons, and solar flare processes	n: 0.6 – 20 MeV Gamma: 0.05 – 10 MeV	5.0	10	5.5	15 × 15 × 25 (sensor head + electronics)	5.5	0.4
Remote-sensing Instruments									
Visible Imager & Magnetograph	VIM	Investigation of the magnetic and velocity fields in the photosphere	400 – 700 nm (1 narrow pass-band of 5-10 nm)	24.3	25	30.4	80 × 40 × 30 optical bench	35	20
EUV Spectrometer	EUS	Investigation of properties of the solar atmosphere	17-100 nm (2-3 narrow bands)	14.4	25	18.0	90 × 30 × 12	35	17
EUV Imager	EUI	Investigation of the solar atmosphere using high resolution imaging in the EUV	13.3 nm, 17.4 nm, 30.4 nm (3 bands)	16.3	25	20.4	each HRI 95 × 10 × 15 FSI 95 × 25 × 20 optical bench	28	20
Visible Coronagraph	COR	Investigation of coronal structures using polarized brightness measurements in Vis	450-600 nm +121.6 nm and 30.4 nm (optional)	14.6	25	18.3	80 × 40 × 25 (optical bench)	30	10
Spectrometer Telescope Imaging X-ray	STIX	Investigation of energetic electrons near the Sun, and solar x-ray emission	3 – 150 keV	4.0	10	4.4	100 × 15 × 15 or 100 × 17 cm diam.	4	0.2
Payload Support Elements	PSE	---	---	21.6	20	26.0	---	4	---
TOTAL						171.5	---	186.0	83.6

(1) Remote-sensing mass values based on [RD5] input and consolidation by industrial study; (2) average power including margins during operations; (3) reference allocation only.

Table 7.2 –Solar Orbiter core payload complement: summary of pointing and accommodation aspects.

Instrument	Acronym	Pointing direction & FOV	LOS pointing stability (RPE)	Instrument accommodation
In-situ instruments				
Solar Wind Plasma Analyzer	SWA	EAS: FOV= 4π Sr, PAS: Sun pointed, FOV = $60^0 \times 10^0$ HIS: Sun pointed, FOV = $60^0 \times 10^0$	NA	PAS and HIS are S/C body mounted with small (10 cm ²) aperture through the heat shield, EAS sensors are on the S/C behind the shield
Radio and Plasma Wave Analyzer	RPW	3-axis sensing	NA	3 × antenna on S/C under direct Sun light, magnetometer loop and 3x search coils on the boom
Magnetometer	MAG	3-axis sensing	NA	2 × sensors located on boom (in the shadow)
Energetic Particle Detector	EPD	Several directions wrt orbital plane Typical FOV of order $60^0 \times 60^0$	NA	5 × sensors located on the spacecraft corners behind the heat shield.
Dust Particle Detector	DPD	1x RAM, 1x orthogonal to RAM, FOV = 120^0	NA	2 sensors mounted on the S/C body in velocity and orthogonal to velocity direction
Neutron Gamma ray Detector	NGD	Sun pointed FOV = 5^0	NA	Located behind shield, no optical aperture is required (but low Z materials)
Remote sensing instruments				
Visible Imager & Magnetograph	VIM	Sun pointing FOV= 2.7^0 FDT, 17^0 HRT	0.02" in 10s	Located behind shield, 2 apertures (12.5 and 1.5 cm diameter) with door and heat rejection filters
EUV Spectrometer	EUS	Sun pointing FOV= $34^0 \times 1.0^0$ slit	1.0" in 10 s	Located behind shield, 1 aperture (7 cm diameter) with door
EUV Imager	EUI	Sun pointing FOV= 16.7^0 HRI, 5.4^0 FSI	0.1" in 10 s	Located behind shield, 4 apertures (2 cm diameter) with doors and baffles, small Al filters
VIS-EUV Coronagraph	COR	Sun pointing FOV= 9.2^0	2" over few s	Located behind shield, 1 aperture (17 cm diameter) with door and occulter (8 cm diameter)
Spectrometer Telescope Imaging X-ray	STIX	Sun pointing FOV= 38^0	2" over few s	Located behind shield, 1 apertures (12 × 12 cm ²) with door (TBC) and filters

Table 7.3 –Solar Orbiter core payload complement: summary of instrument design maturity and related development activities.

Instrument	Acronym	Instrument concept	Critical issues	Maturity Level	Technology Development Activity
In-Situ instruments					
Solar Wind Plasma Analyzer	SWA	Multi-sensor unit (EAS: e-; PAS: p+; HIS: heavy ions) based on high voltage mass spectrometers	Entrance of HIS and PAS under direct Sun illumination; high voltage; multiple locations	3	NA
Radio and Plasma Wave Analyzer	RPW	Multi-sensor instrument based on electric antennas, magnetic coils and 3 dedicated receivers	3 × 5-6 m long antenna exposed to Sunlight, EMC cleanliness	3	Antenna material
Magnetometer	MAG	Dual, 3-axis fluxgate, with boom-mounted sensors	Magnetic cleanliness, need for stable temp environment, periodic calibrations	2	NA
Energetic Particle Detector	EPD	Multi-sensor unit (STE: e-; EPT: e-, p+; SIS: ions; LET: ions; HET: ions, p+, n, e-) based on SSD+MCP	Complex FOV requirements, detectors behavior in relevant environment, Front-End electronics	2	High quality Si material
Dust Particle Detector	DPD	Impact detector	High Voltage required	3	NA
Neutron Gamma ray Detector	NGD	Combined neutron and gamma-ray detector, based on scintillators and PMT's	High-voltage for PMT's and scintillating crystals	5	LaBr ₃ crystal development
Remote-sensing instruments					
Visible Imager & Magnetograph	VIM	2 telescopes (HRT: reflection; FDT: refractive; and a common filtergraph (FO: dioptric+Fabry Perot)	Internal Stabilisation System required to achieve high pointing stability. Fabry Perot and LCVR	4	APS development LiNbO ₃ rad hard qualific.
EUV Spectrometer	EUS	Off-axis normal incidence plus grating spectrometer	Stringent pointing stability, internal mechanisms, heat load without entrance filter, mirror coatings, data rate / data selection approach, cooled APS	4	APS development, thin heat rejection filter
EUV Imager	EUI	4 off-axis reflective system: High Resol. Imager with 3 telescopes, Full Sun Imager with 1 telescope	Stringent pointing stability, internal mechanisms, data rate / data selection approach, cooled APS	4	APS development, thin heat rejection filter
VIS-EUV Coronagraph	COR	Off-axis Gregorian telescope with external occulter	Occulter design, pointing offset compensation, simultaneous visible and EUV bands, data rate / data selection approach, resource demands	4	APS development LCVR developments
Spectrometer Telescope Imaging X-ray	STIX	Indirect imaging technique based on 64 sub-collimators (tungsten grids), CdZnTe detectors. Monitoring of LOS by 2 limb-sensing systems	Image reconstruction, data rate / data selection approach, instrument length, aspect system	2	Modest grid development

⁽¹⁾ Maturity levels: 1 Existing hardware 4 New, Detailed design level
 2 Existing + minor modifications 5 New, Preliminary design level
 3 Existing + major modifications 6 Concept only

Part 2 Description of the Instruments

1 INTRODUCTION

In this part, the baseline design of each Remote-sensing and In-Situ instrument is described and the corresponding resources, in terms of mass, envelope size, power and data rate are quantified. Such estimates play an important role in the context of the definition of the Solar Orbiter mission as they strongly influence the S/C requirements and corresponding resources. Under- or over-estimating the required resources would in fact lead to inaccurate choices at system level, thus significantly increasing the development risks and/or the cost at completion.

The payload study [RD5, RD6] indicated clearly that the P/L resources contained in ref. [RD2] were often underestimated (up to 100%) with a correspondingly large impact on the platform design and overall mission definition. On this basis, following consultation with the chairmen of the PLWG and the Science Definition Team, particular effort was made to define new boundary conditions which, while leaving freedom in the detailed design of each instrument and remaining compatible with the science goals of ref. [RD1], would allow to respect the available payload resource budgets, including realistic margins.

This approach has led to the identification of the so-called *resource efficient payload*, resulting in:

- a) 1-m class, 1 arcsec resolution units in the case of the Remote-sensing instruments;
- b) Possible grouping of the In-Situ sensors sharing common functions.
- c) Introduction of standard Remote Terminal Control units.

2 PAYLOAD SUPPORT ELEMENTS (PSE)

The Payload Support Elements (PSE) are instrument specific items required for a proper accommodation of the instruments on-board the spacecraft. They include thermal control units whose characteristics and procurement is strictly linked to the design of the spacecraft heat shield (e.g., instrument covers/doors, heat rejection windows, thermal straps).

The resource required by the PSE items is accounted for in addition to the payload units.

To date the following items are included in the PSE:

Payload Support Element	Description / justification	Nominal Mass (kg)	Maturity Margin (%)	Total Mass (kg)
Boom	A foldable boom is presently envisaged (total max length 4 m). The boom will be procured as part of the S/C due to the implications on AIV/AIT and platform pointing performance.	5	20	6
VIM filter	A heat-rejecting filter is baselined for VIM. Given its close interface to the S/C heat shield, the item shall be procured as part of the S/C.	1.2	20	1.5
EUS filter (TBC)	A heat-rejecting filter is baselined for EUS. Given its close interface to the S/C heat shield, the item shall be procured as part of the S/C.	0.4	20	0.5
Instrument doors (Several items)	All instruments requiring a direct FOV to the Sun require an aperture through the heat shield and a related (multiple-operation) cover. Given their close interface to the S/C heat shield, such items shall be procured as part of the S/C.	10	20	12
Thermal interfaces (Several items)	As part of the P/L accommodation a number of I/F units will be required to ensure adequate thermal control (e.g. dedicated straps, extra baffling/MLI).	5	20	6
TOTAL		21.6	---	26.0

3 REMOTE-SENSING UNITS

3.1 Visible-Light Imager and Magnetograph (VIM)

The purpose of the VIM is to measure the magnetic and velocity fields in the photosphere. It observes the magnetic boundary for the magneto hydro-dynamic (MHD) processes observed by other remote-sensing instruments and allows surface and subsurface dynamics and structure to be determined, *e.g.*, with the methods of local helio-seismology. It will observe the morphology, dynamics, and strength of the magnetic elements and flux tubes at the photospheric level with a resolution that is consistent with the resolution of the EUV telescopes. It will also provide the first images, Doppler-grams and magneto-grams of the solar poles and of the side of the Sun, which is not visible from the Earth.

VIM will have vector magnetic field capabilities as this is of fundamental importance to understand the nature of photospheric fields. Having vector capabilities is also the only way in which quantitative inferences of the magnetic field in the transition region and corona can be made (from force-free or full 3D MHD extrapolations).

VIM will also produce line-of-sight velocity maps by observing two points on either side of a spectral line. These maps can be used, through local helio-seismology techniques, to investigate subsurface flows. The internal structure and dynamics of the near-polar regions of the Sun is of paramount importance and perhaps *the* key to our understanding of the solar cycle.

3.1.1 Scientific Goals

The principal scientific goals of the Visible-light Imager and Magnetograph (VIM) are:

- To provide measurements of the “magnetic carpet” which drives chromospheric and coronal activity as studied by the UV and X-ray instruments;
- To provide surface and subsurface flows in the field of view of the UV and X-ray instruments;
- To observe and accurately quantify for the first time the surface polar magnetic field of the Sun;
- To measure rotation and flows near the Sun’s poles using techniques of local area helio-seismology, and thereby provide crucial constraints on solar dynamo theories;
- To unveil the small-scale photospheric dynamo;
- To resolve solar magnetism down to its fundamental length scale (<150 km);
- To provide the first magneto-grams and Doppler-grams of the far side of the Sun (in relation to the Earth).
- Subsurface flows, using local helio-seismology techniques applied to line-of-sight velocity maps obtained by observing two points on either side of a spectral line.

Furthermore, by using its vector magnetic field capabilities, VIM will enable studies of:

- The nature of photospheric fields: Are the polar fields vertical unipolar fields? Do they harbour complex neutral lines with horizontal sheared fields?
- The magnetic field in the transition region and corona (using force-free or full 3D MHD extrapolations);

3.1.2 Instrument concept

It is impractical to combine the functions of full-disc and high resolution viewing of the Sun into a single telescope. Therefore two telescopes, a 125 mm diameter (TBC) High Resolution Telescope (HRT), and a 15 mm diameter Full Disc Telescope (FDT) are required. The design allows for them to share the Filtergraph Optics (FO) and the detector. Light from either the HRT or the FDT will be selected by a shutter mechanism. A single set of electronics with control and data processing capability is envisaged.

A functional block diagram of VIM is provided below.

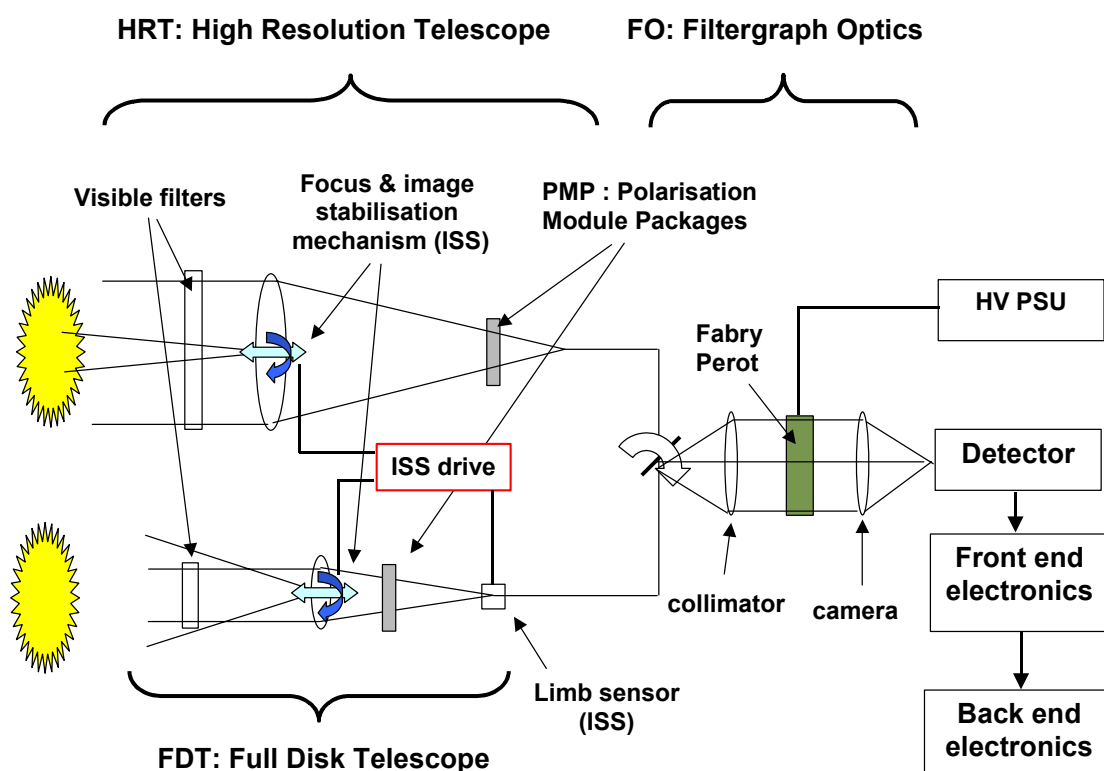


Figure 2.1.1: VIM Functional Diagram

Wavelength of interest and rationale for HRT telescope aperture

For the purposes of the system study, the aperture of the HRT was sized to give a diffraction limited angular resolution of 1 arcsec at 500 nm. This aperture then sets the thermal load into the instrument. The selection of a longer wavelength (e.g. 630 nm) would imply an increased aperture to maintain the same diffraction limit. An increased aperture will lead to higher heat load, a larger filter window and cover, as well as an increase in the volume of the telescope, with impacts on overall payload resources. On this basis, the final choice of the VIM aperture should be the result of an instrument level trade study, including scientific (e.g. resolution, SNR, detector performance, etc.) as well as engineering parameters (e.g., resource envelopes, development risk). Such a trade-off analysis shall aim to be compatible with the allocated instrument resources. A diameter of 18 cm is considered as maximum acceptable.

High Resolution Telescope (HRT)

In agreement with the Scientific Requirements Document [RD1], the HRT presented here is sized to provide a spatial resolution of 150 km (angular resolution of 1'') over the solar surface at perihelion (about 0.22 AU heliocentric distance). This value sets the aperture of the telescope to 12.5 cm ($\lambda=500$ nm, TBC). It is also baselined to have a pixel size equal to half the spatial resolution. A Polarisation Modulation Package (PMP) is included in the optics prior to the FO.

Two solutions were evaluated for the HRT, first, an open solution with ceramic mirrors and a heat stop rejecting most of the solar light outside of the spacecraft and, second, a closed solution with a window (possibly a lens) coated to allow a very small wavelength region entering the telescope. For thermal reasons, the closed solution has been identified as the preferred solution. In this implementation, the only critical element from a thermal point of view is the entrance filter (or lens). Assuming a broad-band absorption of 10%, 38.2 W will have to be disposed off by a dedicated radiator. The main saving compared to the open case is the reduction of critical elements from two (mirror + heat rejection) to one (entrance filter) and lower thermal loads inside the S/C.

Full Disc Telescope (FDT)

The FDT is composed of a lens or entrance filter (with identical performance to the HRT entrance filter) and a first imaging lens followed by a relay system, chosen to provide a full disk image at minimum perihelion distance that fills the detector with the image and working at the diffraction limit. The diameter of the FDT is such that the ratio of the apertures between the HRT and the FDT is equal to the inverse of the ratio of the field-of-view of both telescopes. This ensures the same field-of-view performance for both telescopes of the FO Fabry-Perot units. A coating at the entrance lens reflects most of the incident sunlight so that the radiation load is not a problem for the FDT. A separate PMP is necessary for the FDT in order to perform polarisation modulation within the centred optical path before the first oblique reflection.

Polarisation Modulation Package (PMP)

The PMP will allow VIM to provide longitudinal and transverse magnetograms of the region being observed. The PMP will produce the modulation of the intensity at the APS detector as a function of the input polarisation state. These intensity changes of the detector measurements will be used to recover the Stokes vector of the solar light.

Each PMP will be composed of a couple of Liquid Crystal Variable Retarders (LCVRs) followed by a fixed linear polariser. The LCVR retarders follows the design of ground polarimeters successfully built and used at the Canary Island Observatories. LCVRs produce polarization modulation using simple square waves with amplitudes of up to ± 20 V. They need to be temperature controlled to within 1 degree. LCVRs can be built in such a way that, for no applied voltage, no net retardance is introduced (compensated LCVRs). In this case no effect is produced when only velocity measurements are being made. The LCVRs combination generates 4 independent polarization states that are read by the detector.

LCVRs have been tested to some extent for space applications but a full characterization for the Solar Orbiter environment is needed, in particular sensitivity to UV light and continued performance under vacuum conditions.

Image Stabilisation System (ISS)

Due to the data processing needs (see section 1.1.1), the VIM pointing (LOS) needs to be extremely stable, better than 0.02 arc seconds in 10 seconds (typical integration time), and therefore an ISS is required to

improve significantly over the pointing accuracy of the spacecraft. The ISS can only correct for the LOS, and therefore the spacecraft will provide the required stability (2 arc sec in 10 seconds) around the LOS. The ISS, and the related control loop must also account for the relative rotation of the Sun, and will require inputs on the spacecraft - Sun geometry at observation time. The table below summarises the estimated relative (Sun-S/C) rotation, which is dependant upon the Sun – spacecraft distance, for each of the science phase orbits.

Orbits after GAM	Window	Distance to Sun (AU)	Relative Rotation (degrees/day)	Rotation of the Sun from the perspective of the Spacecraft (arcsec/10 seconds)
Venus 2	max southern helio latitude	0.34	9.3	0.053
	perihelion	0.23	2.8	0.024
	max northern helio latitude	0.61	12.5	0.040
Venus 3	max southern helio latitude	0.36	9.4	0.051
	perihelion	0.25	4.9	0.038
	max northern helio latitude	0.57	12.1	0.041
Venus 4	max southern helio latitude	0.40	9.9	0.048
	perihelion	0.30	7.2	0.047
	max northern helio latitude	0.56	11.8	0.041
Venus 5	max southern helio latitude	0.37	9.0	0.047
	perihelion	0.34	9.0	0.051
	max northern helio latitude	0.55	11.6	0.041
Venus 6	max southern helio latitude	0.39	9.9	0.049
	perihelion	0.37	10.0	0.052
	max northern helio latitude	0.50	10.9	0.042

The ISS uses a limb sensor as a stabilisation source. In essence, a cube beam-splitter sends a small fraction of the light of the FDT to a limb-sensor that drives folding mirrors acting as closed-loop tip-tilt system to stabilise the image to the required level. The ISS must also operate when VIM is observing with the HRT. It will derive the correction signal needed to compensate spacecraft pointing errors and drive a similar tip-tilt mirror in the HRT. In principle the signal could be made available to other remote-sensing instruments (those needing a better pointing accuracy than that provided by the AOCs of the spacecraft, such as EUI). A calibration strategy of all these tip-tilt mirrors with respect to the one on the FDT path needs to be defined to ensure a correct performance during the mission lifetime. A possible implementation of the ISS is given in figures. 2.1.2 and 2.1.3.

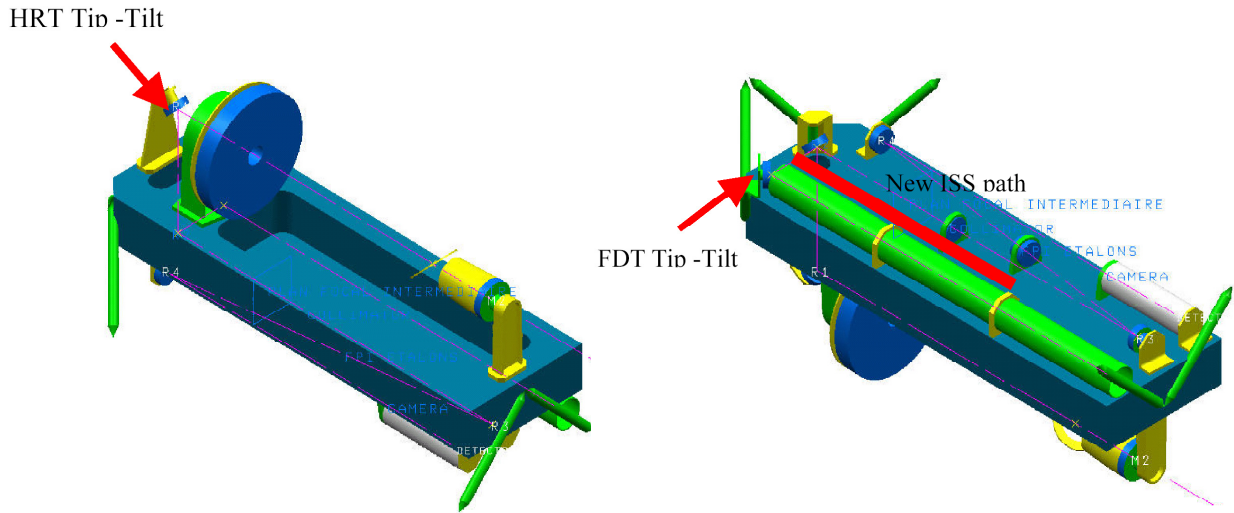


Figure 2.1.2: Possible implementation of the ISS, showing the FDT and HRT Tip-tilt mirrors and the ISS path

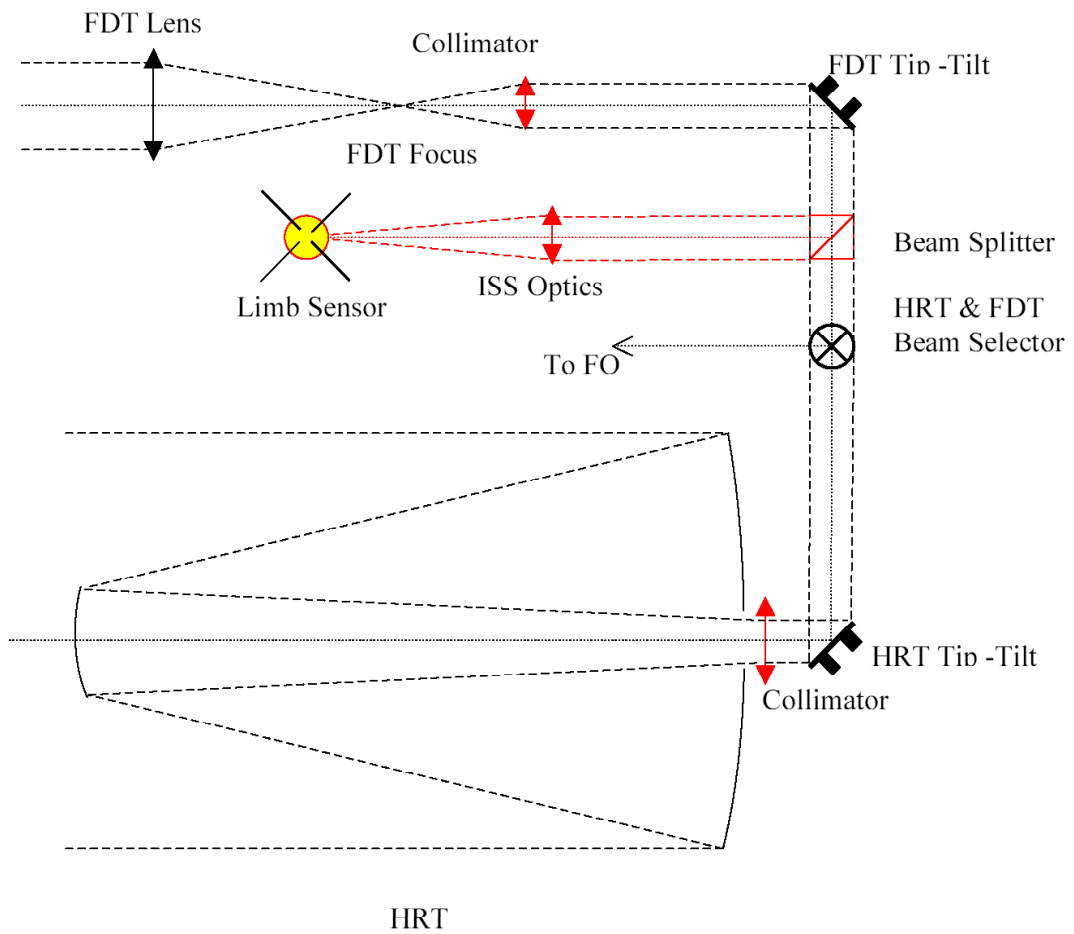


Figure 2.1.3: Optical functional diagram of the ISS

Filtergraph Optics (FO)

The FO consists of a relaying optical system with a magnification that provides an adequate location for all the spectral filter components (prefilter and LiNbO₃ etalons). This location could be either near a pupil plane of the system (collimated case) or near a telecentric image plane. The pros and cons of both options, collimated vs. telecentric, should be carefully considered as they have important implications in terms of instrument calibration.

Two 50 mm diameter Fabry-Perot etalons near the pupil plane provide the required spectral resolution of typically 50 mÅ. One etalon will provide the spectral resolution while the other blocks the secondary transmission maxima of the first. A separate interference filter with a 3Å band blocks the secondary transmission maxima of the combined etalons. It is considered using two LiNbO₃ solid-state etalons with fixed resonator widths, mounted on a temperature controlled oven (0.1 degrees of stability is required for 10 mÅ passband shift). Spectral tuning is achieved by applying voltages to the Fabry-Perots. About ±2 kV is required for a shift of the passband of ±1 Å, which is sufficient to cover both line width and Sun-spacecraft velocity shifts. The LiNbO₃ technology will require a thorough space qualification effort, with particular emphasis on the performance under high particle radiation environments (see section 2.1.8).

A focus mechanism near the telescope focal plane is used for accurate focusing and to re-image the pupil onto the detector (MDI heritage). This includes a calibration mode, which will allow a pixel-to-pixel calibration strategy of VIM for wavelength registration.

APS detector camera

VIM uses only one detector at the focal plane of the FO. The detector is base lined to be a CMOS-APS 2048 × 2048 pixel detector, providing 0.5 arcsec per pixel (8 μm). As VIM operates in the visible range, the operating temperature is presently envisaged to be around 0 deg C. CCD detectors, a potential alternative to APS, in addition to posing significant radiation damage problems, would require a considerably lower operating temperature (-110 deg C). Detector performance plays a critical role with respect to SNR, thus influencing the final choice of the telescope aperture. See section on Open points and critical issues.

Overall optical configuration

The combination of all optical subsystems is shown in Figure 2.1.4 (HRT and FO), 2.1.5 (FDT) and 2.1.6 (optical bench assembly), all for the on-axis design case. As part of the payload study, a specific recommendation was made by industry for considering an off-axis design. A common optical bench provides support to both the HRT and the FDT; the HRT is seen as the top part of the left figure. The FDT is the large cylinder on the left top part of the central figure that also includes the FO. The right figure displays a frontal view of the optical bench with the HRT on the top part and the FDT and FO in the bottom part.

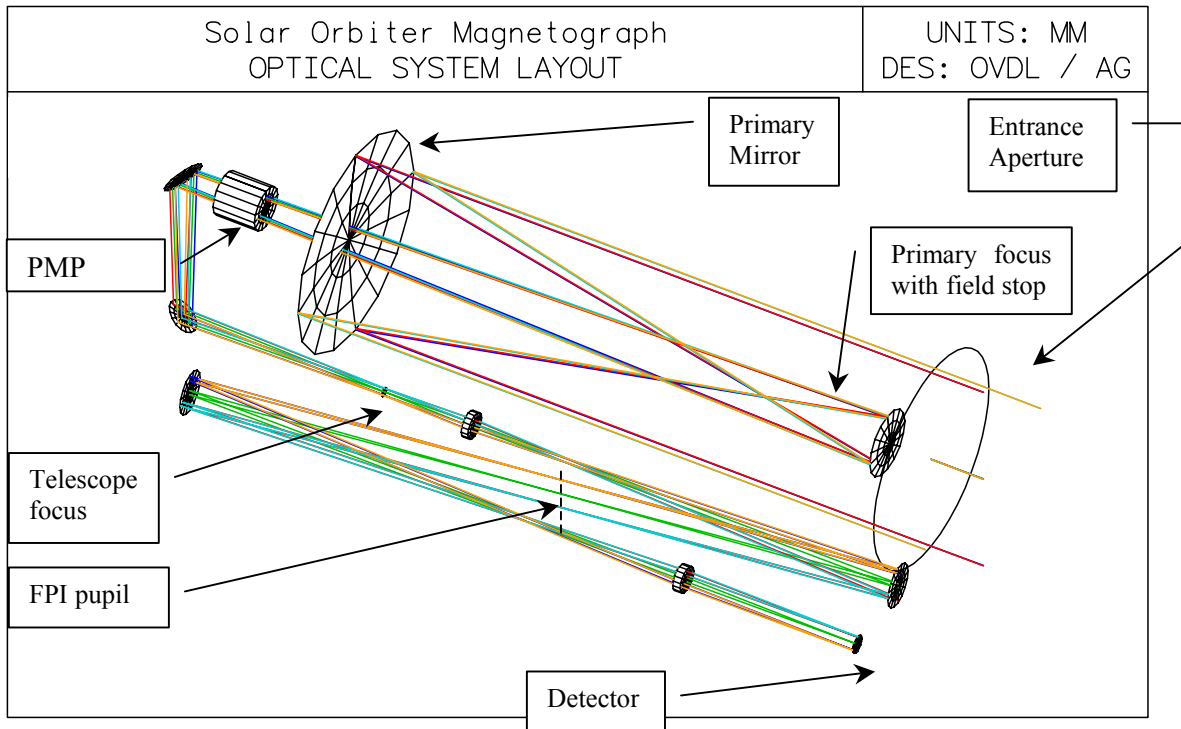


Figure 2.1.4: View of a possible optical layout of the high resolution telescope and filtergraph (under the assumption of an on-axis design).

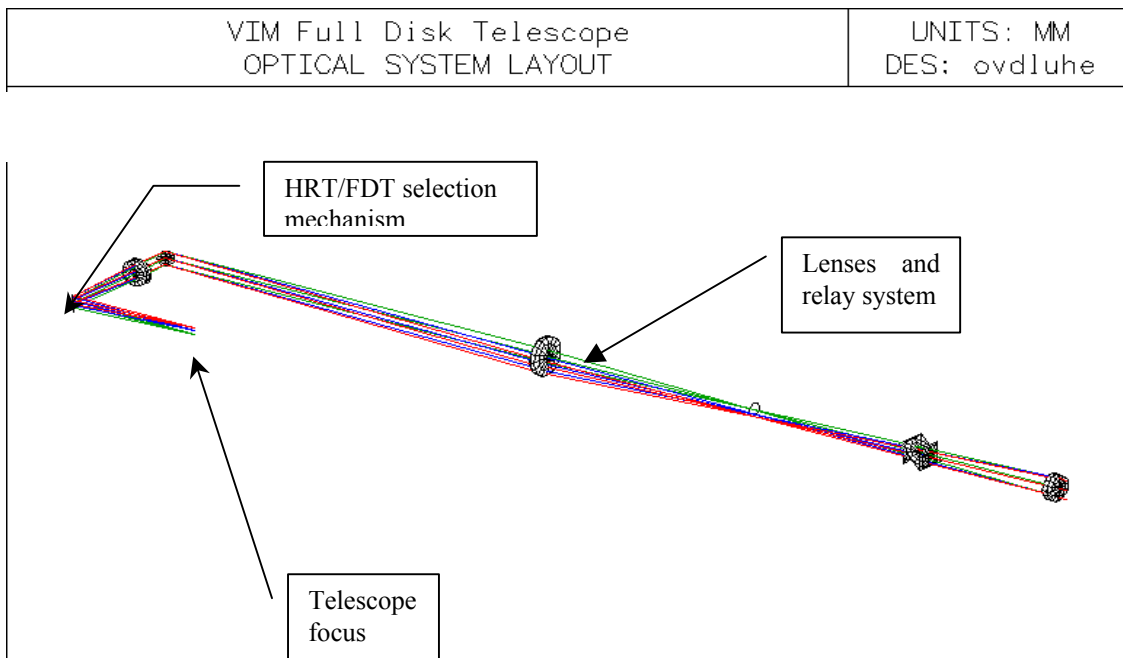


Figure 2.1.5: View of a possible optical layout for the full disk telescope (ISS beam-splitter not shown).

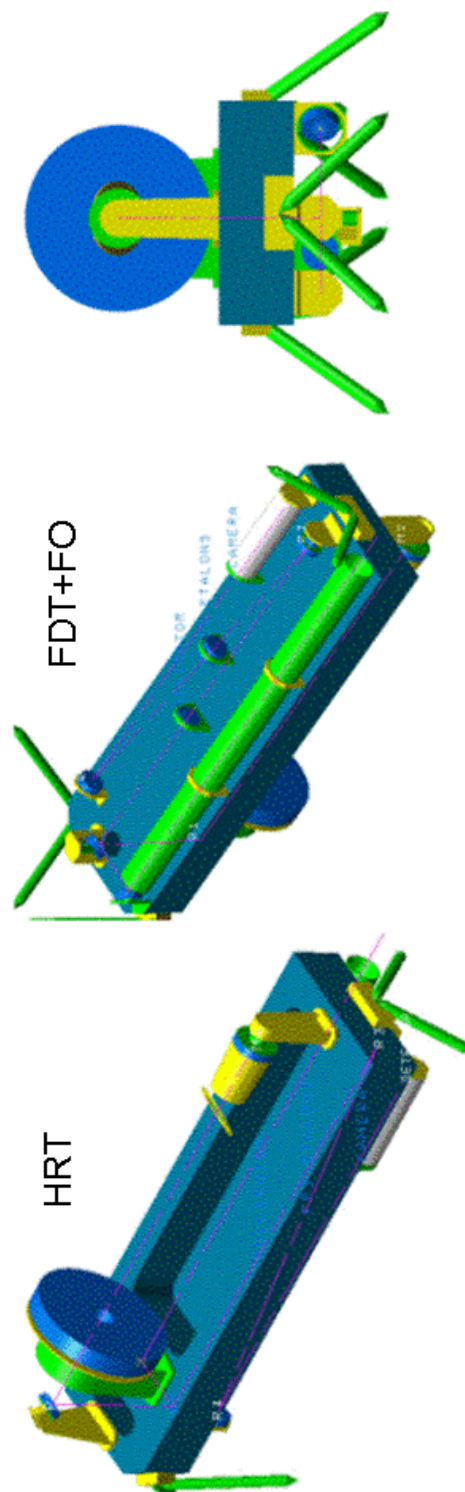


Figure 2.1.6: VIM assembly (on axis design). The HRT is arranged above the FDT and the FO, both of which are mounted on a common optical bench. The optics assembly fits an 800 mm × 400 mm × 300 mm envelope.

3.1.3 Orbit, Operations and Pointing Requirements

The HRT and FDT cannot be used simultaneously as they share the same FO and will be used sequentially during the full observation windows.

The processing requirements are key to a good understanding of the instrument. The Stokes parameters I,Q,U,V provide the longitudinal and transverse solar magnetic field. To obtain them ideally requires 5 wavelengths (one in continuum and 4 within a spectral line). Further the Stokes parameters are required in 4 polarization states leading to an observation sequence as follows:

Time (sec)	Filter setting	Processing
0	λ_1 (continuum)	Obtain image in each of 4 polarization states, 4 × configure PMP, the APS takes the image and sends to processor.
6	λ_2 (inside spectral line)	Another set of 4 polarization states
12	λ_3 (inside spectral line)	Another set of 4 polarization states
18	λ_4 (inside spectral line)	Another set of 4 polarization states
24	λ_5 (inside spectral line)	Another set of 4 polarization states
30		Physical magnitudes (continuum intensity, magnetic field, velocity) are determined in the processor and stored
60	Commence sequence again	As above, or perform in just two polarization states collecting I and V parameters

The line of sight Doppler shift (velocity) is made from a combination of the four points within the line.

3.1.4 Calibration

Outside of the nominal 30 encounter days, a calibration mode of the tip-tilt mirrors in the FDT and HRT path should be included (preferably before the encounter phase and while the spacecraft has direct contact to the Earth). This calibration program (that should be considered by all instruments receiving the VIM stabilisation signal) will allow to set the gains and offsets of the PZT normally included in the tip-tilt mirrors and that, will inevitably, suffer from degradation during the mission lifetime.

3.1.5 Accommodation

The VIM is hard-mounted on the spacecraft, behind the heat shield and aligned to within 2 arcmin to the other instruments. The large aperture of the HRT-VIM in combination with the need for a high thermal stability makes the thermal balance of the instrument most demanding.

3.1.6 Interface and Physical Resource Requirements

Telemetry needs – data compression.

VIM will detect intensity images in different positions within a selected spectral line and in different polarization modes. For calibration purposes, sometimes, these intensity frames (or the Stokes parameters easily deduced from them) will be stored. But these data will represent a small fraction of the total and will not compromise the telemetry rates. Here we consider only the cadences and telemetry rates needed for different observing modes that should constitute the fundamental science operation modes of the instrument. The use of these modes will depend on the science targets selected for each orbit based on the science plans of the spacecraft. In any of these modes, VIM will provide a combination of the following physical magnitudes:

1. I_c or continuum intensity images. A temperature indicator that provides the photospheric context. 8 bits compressed to 4 bits per pixel.
2. V_{los} the line-of-sight (LOS) velocity frames. They provide the Doppler signals needed for local helioseismology. 10 bits compressed to 5, some applications may use only 4.
3. B_{los} the LOS component of the magnetic field. They are basically maps of circular polarization over the observed area. 10 bits compressed to 5, some applications may use only 4.
4. B_{trans} the transverse to the LOS component of the magnetic field. They represent maps of linear polarization. 8 bits compressed to 4.
5. ϕ the azimuth of the transverse component in a plane perpendicular to the LOS. Also obtained from linear polarization measurements. 8 bits compressed to 4.

The final 4/5 bits per pixels estimates provided here, assume a lossless compression scheme with an efficiency of a factor 2. Note that from the original 12 bits, we have first thrown out the 2 to 4 less significant ones. Thus the total reduction factors are between 2 to 3. These compressed estimates have been used in the following description of example observing modes that could produce the desired scientific results from VIM:

Mode 1. Low resolution, high cadence mode: On-chip binning to 512×512 pixels of 1 physical magnitude at a cadence of 1 per minute require a telemetry rate of 22 kbps. This mode can be used for storing V_{los} over the whole FOV at a high cadence adequate for local helioseismology.

Mode 2. Medium resolution, medium cadence mode: Binning to 1024×1024 pixels of 1 physical magnitude at a cadence of 1 every two minutes require a telemetry rate of 44 kbps. This mode can be used for sending I_c , V_{los} or B_{los} for general purposes (e.g., magnetic field evolution).

Mode 3. High resolution, high/medium cadence mode: This mode is similar to the two previous ones but instead of binning pixels, a selection of a subframe (512 or 1024) is done, thus prioritizing spatial resolution at the expenses of FOV and keeping a reasonable cadence.

Mode 4. Photospheric context: In this mode three quantities (B_{los} , B_{trans} and ϕ for vector magnetometry or B_{los} , V_{los} , I_c for dynamical studies) can be sent over the full frame every 5 minutes at a rate of 160 kbps (2K frame and 4 bits per magnitude). The vector magnetometry case enables to follow the evolution of the magnetic field at a sufficiently high cadence adequate for most of the upper atmospheric phenomena.

Modes 1 and 3 have data rates similar to the nominal one 20 kbps. Peak data rates of 3 physical magnitudes over the full frame every minute of 800 kbps (2K frame) must also be considered (with a low duty cycle).

Modes 1 and 2 can be accommodated in different orbits to better achieve the science goals.

VIM DPU Concept

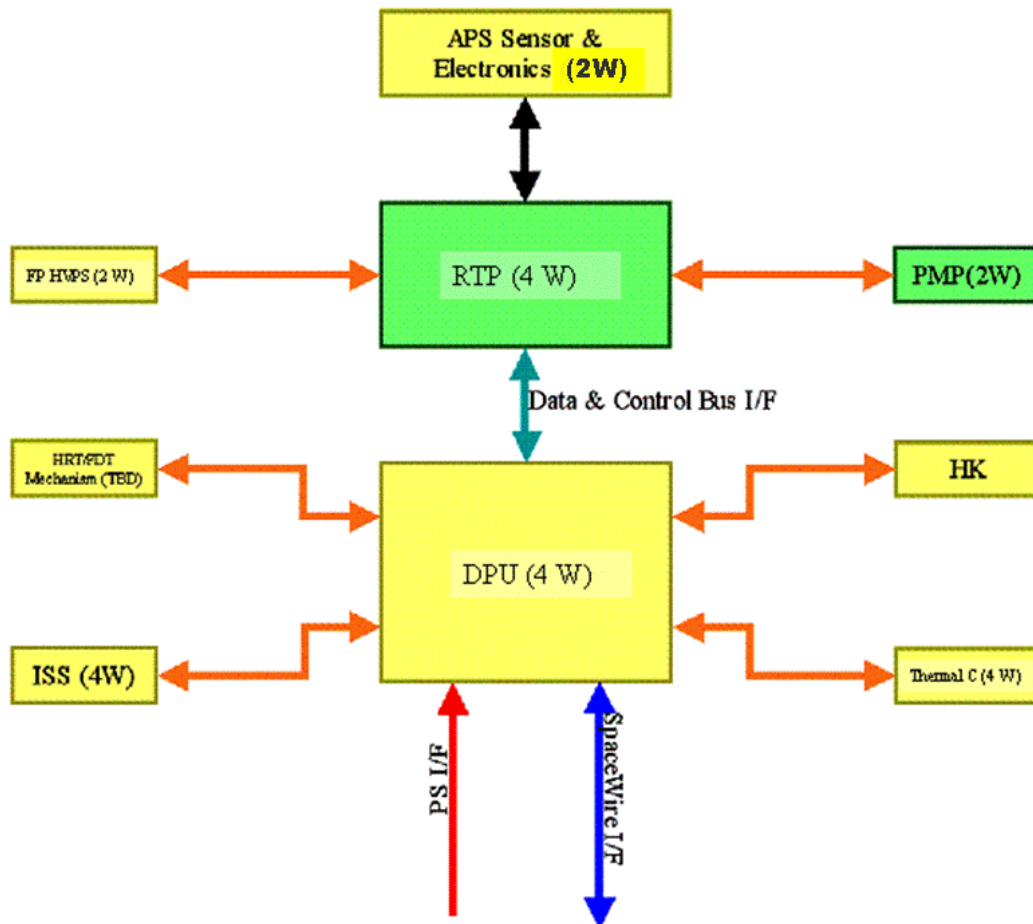


Figure 2.1.7: Schematic of the VIM electronics

Because of the limited telemetry available the instrument must be able to compute physical quantities (magnetic field and velocities) on-board in almost real time. This means that a dedicated DPU unit will be needed for the global control of the instrument as well as a real time processing card (RTP) that consists of a set of FPGA/ASIC components and memory units. The VIM DPU concept is illustrated in Figure 2.1.7.

Allocated mass and power breakdown

Item	Mass (kg)
HRT optics & supports	2.5
FDT optics & supports	1.4
Structure / bench / enclosure	4.5
ISS (tip/tilt + limb sensor unit)	2.0
De-pointing compensation mechanism	0.5
FO optics & supports	1.5
Etalon (incl. Filter & HVPS)	2.5
Focus mechanism	0.5
Detector and related FE electronics	0.3
Thermal subsystem (no entr. Filter)	1.3
Electronics	4
Power Converter Unit	1
VIM cover S/C provided	0
Harness (10%)	2.2
Subtotal	24.3
VIM margin (25%)	6.1
VIM TOTAL	30.4

Unit	Power (W)
APS + electronics	2
Image Stabilisation System	4
Fabry Perot Etalon Oven	1.5
Fabry Perot HV PSU	2
PMP	2
DPU and control electron.	8
Power Converter Unit	1
Thermal subsystem	4
Sub-total	24.5
Margin (25%)	6
Converter losses (>80% eff.)	4.5
VIM TOTAL	35.0

Allocated instrument volume

Similarly to the other RS instruments, VIM has been allocated a maximum length (along +X axis, see section 3) of 100 cm. Based on the spatial resolution requirement of 1 arcsec, and on possible optical design solutions discussed, the VIM envelope fits an overall volume of $80 \times 40 \times 30 \text{ cm}^3$.

3.1.7 Cleanliness, Ground Operations and Other Requirements

Cleanliness requirements.

A similar particulate and chemical contamination plan as followed by the STEREO mission should be adopted (see section XZ). To avoid contamination build-up during operation in orbit, the thermal design of the VIM instruments will ensure that there are no optical surfaces colder than their surroundings. A filter will block the ultraviolet component of the spectrum on a clean, hot surface very early in the optical path. The optical path before this filter will be extremely clean and free of outgassing organic material. The UV filter will block all wavelengths shorter than 360 nm. Since the working passband of the instrument is in the visible, a UV blocking filter at the entrance aperture would be a preferred solution from a cleanliness point of view. A hot telescope with a filter behind the secondary may also be an acceptable solution. In any case, the instrument must be ultimately clean up to this surface, like a solar UV instrument. The filter must be stable against the radiative flux and must be un-polarizing. During all ground operations HRT will be closed by an openable cover (door mechanism) that will allow purging with clean gas.

Operating modes

The VIM instrument will be operating by execution of a limited number of predefined observation sequences to be stored in the DPU. The science modes will define both the instrument operating sequence and the data processing requirements.

3.1.8 Open Points and Critical Issues

1. Thermal concept: the present thermal design is based on a closed system with a heat rejecting window. This has been identified as a critical element since the heat rejection performance of the entrance window will directly impact on the instrument heat load, potentially limiting the maximum aperture size. Moreover, a larger window will have to tolerate larger heat gradients and mechanical loads. The S/C TCS will provide a local environment at room temperature (behind the heat-shield). Heat straps will be connected to different S/C radiators providing heat sinks at different T. A localized heating strategy is proposed to allow for real time alignment of the optical system under different thermal loads. The thermal stability of the lithium niobate solid-state etalons needs to be $\pm 0.025^\circ\text{C}$. A detailed instrument thermal study is required.
2. APS detector: The APS detector is baselined, but significant development is required towards the space qualification of suitable devices (see dedicated section). Detector performance plays a critical role with respect to SNR, thus influencing the final choice of the telescope aperture. Sub-optimal performance would require a larger aperture, with a significant heat load increase.
3. LCVR's and their space qualification: These devices offer a light and low power solution for the VIM PMP. They have been successfully used for ground-based instruments and tested to some degree for space applications. Prototypes have been produced by IAC and an LCD company (Spain) for use in a balloon experiment. Space qualification for the Solar Orbiter case is required.
4. LiNbO₃ etalons: this technology has been used in a variety of instruments for ground applications. MPS (Lindau) is studying their performance for space applications. The LiNbO₃ technology requires space qualification of performance under high particle radiation fluxes and with kilo-volt driving signals. This technology has as main advantage the lack of moving parts combined with finesse

values as high as 30. The high refractive index of the material ($n=2.3$, which simplifies field-of-view problems and has other advantages) is particularly attractive for this mission. LiNbO_3 Fabry-Perots have been used successfully in stratospheric balloon experiments (Flare Genesis). Back-up technologies: PZT spacing controlled Fabry-Perots with flight heritage from the HRDI instrument in the UARS satellite (requiring moving parts) or liquid crystal Fabry-Perots that are under development (in the US) for Earth observing missions.

5. Multilayer coatings: Stability of the coatings for the interference filters and mirrors under high thermal load needs to be verified (e.g. entrance window).

3.2 EUV Spectrometer (EUS)

Spectroscopic observations of emission lines in the UV/EUV region of the electromagnetic spectrum provide important plasma diagnostics of the solar atmosphere, providing the necessary tools for probing the wide range of solar plasma temperatures. These may range from tens of thousands to several million K. The analysis of emission lines, mainly from trace elements in the Sun's atmosphere, provides information on plasma density, temperature, element/ion abundances, flow speeds and the structure and evolution of atmospheric phenomena. Such information provides a foundation for understanding the microphysics behind a large range of solar phenomena.

3.2.1 Scientific Goals

The principal scientific goal of the EUV Spectrometer (EUS) is:

- To determine the plasma density, temperature, element/ion abundances, flow speeds and the structure of the solar atmosphere using spectroscopic observations of emission lines in the UV/EUV.

3.2.2 Instrument concept

The design approach for the EUS instrument is an off-axis normal incidence system (NIS), which fits the spacecraft length requirement of < 1 m class instruments. A single paraboloid primary mirror reflects a portion of the solar image through a heat-stop and slit into a spectrometer, which utilises a toroidal variable line spaced (TVLS) grating in a normal incidence configuration. The solar image is scanned across the spectrometer slit by motions of the primary mirror. The design is stigmatic. The wavelength selections are geared to the bright solar lines in the extreme ultraviolet (EUV) wavelength range, which are emitted by a broad range of plasma temperatures within the solar atmosphere. The instrument structure may be constructed of light-weight CFRP with SiC optical components. Alternatively, the structure and optical components could be SiC, thus avoiding complex thermal control systems. Multilayer coatings will be considered if the final wavelength selection requires it (shorter wavelengths). The extreme thermal situation is recognised and a grazing incidence telescope system is under consideration as a second option; this would ease the thermal control of the instrument, at a cost to the optical performance.

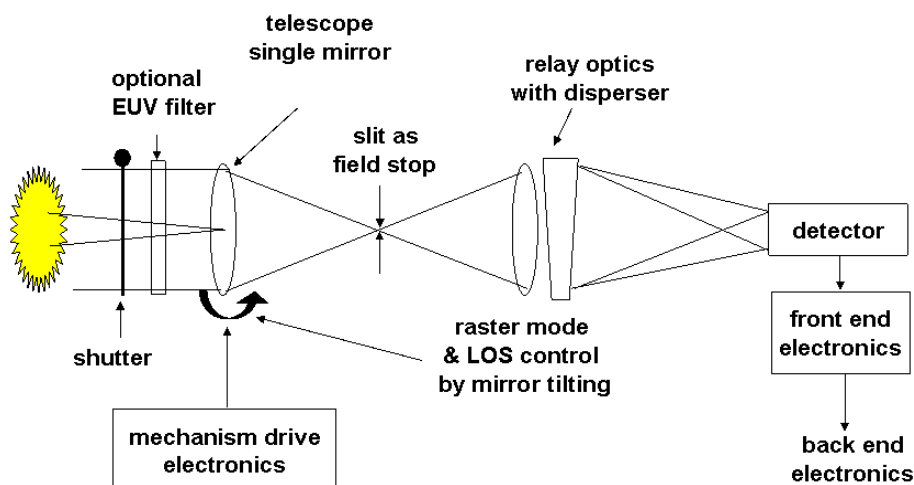


Figure 2.2.1: EUS functional block diagram.

3.2.2.1 Optical configuration

The NIS concept is illustrated in Fig. 2.2.2 below. The instrument aperture stop is the first optical surface, at the front of the instrument, and has a diameter of 70mm. An off-axis parabola primary mirror is used to form an image of the solar disk at the spectrometer entrance slit. The off-axis approach allows us to insert a heat-stop (not shown in the figure) between the primary mirror and the slit. As part of the thermal control strategy, the heat-stop can be used to reflect solar radiation back out of the front of the instrument. Management of the heat arriving at the primary mirror and slit is critical to a successful opto-mechanical and thermal design. The slit presents a selected area of the solar image to the spectrometer. The slit presents a selected area of the solar image to the spectrometer.

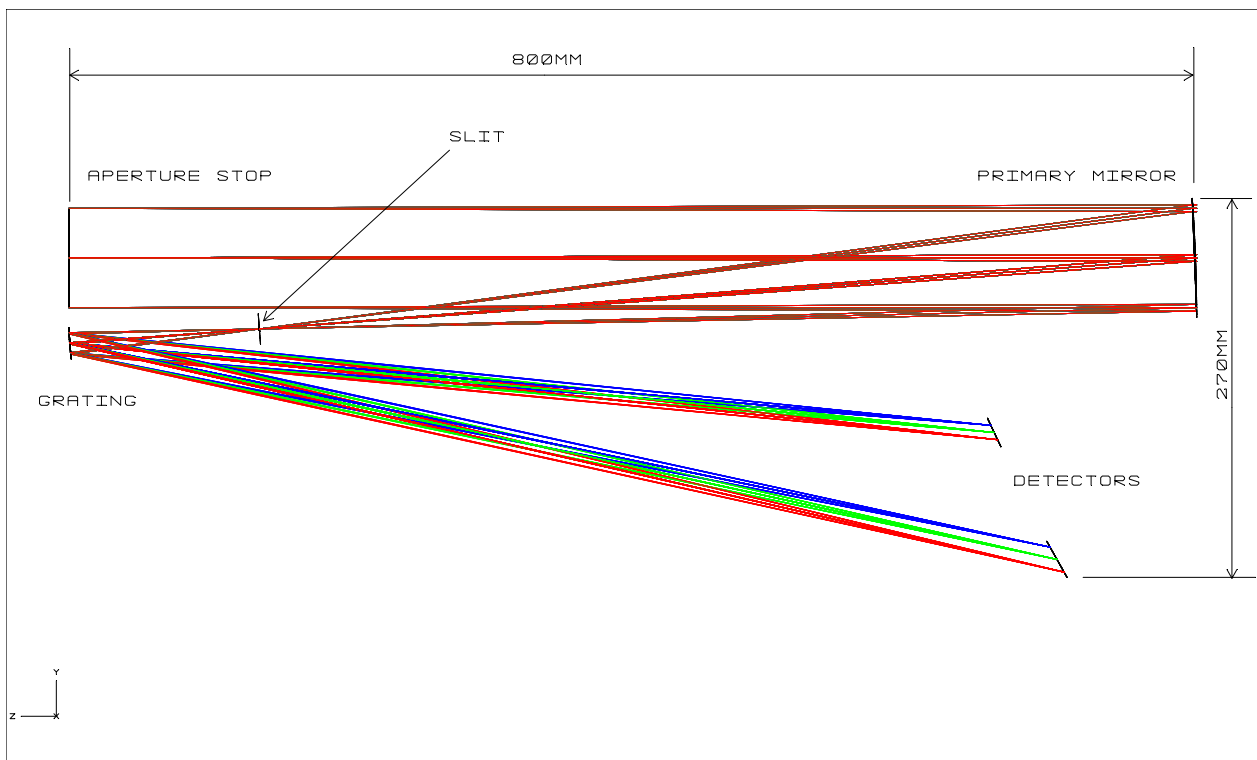


Figure 2.2.2: Optical scheme of the EUS off-axis NIS Concept

The slit assembly lies at the focal plane of the off-axis parabola, and below the heat-stop mentioned above, and beyond this is the spectrometer, with a toroidal variable line spacing (TVLS) grating, forming a focus at a 2-D detector. There is no secondary mirror, as with a Ritchey-Chretien design, for example, and this helps to maintain a reasonable effective area. The TVLS grating approach allows good off-axis performance compared to a uniform grating. It brings the spectrometer 'arm' closer to the axis of the instrument and removes the restriction of a close to unit magnification spectrometer common in other designs, making the envelope smaller.

Figure 2.2.2 illustrates the narrow design of the EUS afforded by the VLS grating and shows the detection of two wavelength ranges through the use of two detectors.

The grating ruling spacing is yet to be decided but values up to 4800 l/mm have been taken as a guide for current design investigations. Several wavelength bands are under consideration, for example, 170-220 Å, 580-630 Å and >912 Å, to obtain spectral information from the corona, transition region and chromosphere,

and we anticipate obtaining one, two or possibly three bands possibly using two orders, a split grating concept (much as is done for CDS/SOHO), or multiple detectors (as in Figure 2.2.2). The 580-630 Å band has been used as the band for design discussions to date. Optimisation of the design is required, but this produces an optical envelope of 80 cm × 27 cm × 7.6 cm leading to a basic physical instrument envelope of 90 cm × 30 cm × 15 cm.

As noted above, the primary mirror presents a portion of the Sun at the slit, and it is this mirror that could be tipped to allow rastered images (*i.e.*, exposures interlaced with mechanism movements to build up images simultaneously in selected wavelengths). Only a small fraction of the solar thermal load will pass through the heat-stop to the slit assembly, possibly of order several hundredths of the disc area.

The pupil diameter of EUS is sized by a combination of the diffraction limit, geometrical aberrations, the heat load and the required light flux. The choice of the sampling resolution needs to take into account the overall instrument radiometric performance, including the actual detector signal-to-noise characteristics.

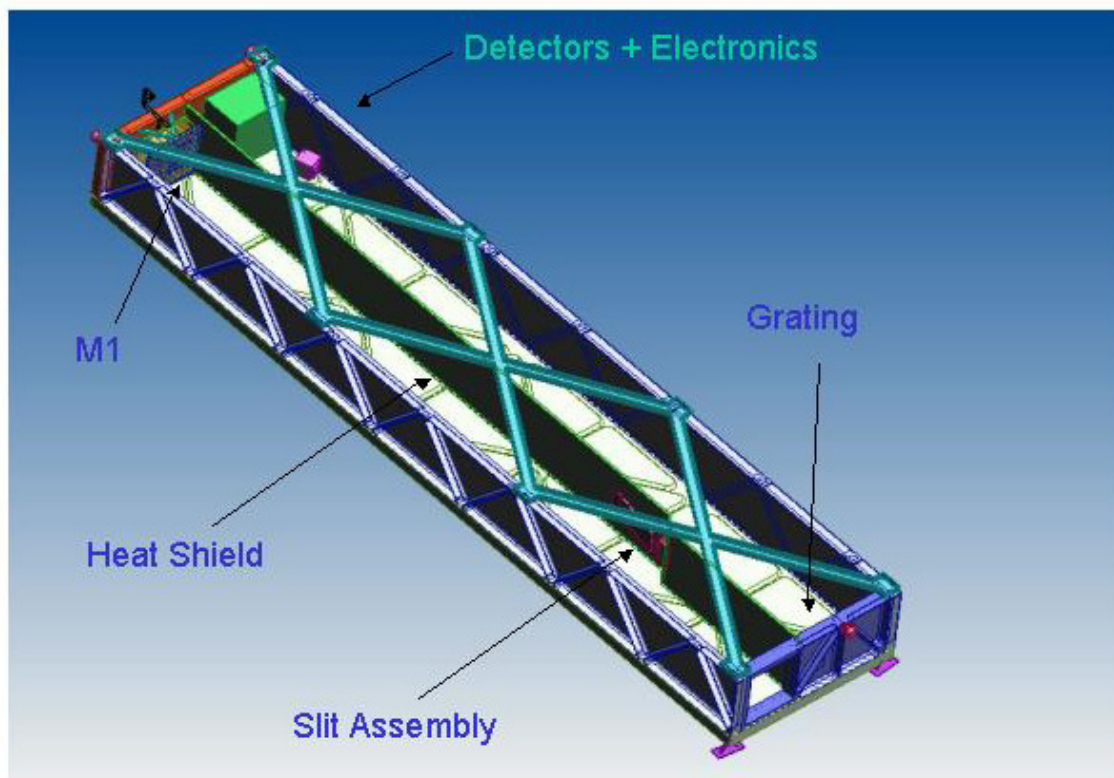


Figure 2.2.3: Possible physical implementation of the EUS telescope.

The design could include a selection of slits, which can be chosen for particular observation programmes. In addition, for simplicity it is assumed that image stabilization will be carried out post-facto by image processing on the ground. Figure 2.2.3 shows a possible physical implementation of the EUS telescope, used for consolidating the instrument mass budget.

The heritage of this instrument concept comes from the SOHO/CDS, SOHO/SUMER and Solar-B/EIS projects.

An alternative design could be based on a grazing incidence concept. This option would make use of the parabolic and hyperbolic mirror reflections of a Wolter II telescope, with light passing into a similar spectrometer to the NIS approach (TVLS grating and APS detector) after reflection in grazing incidence off a plane scan mirror. This concept results in a lower heat power density at the telescope mirrors, which would reduce susceptibility due to polymerization of contaminants on the mirrors, but has poorer optical performance and would probably result in a longer instrument.

3.2.2.2 Thermal design

During the science phase the spacecraft will encounter a thermal load ranging from 2.2 kW/m^2 (at 0.8 AU) to 34.4 kW/m^2 (at 0.2 AU). Careful design will be required to develop a thermal control strategy that will cope with both the wide variation of thermal input and the extremes of the solar encounter.

The industrial study of the Solar Orbiter payload has indicated that the generic strategy for the EUS thermal design should aim to maintain the aperture diameter at no more than 70 mm. The same study calls for adequate baffling and suggests that the instrument could include a novel front-end thin aluminium filter. The aim of the filter is to exclude the extreme thermal input from the optical components completely. It is based on a conductive metallic grid, supporting a thin aluminium foil and connected to radiating fins. It would be part of the spacecraft thermal shield. The adoption of such a filter could greatly simplify the thermal design of EUS as the heat input would be drastically reduced. However, such a filter would considerably reduce the effective area of the instrument and introduce optical effects that must be removed. Whilst this is an option, and should be considered thoroughly, it does introduce a complex component which is a potential single-point failure in extreme conditions. Thus, the baseline is to have an open optical off-axis system

The main heat input to the instrument is via the 70 mm diameter entrance aperture. The solar beam will be incident mostly upon the SiC primary mirror, although a fraction of the load will not strike the mirror. Baffling will be required to absorb or reflect this portion of the solar beam that misses the primary mirror.

The basic thermal design approach is to thermally isolate the instrument from the spacecraft and to separate the spectrometer and the telescope sides of the instrument so that the heat load passed beyond the slit is minimal (see the table). Only a portion of the solar load reflected to the slit will pass through it to the spectrometer. A heat stop fitted around the slit, and separating the two parts of the instrument, will reflect, or possibly absorb, the excess solar load. Ideally this solar load should be reflected out of the instrument, either directly out of the front aperture or via reflection off the primary mirror. The approach adopted may have some bearing on the design of the baffles.

The APS detector system (see below) should run at approximately $-80 \text{ }^\circ\text{C}$. Thermal loads will be minimized by mounting the camera systems on low conductance legs within an enclosure that is radiatively isolated from the instrument. Radiative isolation may be achieved using multi-layer insulation. Cooling will be via a cold finger connection to a spacecraft cold sink. The use of such an enclosure means that there is little difference in terms of thermal design and loads between the use of one or two APS detectors.

3.2.2.3 Resolution/detector

A detector array of $2 \times 2 \text{ k}$, $10 \text{ } \mu\text{m}$ pixels is baselined. Thus, the EUS has a spectral range of 4 nm at 0.002 nm/pixel. The same array will give a spatial extent (vertical distance on the detector = slit length) of $1.0 \text{ arcsec} \times 2048 = 34 \text{ arcmin}$. For a given pointing location (spacecraft pointing), rastered imaging will be

made up from movement in one direction of the primary mirror or the plane mirror, depending on the selected approach.

The choice of detector is dictated by the harsh particle environment, which will be encountered by Solar Orbiter close to the Sun, as well as mass and power constraints. The near solar environment has been investigated and careful consideration of the effects of solar neutrons, and particle storms have to be made. At present APS are baselined as the primary detectors in view of their radiation hardness. In addition the on-chip electronics ensures mass savings and leads to power savings relative to traditional CCD approaches.

Whilst the development of suitable APS devices is well under way, we note that the final wavelength selection may require different detector approaches for different bands. If a long wavelength band is selected, above 700 Angstrom, we cannot use an aluminium filter. This means that whereas for the shorter bands we would use a back thinned APS device with a filter, the long wavelength band would require an APS device with a MicroChannel Plate (MCP). This is proven technology.

2.2.2.5 Instrument count rates

In order to fulfill the science objectives of EUS it is essential that the instrument design yields sufficient count rates in key emission lines to accurately determine intensities and velocities in timescales on which the solar plasma changes (≤ 10 secs). Considering the normal incidence telescope option, the instrument throughput depends on the collecting area of the telescope, the optical surface coatings, the grating efficiency, the type of detector, and any filters in the optical path. The choices for each of these depend on the wavelength ranges considered, and we identify four design options below according to which wavelength bands they cover, either S (170-210 Å), M (580-630 Å) or L (970-1040 Å).

1. S & M: multilayer coating on the mirror and grating; a back-thinned APS detector
2. M only: SiC coating on the mirror and grating; a back-thinned APS detector
3. M & L: SiC coating on the mirror and grating; a MCP with KBr coating for the detector
4. S, M & L: hybrid design with a multilayer coating on the mirror and grating; a UV sensitive APS detector for short and medium bands, and a MCP for the long wavelength band

The multilayer coating is chosen to give high efficiency at short wavelengths, and also moderate efficiency at longer wavelengths beyond 400 Å. The microchannel plate (MCP) can be mated to a standard APS detector via a phosphor screen and fibre-optic cables. The back-thinned APS detector requires an aluminium filter to make it visibly blind. A telescope area of $(70 \text{ mm})^2$ is assumed.

The Table below presents expected count rates for the four design options. Average quiet Sun intensities are obtained from previous solar missions. Actual measured count rates, scaled to 1 arcsec pixel size, from SOHO/CDS for two lines are also presented. Note that the count rates for Fe IX 171 and Fe XII 195 assume the lines are found at the top of the multilayer efficiency curve. A multilayer tuned to 195 will give much lower ($>$ factor 10) counts at 171, and vice versa.

Line	QS intensity (erg/cm ² /s/sr)	Design 1	Design 2	Design 3	Design 4	CDS (measured)
Fe IX 171	758	87	-	-	87	-
Fe XII 195	718	73	-	-	73	-
Mg X 624	40	1.6	12	38	1.6	0.3
O V 629	400	20	109	382	20	2.8

C III 977	963	-	-	2475	122	-
O VI 1032	305	-	-	828	41	-

A lower limit for measuring the intensity and centroid of an emission line is around 100 counts, and these counts should be accumulated in < 10 secs, thus the values given above for the 4 designs all fall within these criteria, except for Mg X 624. This line, however, will be much stronger in active solar conditions.

3.2.3 Orbit, Operations and Pointing Requirements

Given the 1.0 arcsec resolution requirement, two options can be considered to maintain the pointing stability:

- Include an image stabilisation system, possibly making use of VIM limb sensor error signals.
- Do not include an image stabilisation system, assuming that the variations of the spacecraft stability occur on timescales much less than the exposure time of the spectrometer and thus any corrections could be done on the ground;

For the reference instrument design, the latter approach is assumed, since the alternative solution would increase the development risks and resource demands.

The EUS instrument would not require an independent pointing system. The required co-alignment accuracy between instruments is 2 arcmin, based on attaining a reasonable image overlap with the smallest instrument field of view. In addition, in operation, a pointing accuracy of 2 arcmin is required. Fine pointing within the field of view of EUS can be achieved using the mirror mechanism, and stability will be achieved *post-facto* based on the ground analysis of the data.

It is envisioned that operations will be performed in pre-planned sequences and time-tagged in a deferred command store. The sequences will have been selected during the period preceding the solar encounter. The planning and the selection of sequences will be done in concert with the other remote-sensing instruments.

3.2.4 Calibration

The interpretation of spectral emission line intensities, for the production of plasma diagnostic information, requires good instrument calibration. This will be done on the ground and in flight using the following methods, which are used for the SOHO mission with success. A hollow cathode source, calibrated against a storage ring (e.g. BESSY) will be used to illuminate the instrument prior to launch to view lines of known intensity. In flight monitoring of solar quiet-Sun emission line intensities using regular 'spectral atlas' measurements will be used to monitor the instrument performance and cross calibration of intensities against similar lines observed from rocket flights can be used as bench marks. The rocket instruments can be calibrated against the same hollow cathode source. Rocket payloads such as the Goddard Space Flight Center EUNIS experiment, or the Montana MOSES instrument, are appropriate and may be in operation at the appropriate time. Members of the potential consortium are co-investigators of the EUNIS and MOSES instruments.

3.2.5 Accommodation

The EUS instrument requires being Sun pointed. It will be hard-mounted on the spacecraft, behind the heat shield, along with the other remote-sensing instruments. The instrument should be mounted on legs with vents for out-gassing facing the side or back of the instrument. The mount will be on low conductance legs to ensure thermal isolation. A door is required, which can be operated as required throughout the mission, and radiators will be required, in particular for the primary mirror and the detector(s). The assumption here is that

the door and radiators are provided by the spacecraft. It is essential that the EUS slit be aligned in a solar north-south direction (as is done for the SOHO spectrometers) to ensure that in the case of a mechanism failure the rotation of the Sun can be used to construct images.

3.2.6 Interface and Physical Resource Requirements

Telemetry – data compression

The reference average telemetry rate for the EUS instrument is 17 kbps during full operations windows. The full EUS detector image is $2k \times 2k$ pixels. At 12 bits per pixel, it would take 49 min to transmit one exposure without any compression or data selection (at 17 kbps). Since each exposure will form part of a raster, the raster cadence will be significantly longer. Studies from instruments such as CDS/SOHO have shown that careful line selection is far more important than data compression in managing the data return of such a spectrometer. Much of the spectrum is not required. Indeed, specific emission lines are required. A good rule of thumb is that a selection of between 6 and 15 lines is good for most scientific purposes. The particular selection of lines at any time will depend on the specific objective of the current operation and, in addition, the area to be rastered over is subject to the specific scientific application.

The EUS nominal resolving element is 1.0 arcsec along a 34 arcmin slit (2k pixels, with 1.0 arcsec/pixel). The nominal spectral resolution is of order 0.002 nm/pixel. To obtain full line widths for million K lines, plus sufficient nearby background, one would want to return about 0.3 Å, *i.e.* 15 pixels.

The Table shows a selection of potential cases. In each case, a number of required lines is defined as is a selected length along the slit (spatial direction). The spatial length is given in pixels because of the varying distance to the Sun. The time to transmit such an exposure is given with a stated compression factor. The rastered image cadence is then given for four cases. We assume a return of 15 pixels across each line and 12 bit words.

No. of lines	Spatial length along slit (pixels)	Compression factor	Time to transmit exposure (seconds)	Cadences for rasters of 50 arcsec, 200 arcsec, 500 arcsec, 2000 arcsec (minutes)			
				50 arcsec	200 arcsec	500 arcsec	2000 arcsec
6	50	3	1.06	0.9	3.5	8.8	35
6	500	3	10.6	8.8	35	88	353
6	500	10	1.06	0.9	3.5	8.8	35
6	1000	3	21.2	17.6	70	176	706
15	100	3	5.3	4.4	17.7	44	177
15	2000	10	31.8	26.4	106	264	1059

The table assumes 17 kbit/s. Any increase in telemetry allocation will provide significant improvement to the scientific return. However, rastered image sequences with cadences of minutes or less can be obtained depending on the number of lines required and the area over which to raster. Concerning compression factors, it should be noted that by returning line profile parameters rather than the 15 pixels assumed here (*i.e.* line width, intensity and location only) or only returning, say, every third pixel in wavelength space (which may be sufficient for some profile needs) it is possible to achieve compression factors equivalent to 10 or even more. Other compression/selection options include returning image differences.

Given careful data selection and compression, the figures demonstrate that the operation of an EUS instrument is feasible with the 17 kbit/s telemetry allocation, allowing operations such as small area, rapid rasters (*e.g.* to look for small-scale fundamental events in the atmosphere, such as blinkers), spectral atlas observations (*e.g.* studies aimed at detailed emission line identification and monitoring), and single-slit observations (*i.e.* no rastering observations such as those used to look for small-scale velocity events), and options exist to cater for more extreme requirements.

We note that the limitation here is the telemetry allocation, which is based on the spacecraft memory and assumed one ground station. We do have the option to use a ‘burst mode’, *i.e.* accept that we can run a far higher cadence rate but for a limited time, until the memory allocation is full. For particular scientific studies this would be the preferred option for some of the solar encounter periods.

Allocated Mass and power breakdown

The instrument mass breakdown is given in the table. Given the fact that there are two design concepts still under discussion and that the optical designs and thermal designs need considerable optimisation, the mass estimates are necessarily preliminary.

	Mass (kg)	Unit	Power (W)
Primary mirror	0.3	APS+electronics	4
Mirror support	0.2	Scan mechanisms	2
Mirror scan mechanism	0.5	DPU and control electron.	16
Slit assembly	0.3	Thermal subsystem	8
Grating assembly	0.4	Sub-total	20
Detector (including FEE)	0.5	Margin (25%)	5
Structure, cover & baffles	4.7	EUS TOTAL	35
Thermal subsystem	1.3		
Electronics	3.5		
Power converter	1.0		
Harness (10%)	1.3		
Total nominal mass	14.4		
EUS margin (25%)	3.6		
EUS TOTAL	18.0		

Allocated instrument volume

Similarly to the other RS instruments, EUS has been allocated a maximum length (side parallel to the Sun direction) of 100 cm. Based on the spatial resolution requirement of 1 arcsec, and on possible optical design solutions discussed, the EUS envelope fits an overall volume of $90 \times 30 \times 15 \text{ cm}^3$.

3.2.7 Cleanliness, Ground Operations and Other Requirements

Cleanliness and Contamination

A similar particulate and chemical contamination plan as followed by the SOHO/CDS mission should be adopted.

3.2.8 Open Points and Critical Issues

There are a number of critical issues for the EUS and these are issues, which are in common with other instruments:

1. **Detector Development:** The APS detector is baselined, and considerable development work has taken place. However, some effort is required towards the space qualification of suitable devices. Operating temperatures ~ -80 deg C will require the use of a dedicated cooling system for each sensor.
2. **Thermal Control/Design:** The thermal design of the EUS requires further consolidation. Final APS operating temperature is to be fully established and may be significantly colder than -80 deg C to achieve the necessary SNR performance. The thermal strategy needs considerable discussion between ESTEC and the proposing teams; the spacecraft thermal strategy has a very significant impact on the instrument designs.
3. **Thin heat rejection filter:** A front-end filter is considered to be risky and has an impact on the scientific performance. Whilst the thermal strategy and detector blindness must be catered for fully, such an option should be kept in mind.
4. **Contamination/Degradation of Optical Surfaces:** The harsh particle and thermal environment may have detrimental effects on optical surfaces, in particular multilayer coatings, other optical coatings and filters (which should be avoided if possible). Although much information has been acquired, it has been recommended that tests be made to understand the effects on specific surfaces.
5. **Telemetry:** The telemetry allocation is very restricting and requires very careful data selection and significant compression. Whilst the instrument can satisfy the scientific requirements, the increase in performance has been well demonstrated for any increase in the telemetry rate.

3.3 EUV Imager (EUI)

Observations from Yohkoh, SOHO and TRACE in the extreme ultraviolet and soft X-ray wavelengths have revealed a truly complex, highly dynamic solar atmosphere with magnetic loops confining plasmas at widely varying temperatures. The TRACE EUV observations in particular, illustrate the existence of fine-scale structures in coronal loops and reveal continuous dynamic activity at the smallest scales. In the quiet Sun, various "events" of different sizes (*e.g.*, bright points, explosive events, jets, blinkers) all provide evidence for small-scale heating and morphological reorganization, probably related to magnetic reconnection. The observed distribution functions have self-similarity properties, which point at sub-resolution processes. The results from Yohkoh, SOHO, and TRACE led to new questions concerning the basic dimensions of coronal structures, the role played by nanoflares in the heating of the quiet solar corona and the structuring of the corona above the poles.

3.3.1 Scientific Goals

The principal scientific goals of the EUV Imager (EUI) are:

- To provide EUV images with at least a factor 2 higher spatial resolution than currently available, in order to reveal the fine-scale structure of coronal features;
- To provide full-disc EUV images of the Sun in order to reveal the global structure and irradiance of inaccessible regions such as the "far side" of the Sun and the polar regions;
- To study the connection between *in-situ* and remote-sensing observations.

3.3.2 Instrument Concept

A reference instrument design has been defined which would deliver the required scientific performance within the allocated spacecraft resources. It is not proposed that other instrument concepts that fulfill (or even improve) the scientific goals should be precluded however adherence to spacecraft resources such as mass, power, telemetry and heat load is essential. This section will describe the instrument concept that has been studied to date.

A single telescope design, providing both high spatial resolution and a full disc field-of-view, would pose very challenging technical problems. This consideration led to a separation of the EUI into two instruments (the High Resolution Imager (HRI) and the Full Sun Imager (FSI)) sharing a common digital electronics unit.

A High Resolution Imager (HRI) would comprise up to three telescopes operating in different wavelength bands. However, based on the Science Requirements Document, the third wavelength is not required and therefore must be considered as optional, depending on the availability of resources. It is vital for the imagers to observe both the quiet Sun network regions and the coronal loops. The wavelength choices for the reference design were 30.4, 17.1 and 13.3 nm covering temperatures from 5×10^4 K to 1.6×10^7 K.

A Full Sun Imager (FSI) is based on a single telescope concept. This will provide a global insight into changes in the solar atmosphere and in addition will provide context information for other instruments. The operating wavelength for the reference design is TBD in the range 13.3 - 30.4 nm.

The relative fields of view and pixel sizes of the reference instruments are given in the table below:

Parameter	HRI	FSI
Field of View	1000 arc sec	5.4 degrees
Number of pixels in image	2k × 2k	2k × 2k
Pixel size (arc sec)	0.5	9
Pixel size (km at 0.22AU)	80	1450

High Resolution Imager (HRI)

A functional diagram of a telescope is given in Fig. 2.3.1. Different multilayer mirrors are used to select up to three reference wavelength bands which avoids the need for a mechanism and permits simultaneous measurement at all three wavelengths. Solar heat input is limited by the size of the entrance aperture (typically 2 cm diameter). Internal scattering is limited through the use of a forward baffle and field stop. An APS detector array is baselined which will have the necessary radiation tolerance. An off-axis Gregorian design has been chosen for the optics. A thin metal foil entrance filter before the first mirror rejects heat and visible radiation.

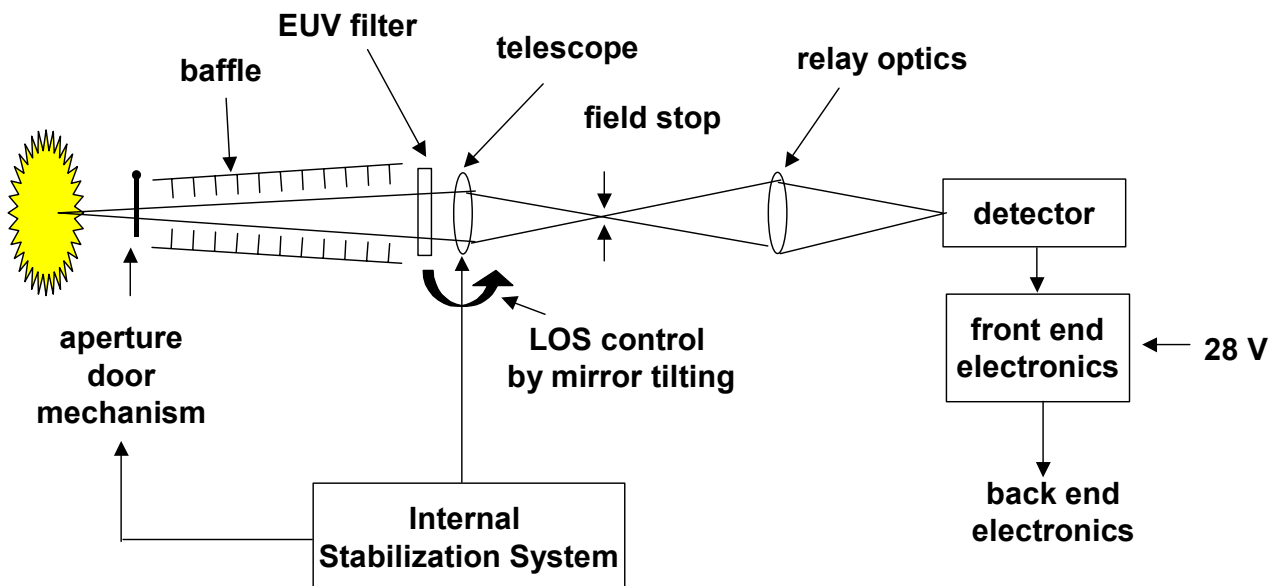


Figure 2.3.1: EUI functional block diagram. The need for an Internal Stabilisation System is to be confirmed.

Figure 2.3.2 shows the optical scheme for the HRI. Up to three telescopes working at 30.4, 17.4 and 13.3 nm are baselined. These wavelengths cover a very wide range of temperatures (from 5×10^4 K up to 1.6×10^7 K) and targets (from quiet Sun to flares). For instance the 13.3 nm band includes a very hot line (Fe XXIII), visible only during flares.

Each telescope is based on an off-axis Gregory design and uses a long baffle to reduce the FOV and the straylight. An entrance filter based on a thin metallic foil is used to reject heat, while the optical elements have multilayer coatings, each optimised for a wavelength band. The Gregory concept allows the placing of stops at the primary focal plane and at the image of the entrance aperture, leading to a significant reduction of straylight.

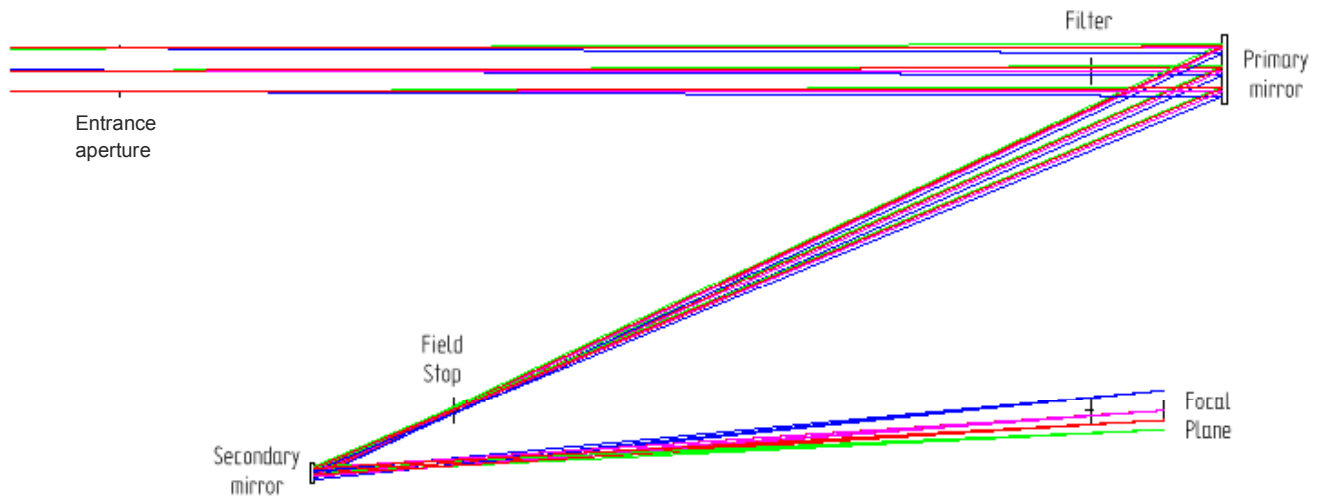


Figure 2.3.2: The HRI optical path showing its basic components. Note the position of the filter is nominal since it can be positioned elsewhere in the optical path.

A carbon-carbon or ceramic structure is planned. It is recommended to use the same material for mirror and structure in order to get a homothetic deformation under heat loads. A possible physical implementation of the HRI with three telescopes and employing a common optical bench is shown in Fig. 2.3.3.

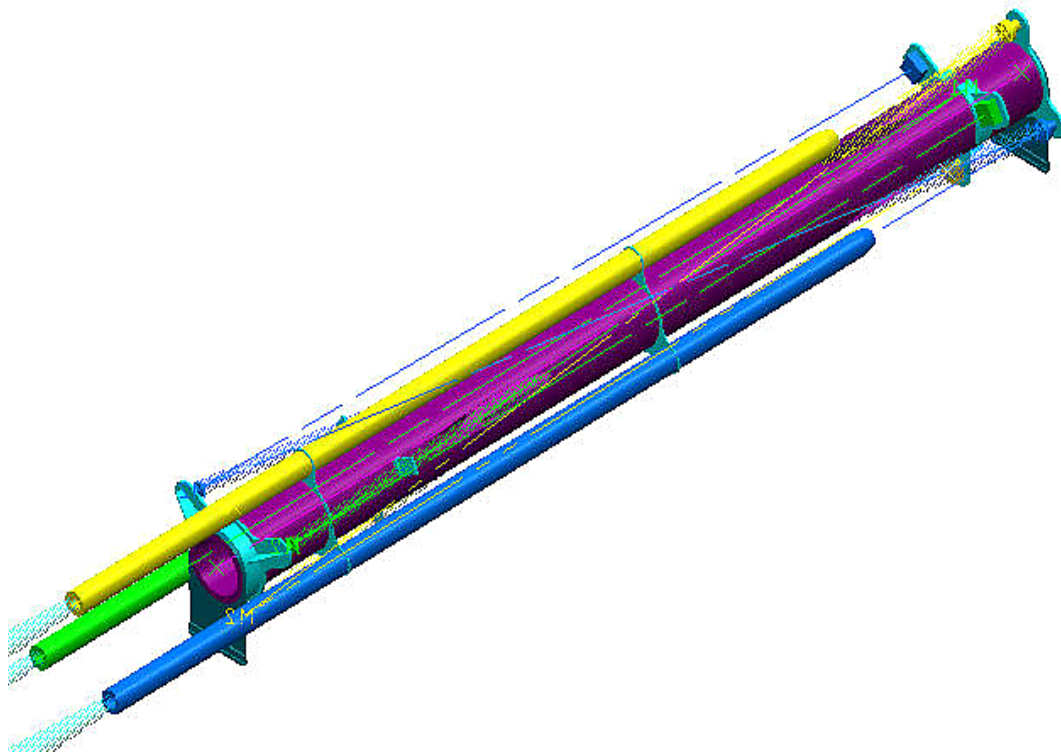


Figure 2.3.3: Possible physical implementation of the three HRI telescopes.

Full Sun Imager (FSI)

The 5.4° field of view will cover the full sun at perihelion with a 50% margin on either direction, accounting for S/C off-pointing capabilities. Solar heat load is reduced by limiting the aperture to a maximum of 2 cm diameter. An off-axis Gregorian optical systems (see figure 2.3.4) reduces the field curvature aberration with the large field of view. This provides an RMS spot diameter less than 9 microns, compatible with typical detector pixel sizes. Figure 2.3.5 shows a possible physical implementation.

As with HRI, a front baffle is used to protect the metal foil filter from the full Solar heat load.

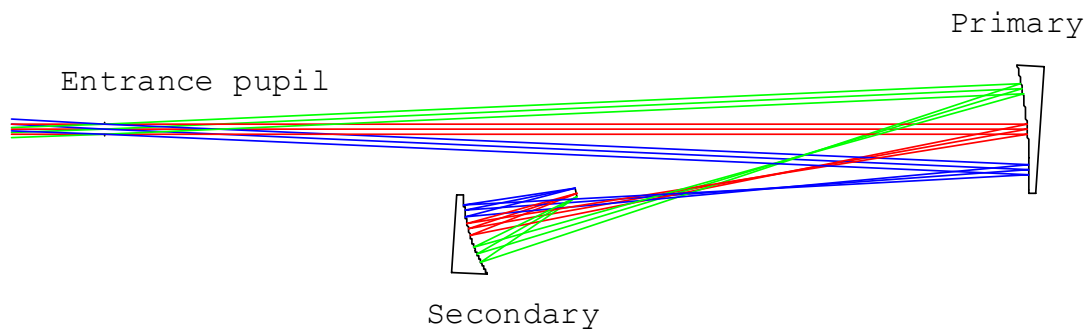


Figure 2.3.4: The Full Sun Imager (FSI) optical scheme.

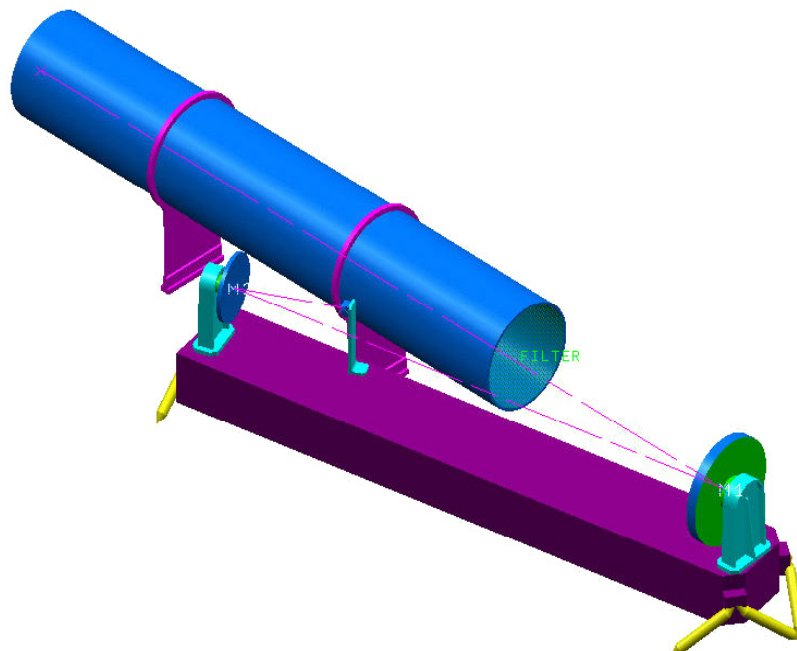


Figure 2.3.5: Possible physical implementation of the Full Sun Image (FSI) instrument.

HRI and FSI resolutions / detectors

At present $2k \times 2k$ array, 8-10 μm pixel APS detectors are baselined for both HRI and FSI. The choice of detector is dictated by the harsh particle environment, mass and power constraints, and recognises the advantages of a common detector concept for both instruments. APS EUV sensitivities are similar to those found in back-thinned CCDs, the technologies being similar in this context. Each detector array will have a

dedicated front-end electronic readout. The back-end electronics (including the DPU) is common to the three detectors and to the FSI telescope.

The FOV of HRI is set to 1000 arcsec with a pixel size of 0.5 arcsec. The pupil diameter of EUI is not sized by the diffraction but by the required light flux. The choice of the sampling resolution (presently assumed to be 0.5 arcsec/pixel) needs to take into account the overall instrument radiometric performance, including the actual detector S/N characteristics. Radiometric budget considerations may lead to a larger sampling resolution (e.g. 1 arcsec/pixel).

The FOV of FSI is set to 5.4 deg. This corresponds to an equivalent pixel size of 9 arcsec (1450 km on Sun at minimum perihelion).

3.3.3 Orbit, Operations and Pointing Requirements

HRI stability/pointing

The stability of the spacecraft platform will be at worst 1" over a 10 second period. Methods will have to be considered to maintain the spatial resolution of the instrument. One method can be to reduce the integration time, another to use a fiducial signal (e.g. from VIM or an internal system within EUI), or to attempt to deconvolve the blurring due to image drift on the ground. It is preferred to avoid the complexity of an image stabilization system within the instrument.

3.3.4 Calibration

The calibration requirements are TBD. However the instrument team will be expected to commission a well-calibrated instrument, and to identify procedures for ongoing calibration throughout the mission. This will require a combination of pre-launch and post-launch calibrations.

3.3.5 Accommodation

The instrument should be co-aligned with S/C and other instruments to within 2 arcmin. Common wavelengths between the RS instruments (EUS, COR) would be an advantage for radiometric cross-calibrations. EUI has been allocated a maximum length (side parallel to the Sun direction) of 100 cm. Based on the reference design, the FSI fits within an envelope of $95 \times 25 \times 20 \text{ cm}^3$ and each HRI within an envelope of $90 \times 10 \times 15 \text{ cm}^3$.

3.3.6 Interface and Physical Resource Requirements

HRI telemetry

Observation cadences of 10 seconds are envisaged to provide sufficient signal-to-noise in the data. Actual observation sequences will be specific to individual science targets/goals and will need to accommodate the limited telemetry available. While the instrument itself has the potential for many Mbps, only an average of 20 kbps is available to the EUI for transmission to the Earth. Short-term high data rates from the EUI will need to be buffered either within the instrument or at spacecraft level (TBD). To manage the above one of the following options will be necessary to implement for some observations:

- Non-simultaneous observations with two HRI telescopes (a third telescope is optional)
- Lossy data compression
- On-board analysis

- On-board target selection

FSI telemetry

An average rate of 0.5 kb/s is sufficient to transmit one compressed full Sun image every 4800 s (about every hour and 20 minutes).

HRI and FSI mass budget

The overall HRI and FSI mass budget is given in Table 2.3.1 assuming 3 HRI telescopes (TBC). A further breakdown (mass of each unit/element) is required.

Component	Mass (kg)
FSI Structure / mirrors (including the baffle)	3.6
Detector (including FE electronics)	0.3
Thermal control HW	0.3
FSI total (without margin)	4.2
FSI with 25% margin	5.3
HRI Structure / mirrors (3×, including baffle)	4.1
Detectors (3×, including FE electronics)	1.0
Thermal control HW	0.7
HRI Total (3 telescopes – no margins)	5.8
HRI with 25% margins	7.5
Common enclosure	1.0
Enclosure with 25% margins	1.3
Electronics shared between the 4 telescopes	4.0
Power converter	1.0
Electronics with 25% margin	6.3
Total for the EUI (with margins)	20.4

Table 2.3.1: Mass breakdown of EUI (assuming 3 HRI telescopes)

HRI power budget

The power consumption has been estimated for the detector and electronics. For a given telescope, a constant power of about 4 W is anticipated for the cycling (power on, integration, dump to memory). With reasonable margins and the required power for pointing, the total is 5 W. If the three (TBC) telescopes are working simultaneously, they will consume about 15 W for basic functions to which one has to add about 7 W for data compression and dumping by the common DPU. The maximum power consumption is estimated at 22 W. Non-simultaneous (sequential) observations will lead to smaller power consumption.

FSI power budget

Power is only required for the detector (3 W), since the electronics is common with HRI.

Unit	Power (W)
3× HRI (4W)	12
1× FSI	3
DPU and control electronics	7
Sub-total	22
Margin (25%)	6
EUI TOTAL	28

3.3.7 Cleanliness, Ground Operations and Other Requirements

A similar particulate and chemical contamination plan as followed by the STEREO mission should be adopted.

3.3.8 Open Points and Critical Issues

1. APS detectors: The baseline design relies on the use of APS as the active sensors. Operating temperatures below ~ -60 deg C will require the use of a dedicated Peltier cooling system for each sensor, with a corresponding impact on the power budget.
2. Telemetry: The telemetry allocation is very restricting and requires very careful data selection and significant compression.
3. Thin heat rejection filter: ageing of the metal foil filters under 25 solar constants is a concern. Qualification tests are required including mechanical behaviour of the foil filter under vibrations and venting launch environment.
4. Internal Stabilisation System: if required, ISS strategy and implementation needs to be defined.
5. Development risk: The allocated resources favour a 2 HRI plus 1 FSI implementation rather than a 3 HRI plus 1 FSI instrument. It should be pointed out that a third wavelength is not required in the Science Requirements Document and would significantly increase the overall development risk due to the resource constraints.

3.4 Coronagraph (COR)

Co-rotation, during the helio-synchronous phases of the orbit, will freeze coronal structures in the plane of the sky for many days. This will allow us to investigate the evolution of the magnetic configuration of streamers to test the hypothesis of magnetic reconnection as one of the main processes leading to the formation of the slow solar wind. The out-of-ecliptic vantage point will also allow a unique view of the plasma distribution and solar wind expansion in the coronal low-latitude/equatorial belt. Therefore, it will be possible to measure the longitudinal extent of coronal streamers and coronal mass ejections. These parameters, that at present are unknown, are essential to determining the magnetic flux carried by plasmoids and coronal mass ejections in the heliosphere.

A third scientific question addressed by COR will be the large-scale structure of the F-corona (the dust) and the detection of the cometary sources of the dust near the Sun. The total brightness detected by a white-light coronagraph is a convolution of the K-corona (the "true" corona, caused by electron Thomson scattering of photospheric radiation) and the F-corona (the dust). These components can be separated by polarization techniques, and this will provide important information for the *in-situ* instruments in the payload that measure plasma and dust.

COR is designed to primarily measure the polarized brightness (pB) of the visible-light K-corona. From this measurement the coronal electron density can be derived.

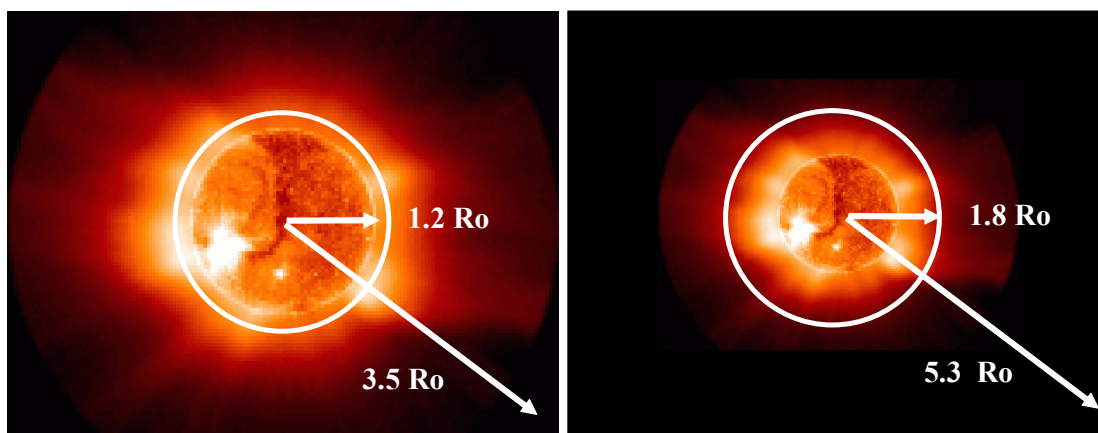


Figure 2.4.1: (Left) Field-of-view of COR at 0.21 A.U. (Right) Field-of-view of COR at 0.3 A.U.

3.4.1 Scientific Goals

The principal scientific goals of the Coronagraph (COR) are:

- To investigate the evolution of the magnetic configuration of streamers in order to test the hypothesis of magnetic reconnection as one of the main processes leading to the formation of the slow solar wind during the quasi helio-synchronous phases of the orbit;

- To measure the longitudinal extent of coronal streamers and coronal mass ejections from an out-of-ecliptic advantage point. These data are essential to determine the magnetic flux carried by plasmoids and coronal mass ejections in the heliosphere;
- To investigate the large-scale structure of the F-corona (the dust) and the cometary sources of the dust near the Sun. This will provide important information for the in-situ instruments in the payload that measure plasma and dust.

Additional goals that could be achieved if sufficient resources are available are:

- To acquire narrow-band images of UV, and as a high-priority augmentation EUV, line emission from the most abundant coronal elements: hydrogen and helium. Helium, the second largest contributor to the density of coronal plasma, is important for the dynamics of solar wind, and it may act as a regulator to maintain a nearly constant solar wind mass flux;
- To determine the differential outflow speed of the major components (H, and optionally He) of the solar wind and discriminate the mechanisms of solar wind acceleration.

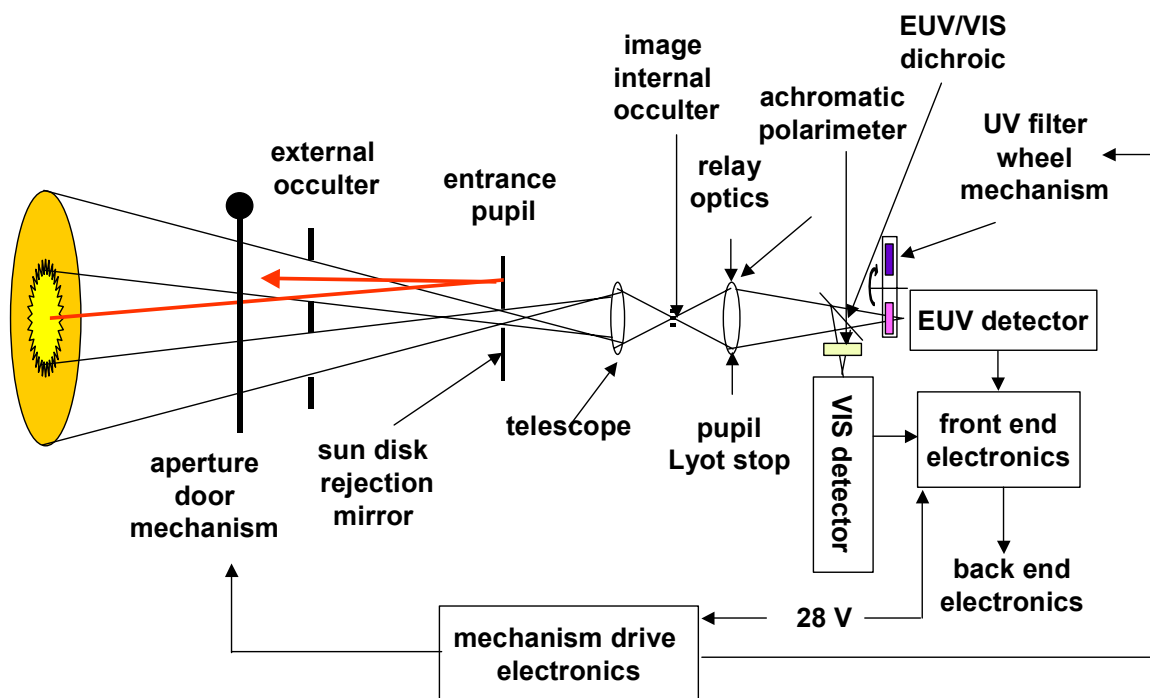


Figure 2.4.2: Functional block diagram of the Coronagraph (including optional EUV channel).

3.4.2 Instrument concept

COR is an externally occulted telescope designed for broad-band polarisation imaging of the visible K-corona and for narrow-band imaging of the UV corona in the H I Lyman- α , 121.6 nm, line in an annular field of view between 1.2 and 3.5 solar radii, when the Solar Orbiter perihelion is 0.22 AU. The design described here also includes an EUV channel, but it is understood that this is not required to satisfy the baseline mission scientific objectives as specified in [RD1]. When at 0.3 AU, the COR field-of-view is within 1.8 and

5.3 solar radii (*c.f.*, Fig. 2.4.1). The telescope optical configuration is an off-axis Gregorian. The UV Lyman- α line is separated with multilayer mirror coatings and (optionally) EUV transmission filters. These mirrors could have coatings optimized for 30.4 nm but still have good reflectivities at 121.6 nm and in the visible. The visible light channel includes an achromatic polarimeter, based on electro-optically modulated liquid crystals.

Optical design - telescope

A functional block diagram of the optical system is shown in Fig. 2.4.2 and a diagram of the optical paths given in Fig. 2.4.3. The external occulter ensures both thermal protection for the optics and better stray-light rejection. A Gregorian telescope design has been chosen because it gives real images of the external occulter and the edges of the telescope primary mirror (see Fig. 2.4.3). A Sun-disk rejection mirror reflects back through the front aperture the disk light. On this mirror, there is a hole, in the shadow of the external occulter. This hole is the entrance aperture through which the coronal light passes to be collected by the primary mirror of the telescope. A light trap behind the secondary mirror ensures that only the light reflected by the mirror enters the filters and detector assembly structure.

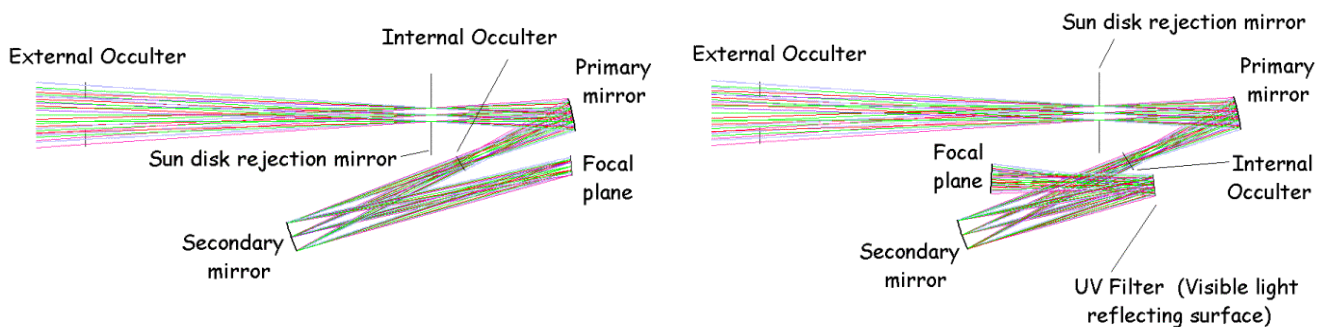


Figure 2.4.3: Concept optical layout of COR for visible light (right) and for optional UV (left).

This “Lyot” trap will be used to reduce stray light and diffracted radiation from the entrance aperture on the disk-light rejection mirror. The direct light from the solar disc is mostly rejected to space, though a portion of it may be used for radiometry and / or coarse imaging of the solar disc in the three wavelength bandpasses.

Visible-Light and UV Channels

The instrument structure is made of carbon fibre, with Zerodur optical components. Zerodur is used for the mirrors' substrate because of its extremely small thermal expansion coefficient. Optics made with this material can be polished into non-spherical figures with sub-angstrom rms surface roughness. The mirrors are coated with a UV coating. The key element in the COR instrument concept is that the mirrors with coatings optimized for the UV (*e.g.*, 121.6 nm) still have good reflectivity in the visible. Figure 2.4.3 shows how appropriate filters will separate the broad-band visible light from the UV line emission.

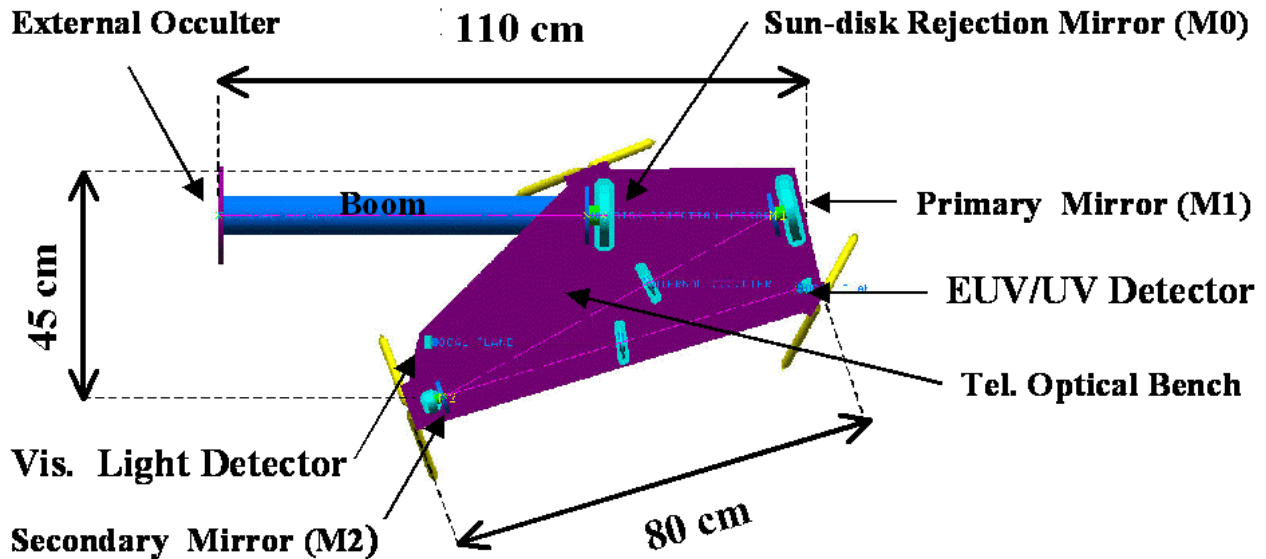


Figure 2.4.4: Possible physical implementation of COR, including optional EUV/UV channel.

The choice of the sampling resolution of COR (presently assumed to be 16 arcsec/pixel, based on a FOV of about 9 deg and a 2k × 2k APS array) needs to take into account the overall instrument radiometric performance, including the actual detector S/N characteristics. Radiometric budget considerations may lead to different sampling resolutions.

The basic specifications and drivers of the instrument are summarised in Table 2.4.1.

Parameter	Value
Telescope type	Externally occulted off-axis Gregorian
Aperture diameter	180 mm
External occulter diameter	60 mm.
Sun disk rejection mirror diameter	230 mm
Primary mirror diameter	92 mm.
Secondary mirror diameter	82 mm
Effective focal length	400 mm
Exit pupil diameter	90 mm
Lyot trap diameter	92 mm

Parameter	Value
Field-of-view	Annular, Sun-centred. Coverage: 1.2 – 3.5 R at 0.21 AU, (perihelion at mission start) 1.8 - 5.3 R at 0.30 AU, (perihelion at mission end)
Spatial resolution	Visible (500 nm): 40 arcsec entire FOV UV (30.4 nm, 121.6 nm): 16 arcsec at 1.2 R 40 arcsec at 3.5 R
Stray-light levels	< 10 ⁻⁹ (visible light); < 10 ⁻⁸ (30.4 nm, 121.6 nm)
Wavelength band-pass	1) Visible (450 - 600) nm; 2) H I (121.6 ± 10) nm; 3) He II (30.4 ± 2) nm (optional augmentation)

Table 2.4.1: COR instrument summary.

Structure

The instrument structure will utilize carbon fibre/cyanate or carbon-carbon composite and will be designed for zero coefficient of thermal expansion in the axial direction. It is in the form of a rigid rectangular baseplate to which are bonded appropriately placed brackets (also of composite) for the support of the optical and detector elements. The focus and orientation of each element is set and maintained by a precision spacer located between the element and its support bracket. The optical system is surrounded by a lightweight rectangular composite enclosure and baffle structure that attaches to and further strengthens the baseplate. Removable covers on the top of the enclosure allow for installation and servicing of the optical and detector elements. An external door mechanism shields the telescope aperture when the instrument is not observing.

Thermal

The thermal control approach is based on shielding the instrument from most direct solar radiation, rejecting light from the solar disc that enters the annular entrance aperture, and an opto-mechanical design that is insensitive to bulk temperature changes. The use of a carbon fibre composite structural system allows the optical system to be almost completely a-thermalised. Moreover, the use of a low secondary magnification factor in the telescope (*i.e.*, 3:1) makes the optical system less sensitive to dimensional changes compared to more traditional space instruments such as TRACE. Preliminary estimates suggest that the allowable temperature range of the opto-mechanical system may be as much as ±50° C. Local temperature control will be needed for the liquid crystal polarisation module (LCPM), which has a smaller allowable temperature range. Thus, we consider it prudent to include a small power allocation for thermal control heaters (*e.g.* 1 W) pending further analysis.

The occulter is the element of the coronagraph which reaches the highest temperature, since it is directly exposed to the Sun. The occulter has an exiguous conductive link (represented by the thin rods of the support) with the rest of the structure. The occulter and supporting links are made of titanium and are arranged in a conical geometry such that thermally induced strain is absorbed without de-centring the occulter disc.

The temperature achieved by the occulter has been estimated by assuming a purely radiative heat transfer and an external coating of the same type as that utilised for the sunshield of the payload module. The thermal flux incident on the occulter is 29.2 kW/m² at 0.22 AU and 1.8 kW/m² at 0.9 AU. The temperature difference experienced by the occulter along the observation phase is at maximum 266.5° C. A small reduction of the temperature will be caused by the transport of part of the heat through the occulter supports.

Detectors

In the present COR implementation, one detector is baselined optimised for the Visible region (450 – 600 nm). As a high-priority augmentation, this could be extended to include the UV (121.6 nm) and the EUV (30.4 nm). Both detectors have 8-10 μm pixels and an array size of 2048×2048 . The baseline visible and UV detector is an Active Pixel Sensor (APS). This detector system is based on CMOS technology, which is attractive for high radiation dose environment. In addition, the APS architecture has the potential to allow on-chip differencing of the polarimetric signals, yielding substantial improvements in signal-to-noise performance compared with conventional CCD detectors.

APS detectors have addressable pixels, permitting the dynamically programmable read-out of individual pixels and sub-arrays. This feature will be used in COR for limiting the readout area to the solar corona (excluding the occulted portion field) and for defining “Regions of Interest” to be observed with higher time resolution.

3.4.3 Orbit, Operations and Pointing Requirements

The Solar Orbiter spacecraft is expected to have the capability of offset pointing from the nominal sun-center direction with an angular range of about $\pm 2^\circ$ (that is, less than $\pm 1 R_\odot$ at 0.2 A.U.). This capability will allow the pointing towards the solar poles, during the out-of-ecliptic encounters, of the high spatial resolution remote-sensing instruments with limited field-of-views.

The COR’s external occulter should be sized for optimum observations up to the closest encounter, that is, at 0.21 A.U. The geometrical requirement driving this sizing is that no sunray from below $1.2 R_\odot$ at 0.21 A.U. enters the instrument. That is $\pm 1.6^\circ$ from the sun-center direction, corresponding to $1.8 R_\odot$ at 0.3 A.U.

During the spacecraft off pointing, the COR instrument may just not observe. In this case, COR would i) turn off the detector(s), and ii) partially close the entrance door, in order to protect the telescope mirrors from the thermal load. If, then, the off pointings were $\leq 0.5 R_\odot$ at 0.3 A.U. (i.e., $\leq 0.5^\circ$), the telescope entrance aperture would still be in the shadow of the external occulter. In this case, there would be no need for closing the entrance door, provided that the sun-disk rejection mirror and baffling system be design to accommodate the dumping of the sun-disk light at the off-pointing angles. With modest spacecraft off pointing (i.e., $\leq 0.2^\circ$, at 0.3 A.U.), COR may even take advantage of this manoeuvre by observing the corona closer to the limb, in the direction of the off pointing.

In either case, that is, when not observing because of large off pointings, or when continuing operations because the slightly off-centred sun-disk is still occulted, COR would not need a re-pointing mechanism

3.4.4 Accommodation

The coronagraph aperture is located behind the sun shield. The hole through the shield is sized and shaped so to avoid that the stray-light generated by sunlight reflection and diffraction on the hole rim enter in the instrument with an angle close to the line of sight.

The instrument should be co-aligned with S/C and other instruments to within 2 arcmin. Similarly to the other RS instruments, COR has been allocated a maximum length (side parallel to the Sun direction) of 100 cm. The present COR reference design has an optical bench ($80 \times 40 \text{ cm}^2$) compatible with the 1 m requirement, while the fixed occulter, on a dedicated boom, protrudes through the 1 m envelope, to a total length of about 110 cm. The accommodation of such a specific design is presently considered as problematic

and therefore alternative solutions should be considered. For the present design, assuming a fixed occulter design solution, the COR envelope fits an overall volume of $110 \times 40 \times 25 \text{ cm}^3$.

3.4.5 Interface and Physical Resource Requirements

Data rates and volume

The primary driver of the data rate is COR efficiency in the two main channels. In the UV, the coronal signal is weaker and the instrument efficiency lower than in the visible band. Therefore, longer exposure times will be required for the UV coronal observations. On the basis of the count-rate for HI Lyman- α emission estimated from a coronal hole (*i.e.* worst case), we assume an average exposure time of 100 sec. to 600 sec. A single image (2048×2048 pixel) with 16 bit (b) per pixel takes about 67 Mbit of memory. We assume that only 50% of the image is used (the rest is occulted disc, extreme corners of the square matrix, etc.). The two detectors operate in parallel but with HI Lyman- α at 50%. A full 1-pixel resolution will only be used in 20% of the observing sequences, while in the remaining 80%, imaging will be acquired with a 2×2 pixel binning. A compression level of 5 can be achieved with an acceptable loss of information with schemes such as the "Adaptive Discrete Cosine Transform" (ADCT). So every $\sim 10^2$ sec, there is a data volume of 5 Mbit. For the purpose of obtaining "quick-look" images during the perihelion passage, a telemetry rate of 10 kb/s would allow to transmit those data in less than 10 min.

Mass

The COR mass breakdown is given in Table 2.4.2. The estimate of the electronics mass has been obtained by assuming a stand-alone electronics box. A further breakdown of the mass budget is required.

Component	Mass (kg)
Optical bench & boom	4.0
Cover & fixtures	1.0
Mirrors & supports	1.5
Thermal control	2.0
Mechanisms	0.5
Detectors (2 \times , including FE electronics)	0.6
Control electronics	4.0
DC/DC converter	1
Total without margins	14.6
Margins (25%)	3.7
TOTAL instrument	18.3

Table 2.4.2: Mass breakdown of COR (including the optional EUV channel).

Power

In order to minimize power consumption, four basic operating modes have been considered. In each of these modes, only the relevant components are supplied with power. The modes are: a) Data acquisition; b) Data compression; c) Instrument configuration; d) Stand-by. The Power consumption of each of the four modes is given in Table 2.4.3.

Component	Operative Modes Power (W)			
	Standby	Data acq.	Configuration	Data compression
CPU & Interface	10	10	10	10
DC/Dc converter	5	6	6	6
Data compressor				9
Detector		4		
ADC		5		
Motor drive			5	
Stepper Motor			4	
Sub-total	15	20	20	25
Margin (25%)	3	4	4	5
Total	18	24	24	30

Table 2.4.3: Power budget of COR.

3.4.6 Cleanliness, Ground Operations and Other Requirements

A similar particulate and chemical contamination plan as followed by the STEREO mission should be adopted.

3.4.7 Open Points and Critical Issues

1. APS detectors: the baseline design relies on the use of APS as the active sensors. The need for a solar blind UV detector needs to be demonstrated.
2. Occulter design: the occulter design and overall pointing / observing strategy needs definition.
3. Optical design: overall optical design requires further definition, taking into account the required FOV, the baselined focal plane array and the accommodation constraints (1m envelope and interface to heat shield).
4. Liquid crystal polarimeter: this unit requires further definition. Qualification status and/or need for dedicated development activity must be verified.

3.5 Spectrometer/Telescope for Imaging X-rays (STIX)

Bursts of hard X-rays (> 20 keV) are the most common signature of the impulsive phase of a solar flare. In fact, the X-ray continuum is the most direct signature of energetic electrons at the Sun. The X-rays are bremsstrahlung, produced by accelerated electrons colliding with the ambient solar atmosphere. STIX is an X-ray imaging spectrometer, operating from 3 to 150 keV, which determines the location of X-ray emission from the Sun as a function of time and energy to a spatial precision of 1 arcsec over a 38 arcmin imaging field of view and 2 arcmin over a wider 5 degree field of view.

3.5.1 Scientific Goals

The principal scientific goal of the Spectrometer/Telescope for Imaging X-rays (STIX) is:

- To establish the timing, location and spectra of energetic electrons near the Sun. This will enable these electrons to be related to subsequent observations by the in-situ solar energetic particle and radio instruments. In this way, STIX serves as a high-energy link between imaging and in-situ observations.

Secondary science objectives are:

- To determine the size and morphology of hot thermal and non-thermal X-ray sources with 2.3 arcsec resolution (350 km at 0.22 AU);
- To use comparisons with observations from 1 AU, or other solar-orbiting spacecraft (if available), to measure the directivity of solar X-ray emission. This will provide the first direct measurements of beaming at the Sun;
- To use observations of ‘*over-the-limb*’ flares (in conjunction with other spacecraft, if available) to isolate the weak coronal component of hard X-ray bursts, so as to characterize the chromospheric/coronal transport of energetic electrons.

3.5.2 Instrument Concept

STIX imaging uses the same indirect imaging technique as used on Yohkoh / HXT. Imaging information is encoded in the relative count rates in separate detector elements located behind pairs of grids, each of which absorbs a distinct directionally-sensitive fraction of the incident flux.

The telescope hardware employs a set of 64 sub-collimators, each of which consists of a pair of widely separated, X-ray opaque grids with an X-ray detector element located behind the rear grid (see figure below). Front and rear grid pairs have identical pitch and orientation, whose choice determines the spatial frequency to be measured. As was demonstrated by Yohkoh/HXT, the relative count rates of a pair of sub-collimators, one of whose grids is displaced by one quarter of its pitch, can be used to accurately measure both the real and imaginary parts of one Fourier component of the angular distribution of the source. With 64 sub-collimators, the imaging system then measures 32 different Fourier components. This data can then be used to reconstruct the source image, using well-established techniques used by radio astronomy, Yohkoh/HXT and RHESSI.

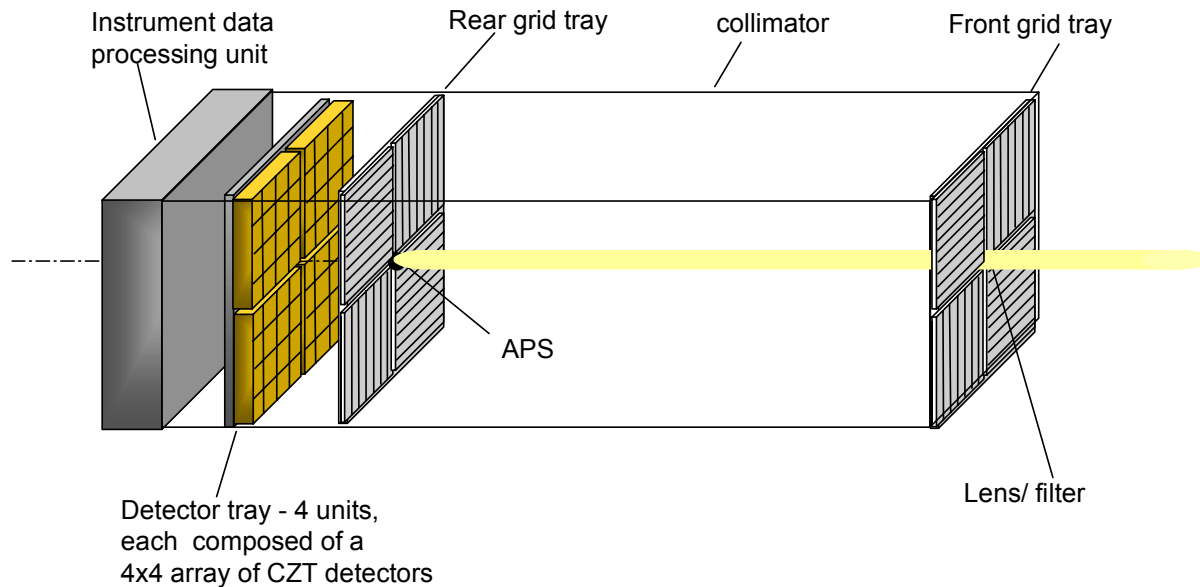


Figure 2.5.1: STIX configuration. A conceptual illustration of the STIX instrument that does not show the current aspect system or sunshade, both of which are described below. The overall dimensions are $12 \times 12 \times 100 \text{ cm}^3$.

Since the detector spatial resolution need match only the $\sim \text{cm}$ dimension of the sub-collimator, detectors can be optimized for their spectral resolution. This enables the imaging to be done as a function of energy, resulting in an instrument which functions as an imaging spectrometer. Such a detector system consists of a set of four identical 3 mm thick CdZnTe solid-state detector modules each of which is divided into sixteen 1 cm square elements. Operating at room temperature, they provide a total of 64 detector elements, each of which provides an energy resolution of 2 to 4 keV (FWHM) from 3 to 150 keV.

The front and rear grid assemblies are each constructed as a unit by stacking sets of etched tungsten sheets to a thickness of 1 mm. Grid pitch values range from 20 microns to 2.8 mm. At a separation of 900 mm, the corresponding spatial resolution of the individual sub-collimators (defined as one half of the ratio of grid pitch to separation) is 2.3 arcsec to 5.4 arcmin. At 0.22 AU the former is equivalent to 0.5 arcsec at 1 AU.

The FWHM imaging field of view, given by the ratio of the sub-collimator diameter (1cm) to separation is 38 arcmin. Even at 0.22 AU this is sufficient to fully encompass an active region. In addition, STIX also can do spatially-integrated spectroscopy over a much wider field of view (5 deg). Such a field is sufficient for observing events anywhere on the Sun, even from 0.22 AU. Furthermore, within this wider field of view STIX can determine the centroid of the source location to an accuracy of 1 arc-minute. This 5-degree locating field of view enables every transient X-ray event on the Sun to be associated with its active region of origin and so provides a capability that could provide useful input for target selection. The overall effective area of the system for imaging is about 16 cm^2 , which at 0.22 AU is equivalent to more than 4 times that of RHESSI.

3.5.3 Orbit, Operations and Pointing Requirements

Elements of a pair of limb-sensing aspect systems are embedded into the grids. For each aspect subsystem, the front grid contains a Fresnel lens element, whose openings are restricted to a narrow band in 1-

dimension. This focuses a one-dimensional profile of the Sun onto the rear grid plane, where a wavelength-filtered linear APS detector, mounted on the rear grid plane, determines the effective limb position in 1-dimension with ~ 1 arcsec precision. An identical, but orthogonal subsystem determines the limb position in the other dimension. The combination of these two systems determines the pitch/yaw offset of the STIX imaging axis with respect to Sun center. The concept is an adaptation of the aspect system on RHESSI which determines the solar aspect to ~ 0.4 arcsec rms at up to a 128 Hz cadence. For STIX, the cadency requirement could be significantly eased. The output of this system could be made available in real-time to provide \sim arcsec relative aspect for use by other instruments. To enable accurate, absolute placement of images on the solar disc, STIX will rely on S/C systems to provide absolute roll aspect to ~ 1 arcmin.

The use of Fresnel lens elements eliminates the possibility of degradation of optical surfaces and restricts the internal solar heat load to a few 10's of milliwatts. As demonstrated by RHESSI, the use of an embedded aspect system significantly eases alignment and pointing requirements. This enables the use of a relatively lightweight metering structure between the front and rear grid planes. The primary alignment requirement is to maintain the relative twist of the front and rear grid assemblies to about 2 arcmin, which is about 10 times less stringent than on RHESSI. Thus STIX instrument provides arcsec-class imaging with arcmin-class alignment requirements. In effect it substitutes aspect knowledge for mechanical control. As described, the system will determine the absolute location of X-ray sources to 1 arcsec within a 38 arcmin field of view.

STIX should be Sun-pointed and co-aligned with the other imaging instruments to ~ 3 arcminutes to provide imaging overlap. Operations would be autonomous, based on preloaded parameter settings. Examples of such parameters include gain-setting parameters (to match gains of the individual detector elements) and parameters used by the instrument data processor algorithm for the selection of imaging intervals.

The science output of the STIX instrument would be greatly enhanced by observations during the cruise phase. The telemetry requirements during this period could be tailored by selecting only large flares for analysis.

3.5.4 Calibration

Specific on-ground and in-flight calibration requirements need to be defined by the STIX instrument team.

3.5.5 Accommodation

The challenge is to accommodate the instrument in the spacecraft such that it is Sun pointing, blocking low energy X-rays while allowing X-rays above 3 keV to reach the instrument and not receiving too much thermal flux. The low energy X-ray flux must be suppressed to prevent saturation and preventing the detectors' ability to handle individual photons.

Such a requirement on X-rays leads to a sunshade with a thickness equivalent to ~ 1 mm of carbon or 3 mm of beryllium. Unfortunately this is not in line with the envisaged designs of the Sun shield and hence a specific aperture needs to be designed. One possible design is to use a thin carbon layer at the outside of the Sunshield which would block the direct Sun light and allow the higher energy X-rays through. This layer must be at the outside of the Sun shield to conform to its multilayer design. Since both this layer and the surrounding Sun shield radiate from high temperatures then a baffle is required to prevent flux entering and provide a larger radiating surface. A thin reflective coating could be applied to the grids without affecting their imaging performance, minimise the heat flux into the instrument and hence the spacecraft. Analysis will be required to determine whether intermediate layers of X-ray transparent yet heat reflective materials are required, and/or whether radiators to the STIX instrument will be required.

A further complication is the requirement for 2 open apertures (each $\sim 0.1 \times 50 \text{ mm}^2$) in front of the aspect elements. At 0.22 AU such apertures would transmit about 300 mW. About 50 mW of this would be transmitted to the lower grid tray inside the instrument while the remainder would be absorbed or reflected by the top tungsten grid. An additional design issue is the trade-off between co-alignment accuracy of the open apertures (that determines their width and transmitted heat load) and the feasible level of heat dissipation/reflection by the front grid.

3.5.6 Interface and Physical Resource Requirements

Data handling and telemetry

Expected count rates from the detector system will vary from a few counts/second during background periods to more than 10^6 counts/second during intense flares. The key on-board data handling challenge is to process and compress this data in order to allow ground-based image reconstruction from a modest telemetry volume. No image reconstruction is done on board.

Each detected photon generates an output pulse from a single CZT detector element. Such analog pulses are shaped and amplified by front-end electronics and then digitized into one of 16 energy channels. Initial data processing consists of accumulating such events according to their energy and detector into one of 16×64 (1024) energy/detector bins. A basic instrument time resolution of 1/8 second results in an initial data rate of ~ 16 kbyte/second. A rotating 64-Mbyte buffer stores ~ 1 hour of this full-resolution data within the instrument.

Within the context of this 1-hour time frame, an autonomous instrument processor is used to form detector- and time-averaged spectra and detector- and energy-averaged light curves. Enhanced count rates in the light curves are used to identify flare time intervals for imaging. The processor then calculates statistically significant sums over adjacent time bins and/or energy channels. The data for a single image is then in the form of 64 2-byte numbers, representing the counts in each detector element for the selected time/energy interval. The image morphology and location is represented by the relative values of these counts and can be expressed as a corresponding set of 64 4-bit binary fractions relative to the maximum count among the 64 values. Compressing the total counts to 8 bits, the image can then be stored as this 8-bit total plus 64×4 bit of relative counts plus 7 byte of miscellaneous information for a total of 40 byte per image.

Assuming a long-term average of 6 minutes of flare data per hour, imaging in an average of 10 energy bands with an average 2-second cadence implies a requirement of 1800 images per hour. Adding 25% for aspect, housekeeping and non-imaging datasets results in an average data rate of 200 bits/second.

Allocated mass and power budget

The estimated mass of STIX is 4 kg. This is based on a well-calculated mass of 0.25 kg for each grid, 0.2 kg for the sunshade and 1 kg each for the metering structure, detectors and electronics. Considering the higher design maturity level of STIX, maturity margin is reduced to 10%. A further consolidation of the mass breakdown is required.

Unit	Mass (kg)
Grids	0.5
Sunshade	0.2
Metering structure	1
Detectors	1
Electronics	1
Harness	0.3
Margin (10%)	0.4
STIX TOTAL	4.4

The instrument power is estimated to be 4 W. A detailed power budget is required.

Allocated instrument volume

Similarly to the other RS instruments, STIX has been allocated a maximum length (side parallel to the Sun direction) of 100 cm. Based on the present design baseline, the STIX envelope fits an overall envelope of $100 \times 15 \times 15 \text{ cm}^3$.

3.5.7 Cleanliness, Ground Operations and Other Requirements

No specific needs identified (closed unit, X-ray instrument).

3.5.8 Open Points and Critical Issues

1. Aspect system: The primary technical issues to be resolved are related to the aspect system. Suitable sensors need to be identified and evaluated for radiation hardness. In addition, ground tests of a prototype aspect system should be undertaken to provide early validation of its optical design.
2. Radiation damage: The radiation tolerance of the CdZnTe may prove inadequate at 0.22 AU from the Sun due to solar energetic particles.
3. Thermal Concept: The low energy X-ray opaque sunshade and its interface to the multilayer Sun shield need to be defined. Heat rejection performance of the grids needs to be validated.

3.6 Remote-sensing Instruments: Open Issues & Critical Items

3.6.1 APS Detectors

At present all the remote-sensing instruments are base-lining Active Pixel Sensors (APS) for the optical elements. This is because the particle environment encountered by the Solar Orbiter, means that CCD-type detectors will most likely be inappropriate. We may anticipate a solar wind ‘background’ proton flux some $20 \times$ that of SOHO ($1/r^2$). For an average flux at 1 AU, of density 9 cm^{-3} (average speed and temperature of 450 km/s and $1.2 \times 10^5 \text{ K}$ (1 keV)) we expect 200 cm^{-3} at 0.22 AU. Thus, the nominal particle environment will be similar to some modest storm events detected occasionally by SOHO.

There may also be an increased chance of encountering proton ‘storms’ from shocks associated with mass ejection, with up to thousands of proton hits per second. One might expect events similar to those experienced by SOHO, with greater intensity, and, in addition, some near-Sun events may be generated by lateral expansion of CME disturbances, whose exact intensities remain unknown.

Also, we anticipate occasional impacts from solar flare neutrons whose 15.5 minute lifetime means that most missions do not encounter them. Finally, we anticipate a similar cosmic ray (non solar) flux to that at SOHO. The net effect is a gross increase in particle hits during extreme conditions.

The radiation damage in CCD’s is primarily caused by the creation of charge traps that reduce the charge transfer efficiency (CTE). The radiation hardness of silicon APS detectors is much higher because CTE degradation is unimportant; charge is not transferred across the array of an APS detector, since the on-chip electronics extracts and amplifies the charge from each pixel individually. On-chip electronics also provides additional low mass and power advantages, compared to CCD’s.

Thus, APS detector systems would seem to be an ideal solution for the optical sensors onboard Solar Orbiter from a particle environment point of view. We note, however, that such devices are still under development and their implementation on Solar Orbiter is not assured. Towards this end, a TDA program is explicitly targeted for APS development. In order to focus the activities, aid procurement and ensure the greatest chance of success, we recommend that all instruments use the same APS design and architecture, namely a 2048×2048 array with 8-10 micron pixels. (The actual pixel size could vary between 8-10 mm depending of the outcome of a planned Technical Development Activity). At the present stage of development it is not clear what the actual operating temperature of the devices will be. Estimates vary from 0 to -100 deg C . Since the lowest anticipated radiator temperature will be of order -50°C , Peltier cooling is likely to be required for the EUV sensors, with associated impact on mass and power resources. Finally, detector performance plays a critical role with respect to SNR, thus influencing the final choice of the telescope aperture. Sub-optimal performance would require a larger aperture, with a significant heat load increase.

3.6.2 Cleanliness requirements

EUV optical surfaces in space are renowned for experiencing significant degradation in performance with time.

Under high irradiation, particularly in the ultraviolet, any contaminant deposited on an optical surface, even in very minute amounts, polymerizes, so the reflectivity of the surface drastically decreases. This effect is well known for synchrotron radiation optics as well as for some space instruments, but has been well avoided

by the SOHO UV/EUV instruments. The degree to which the reflectivity decreases depends on the irradiation exposure and on the partial pressure of the contaminant.

The Solar Orbiter situation is more difficult than it was for SOHO; due to the changing distance from the Sun, the level of UV irradiation will be higher and the thermal environment more variable.

Even with the most stringent procedures in the handling and assembling of the optical components, under the extreme irradiation conditions at 0.22 AU, there is a risk of a serious rapid degradation of the reflectivity, especially in the EUV. The variable thermal environment during the orbit makes evaporation and out-gassing from surfaces with increasing temperature unavoidable.

The decreasing reflectivity could be severe for optics at normal incidence, where the EUV reflectivity is relatively low and the EUV absorption is high. For example, gold could be a good candidate as an EUV coating for mirrors at normal incidence, since it has high visible reflectivity and also discrete EUV reflectivity (0.16 at 1200 Å and 0.13 at 600 Å), but a thin layer of contaminants deposited on its surface could drastically reduce the EUV response, and thus the effective area.

The effects could be less severe when the optics is used in grazing incidence. Firstly, the portion of the optics illuminated at grazing incidence is much larger than in normal incidence (for the same aperture) and correspondingly the flux decreases (this is beneficial also for cooling the optics); secondly, the effect of polymerization results in much less degradation of the reflectivity than in normal incidence.

It should be noted that the mirrors can be operated at relatively high temperature and this could help to reduce the deposition of contaminants.

In addition, steps can be taken to reduce the levels of potential contamination in space. The most important procedure would be a long out-gassing period prior to opening of the instrument doors. For the CDS and SUMER instruments on SOHO, the out-gassing period was 3 months from launch, and this was a deliberate (and successful) policy. With the inclusion of vents allowing out-gassing materials to escape, the long period certainly enabled the contamination to be reduced. Such a policy must be adopted for Solar Orbiter – possibly for several instruments. For efficient venting, the opening to space must be large (*e.g.*, a partly opened aperture door, a door specifically designed for venting, or a permanent vent) and, in addition, the instrument interior must be preferentially heated (by passive or active heating).

Any EUV instrumentation must be developed with the most stringent contamination policy, both in the laboratory and in operation (*e.g.*, out-gassing). Possible effects must be assessed thoroughly by the proposing teams and optical and procedural policies adopted.

Counter-measures

The varying thermal environment, as well as the changing apparent size of the Sun, increases the risk of redistribution of out-gassing contaminants during the orbit. The deposition of these species on the optical components is extremely enhanced on cold surfaces and on surfaces exposed to solar UV light and particle flux, leading to irreversible deposition by polymerization of the organic substances. To avoid contamination build-up during operation, the thermal design of the instruments should ensure that there are no optical surfaces colder than their surroundings. The availability of a surface acting as a cold trap for the contaminants, in close proximity of the sensitive areas, will provide a protection against the deposition.

Requirements applicable to the Solar Orbiter

Cleanliness requirements applicable to the Solar Orbiter have a large impact on AIV/AIT activities at both instrument and system level. Specific requirements will be established at a later stage of the mission definition. Based on past experience, the cleanliness requirements defined for the ESA SOHO mission and for the NASA STEREO mission provide representative guidelines to be followed by the Solar Orbiter project.

3.6.3 Thermal Control

Because of Solar Orbiter's proximity to the Sun, thermal issues are a key concern and especially for the Remote-sensing Instruments in view of their necessity to view directly the Sun. In fact thermal issues derived from the heat load associated to the instruments apertures can very easily drive the spacecraft design. The key to thermal control is: a) keep the heat out of the instruments (closed solution) and b) reduce the aperture sizes. The P/L industrial study has recommended an approach whereby only the spectral bands of interest are allowed to penetrate inside the instruments.

3.6.3.1 VIM thermal architecture concept (on-axis design)

The thermal concept of VIM instrument has been studied for two configurations. The on-axis design represents the description of the reference instrument, whereas the off-axis design is an alternative concept. The entrance of the HRT telescope is significantly greater than the FST telescope and therefore the preliminary analysis is just for the HRI part.

Figure 2.6.1 shows a possible on-axis design of the HRT telescope considering the solar flux as the only thermal source. In order to limit the thermal load on the detector a heat stop is introduced.

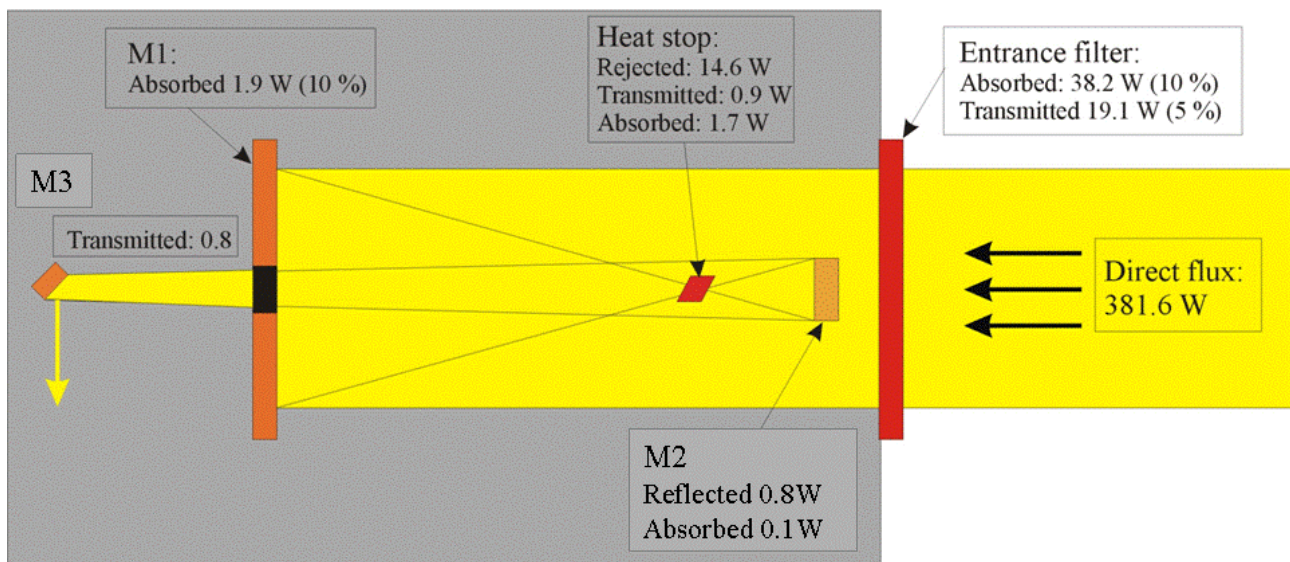


Figure 2.6.1: VIM HRT on-axis thermal architecture concept with a 12.5 cm entrance aperture.

3.6.3.2 VIM thermal architecture concept (off-axis design)

The alternative concept for an off-axis design is detailed figure 2.6.2. A narrow-band filtering window (one candidate material is Suprasil) is mounted on the spacecraft structure, decoupled from the instrument itself. The proposed off-axis design enables the accommodation of a further heat stop between the primary and the secondary mirror, without obstructing the main optical path and to envisage simple cooling devices for this heat stop.

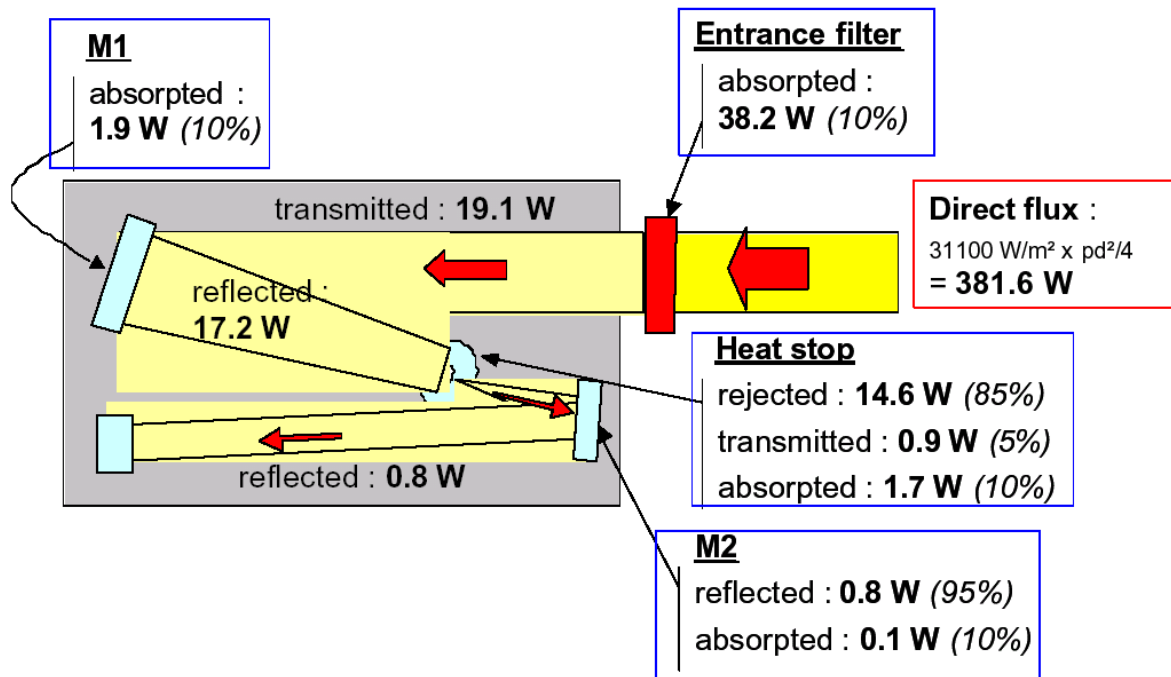


Figure 2.6.2: VIM HRT off-axis thermal architecture concept with a 12.5 cm entrance aperture.

3.6.3.3 EUS thermal architecture concept

The EUS instrument requires a 70 mm diameter aperture (TBC), which will induce a large heat load in the instrument, while the thermal load associated with the extreme UV part of solar spectrum targeted by the instrument is close to zero. A possible solution to reduce the heat load into the instrument is the adoption of a EUV filter based on a thin aluminium sheet (about 15 microns thick), cooled by a support grid acting as a stand alone radiator.

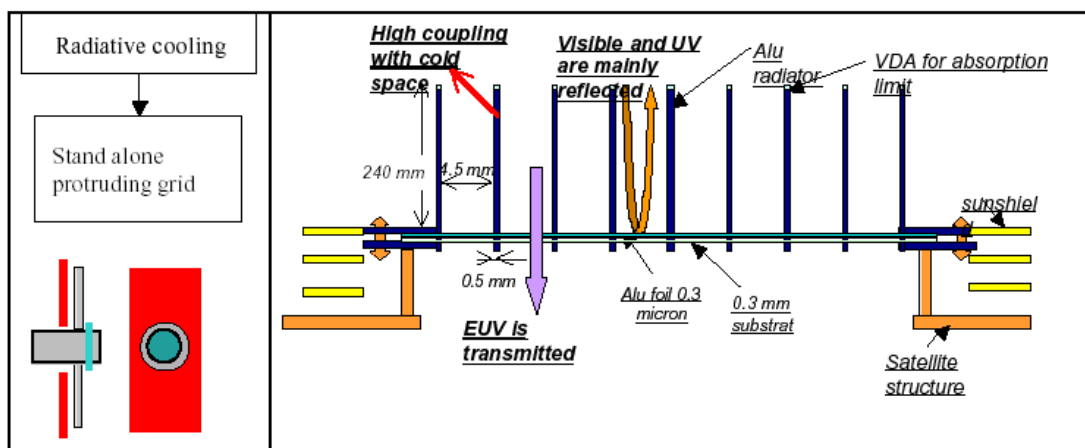


Figure 2.6.3: Filter and filter cooling principle for EUS.

This solution has the disadvantage of reducing considerably the signal photon flux transmitted to the detectors. In case such a filter cannot be adopted or developed for EUS, an open telescope design will have to be implemented, such as that shown in figure 2.6.4.

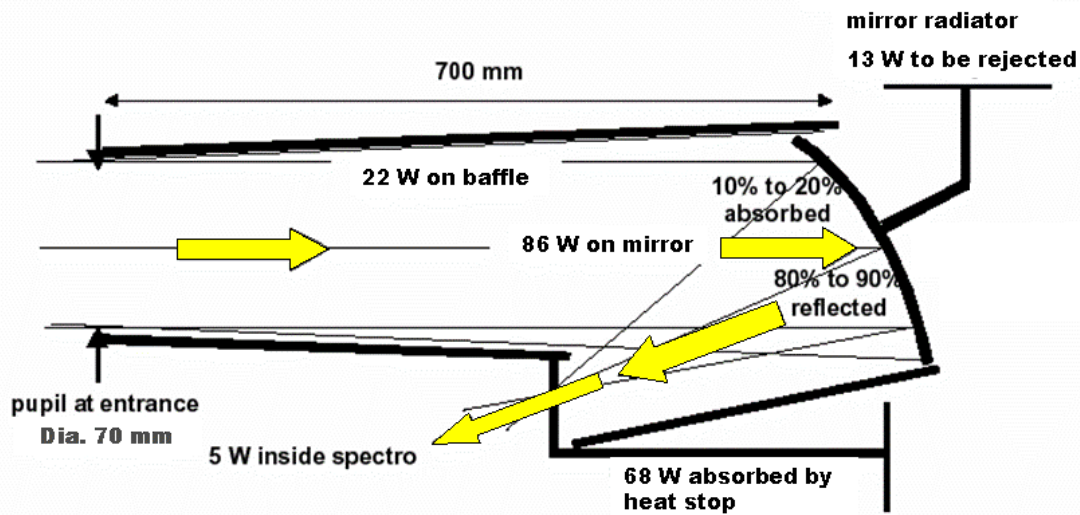


Figure 2.6.4: Open Telescope option for EUS.

3.6.3.4 EUI thermal architecture concept

HRI and FSI telescopes have 20 mm diameter entrance apertures, limiting the solar heat loads inside the instrument. A standard EUV thin aluminum filter sheet is placed at the tip of a baffle. Figures 2.6.5 and 2.6.6 show the loads on the different parts of the two telescopes.

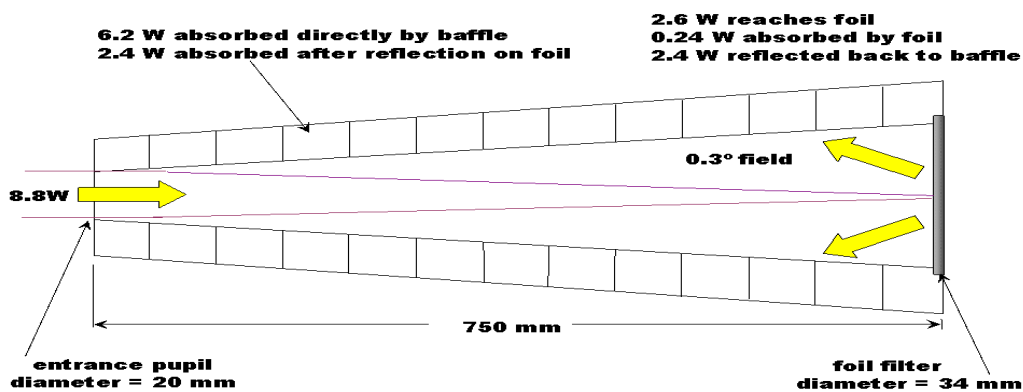


Figure 2.6.5: Solar heat flux management within the HRI baffle under the assumption of a 20 mm diameter.

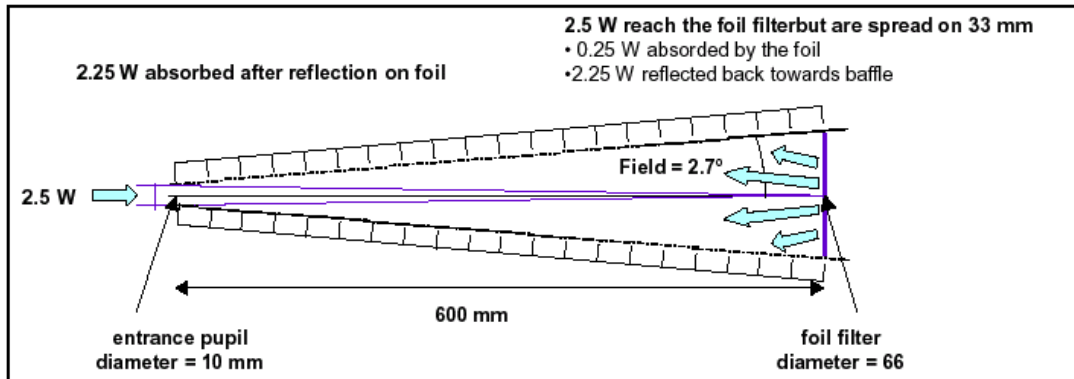


Figure 2.6.6: Solar heat flux management within the FSI baffle (under the assumption of a 10 mm diameter)

3.6.3.5 COR thermal control concept

The coronagraph is characterised by its design enabling to occult before the optical elements all flux coming directly from the Sun disk, as shown in figures 2.6.7 and 2.6.8. The spacecraft thermal control will have to manage the important heat load of the sun disk rejection mirror.

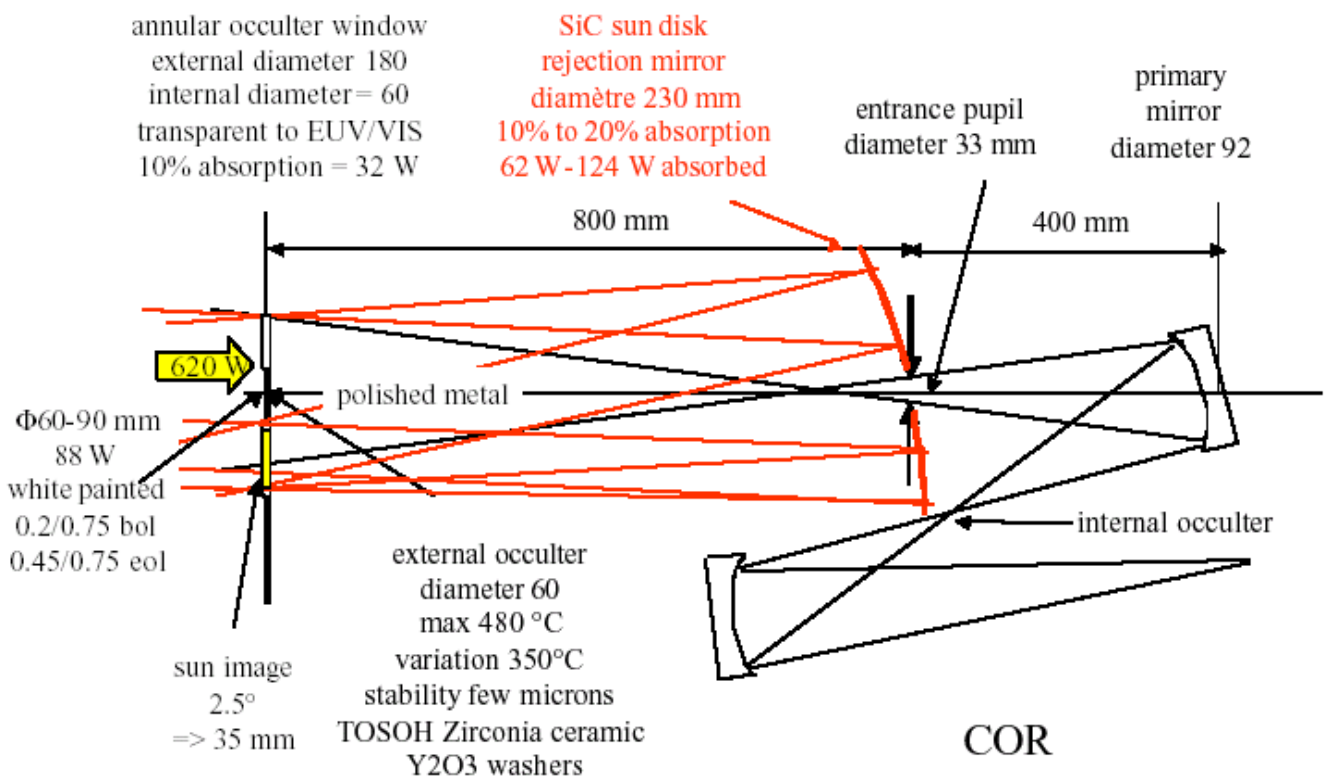


Figure 2.6.7: COR thermal loads assessment.

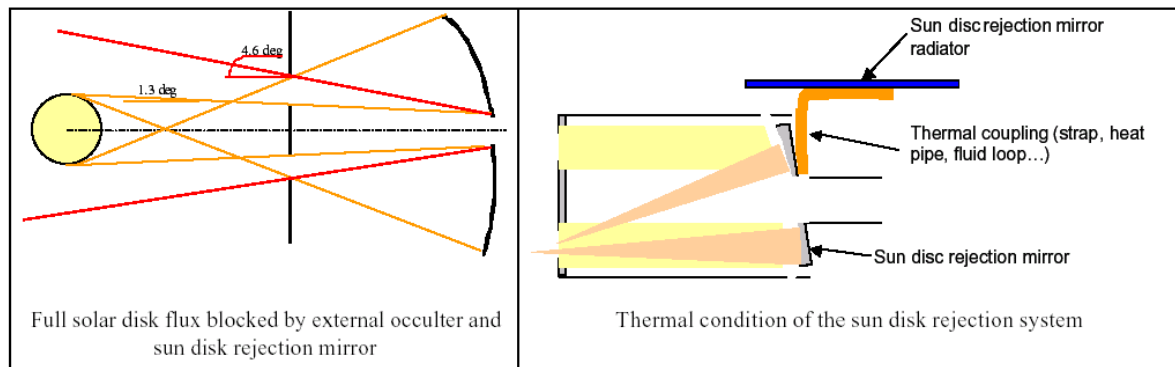


Figure 2.6.8: The COR internal Sun rejection mirror and related heat related approach.

3.6.3.6 STIX thermal control concept

The STIX thermal design is in principle simpler than for the rest of the Remote-sensing Instruments. The actual interface between instrument's sunshade and entrance with the heat shield need to be addressed in more detail. Details can be found in the corresponding instrument description (2.5.5).

3.6.4 Instrument doors

The instrument covers/doors are required in order to cope with contamination issues and to guarantee the physical continuity of the heat shield, especially in case of unexpected problems with heat rejection devices. In order to maintain the integrity of the Thermal Control System, the instrument doors should be considered as an integral part of the heat shield. On these grounds, the instrument doors have been identified as Payload Support Elements and are ESA procured items.

3.6.5 Data Rates

With the exception of STIX, there is a wide disparity between the amount of front-end data generated by the Remote-sensing instruments and the available telemetry. The problem is exacerbated by the fact that these instruments are only operated for 30 days during the 150 day orbit, and thus one should be careful when considering orbit averaged data. Because of the limited amount of telemetry allocated to the remote-sensing instruments, innovative solutions to onboard data compression and reduction are essential if negative impacts on science are to be avoided.

The raw data and processing needs for each of the remote-sensing instruments are summarized Table 2.6.1. The values are consistent with the spatial and sampling resolutions of VIM, EUS and EUI. The processing distributions between the instrument specific front end electronics and the instrument-shared common electronic (PDMU) are given in Table 2.6.1

It is important to note that the instruments are only operating during full operations windows. For all remote-sensing instruments to best utilise the limited TM to achieve the science objectives the operations must consider the following:

- A range of fields-of-view,
- Binning over multiple pixels implying a reduction in resolution,
- Compression techniques,

- Imaging rates.

Table 2.6.1: Data handling needs for the Remote-sensing Instruments

Instrument		Allocated TM Rate
VIM	VIM typically needs a minute to obtain 20 images in 5 different wavelengths and in four different polarisations and then calculate parameter images. There are then options as to how many parameter images are required, the resolution, and also the cadence. Using a lossless compression ratio to average 5 bits per pixel allows modes to generate TM rates from 22 to 800 kbps.	20 kbps
EUS	Instead of transmitting complete spectrum, a number of lines, 6 to 15 are selected. For each line 15 pixels are required for 0.3Å width <i>e.g.</i> only 90 of the 2048 pixels for 6 lines. The complete field of view is not always required, and hence imaging ¼ of the FOV could be performed every 106 minutes (based on a compression ratio of 10). Onboard calculation and down-linking of the spectral parameters of each line would reduce the TM requirements further compared to transmitting the full spectrum.	17 kbps
EUI	The instrument contains up to 3 HRI telescopes configured for different wavelengths. If the 2k × 2k images of 14 bits can be compressed by JPEG2000 by a factor of at least 25. This would result in images on average every 6 minutes for an average of 20 kbps. MPEG should be investigated to see whether this is more appropriate for faster sampling. FSI telescope: An image will be taken every 80 minutes, creating a data rate of $2k \times 2k \times 12 \text{ bit} / 4800 / 20$ (compression) = 0.5 kbps	20 kbps
COR	Single images 2k × 2k × 16 bit require 64Mbit. 50% of image can be discarded as occulted disk, extreme corners etc. The HI Lyman-α detector works in parallel at 60% cadence of visible light detector. Such images can be performed every 540 seconds to achieve the TM rate.	10 kbps
STIX	A matrix of 64 detector bins over 16 energy levels at 16 bit counts requires 16 kbit. Data rates of 8 per second are possible, but images will be selected for the most interesting 10% of time and at a 2 second interval. By just selecting 10 of the 16 energy bands, an image every 2 seconds is sufficient. An image is compressed by recording the maximum value in 16 bit, and providing the 64 bin images of relative sizes to the maximum value in 4 bit/bin. With some bits for time etc then 320 bit is sufficient resulting in the allocated rate of 0.2 kbps.	0.2 kbps

4 IN-SITU UNITS

4.1 Solar Wind Plasma Analyser (SWA)

4.1.1 Science Goals

The principal scientific goals of the Solar Wind Plasma Analyzer (SWA) are:

- To provide observational constraints on kinetic plasma properties for a fundamental and detailed theoretical treatment of all aspects of coronal heating;
- To investigate charge- and mass-dependent fractionation processes of the solar wind acceleration process in the inner corona;
- To correlate comprehensive in-situ plasma analysis and compositional tracer diagnostics with space-based and ground-based optical observations of individual stream elements.

Furthermore, the SWA will enable the investigation of:

- ^3He and “unusual” charge states in CME-related flows;
- The interaction of solar wind ions on dust grains in the heliocentric distance range associated with the “inner source”. Freshly produced pick-up ions from this inner source are specially suited as test particles for studying the dynamics of incorporation of these particles into the solar wind or their further re-energization.

The SWA will measure separately the three-dimensional velocity distribution functions of the major solar wind constituents: protons, α -particles and electrons. The basic moments of the distributions, such as density, velocity, temperature tensor, and heat flux vector will be obtained under all solar wind conditions and be sampled sufficiently rapidly to characterize fully the fluid and kinetic state of the wind. In addition, measurements of representative high-FIP elements (the C, N, O group) and of low-FIP elements (such as Fe, Si or Mg) will be carried out in order to:

- Obtain their abundances, velocities, temperature anisotropies and charge states;
- Probe the wave-particle couplings (heavy-ion wave surfing);
- Determine the freeze-in temperatures (as a proxy for the coronal electron temperature).

4.1.2 Instrument concept

In view of the limited resources of mass, volume and telemetry allocated to the SWA, a compromise between sensitivity, mass/charge- and mass- and time resolution has to be found. The SWA has to cover a large dynamic range in ion fluxes. Since there is an enormous difference between the proton fluxes at perihelion (typically $10^{14} \text{ m}^{-2} \text{ s}^{-1}$) and the fluxes of relevant minor ion tracers at 1 AU (e.g. Fe^{10+} at typically $10^8 \text{ m}^{-2} \text{ s}^{-1}$ etc.) it is suggested to implement three different sensors:

- A **Proton/ α -particle Sensor (PAS)** with the principal aim to investigate the velocity distribution of the major ionic species at a time resolution equivalent to the ambient proton cyclotron frequency. The sensor is Sun pointing.
- An **Electron Analyser System (EAS)** consisting of two (three optional if resources allow) sensors to cover nearly 4π ster of viewing space and to allow the determination of the primary moments of the electron velocity distribution with high temporal resolution.
- A **Heavy Ion Sensor (HIS)** which allows the independent determination of the major charge states of oxygen and iron and a coarse mapping of the three-dimensional velocity distribution of some prominent

minor species. Also, pick-up ions of various origins, such as weakly-ionised species (C^+ , N^+ , Ne^+ , Mg^+ , Si^+ , *etc.*) should be measured. The sensor is Sun pointing.

The three instruments combined in SWA need to cover a wide range in time and dynamic ranges. The shortest time scales are associated with the electron timescales, followed by the proton and ion kinetic time scales. Measurements of these short time scales are not required during ordinary operation because these time scales are not always present in the solar wind. Hence the SWA instruments need to be capable of measuring short time scales in a "burst mode" (see below), while compressing data to longer time averages during normal operation.

Modes of operation

- **Normal mode**

PAS: A typical time resolution of 3s for 3-D velocity distribution functions (transmitted as moments) of protons and alpha particles is required.

EAS: A typical time resolution of 3s for 3-D velocity distribution functions (transmitted as moments) of electrons is required.

HIS: A typical time resolution of 300s for coarse 3-D velocity distribution functions (transmitted as moments) of the most prominent heavy ions.

- **Burst mode**

Burst mode can be triggered either by external instruments (*e.g.* the RPW or MAG), internally, or by a combination of measurements (requires sophisticated algorithms implemented in DPU). Trigger criteria could include *e.g.* shock passage, unusual wave activity, or passage of other transients or discontinuities. In this mode, the following measurements are required:

PAS: Measurements of 2-D distributions of solar wind protons and alpha particles to resolve typical growth times of instabilities, *i.e.* at a cadence of 0.1s.

EAS: Measurements of 2-D distributions of solar wind and supra-thermal electrons to resolve typical growth times of instabilities, *i.e.* at a cadence of 0.1s.

HIS: Measurements of 2-D distributions of solar wind heavy ions to determine kinetic properties and compositional boundaries at a cadence of 30s. Ideally, the instrument would allow faster determination of the abundances of the most common ionic charge states *e.g.* by an interleaved E/q stepping scheme.

All SWA instruments should be capable of routinely measuring in burst mode covering several instability growth times at least once every hour. Because the fluxes will vary strongly in the course of the spacecraft orbit, lower time resolution/cadence is acceptable at large heliocentric distances. This reflects the changing telemetry allocation during the orbit. A duty cycle of the order of 1% can be achieved.

4.1.3 Sensors

4.1.3.1 Proton and Alpha Particle Sensor (SW-PAS)

The SWA PAS sensor uses electrostatic optics to separate and analyze protons and alpha particles. In essence it consists of four components – three electrostatic lenses and a detector (see fig. 3.1.1). The first component

is a pair of electrostatic deflectors located either within, or at the rear of the Sun shield. The second component is a set of electrostatic optic components which are outside of the direct view of the aperture and steer the particles towards a third set of deflectors which guide the particles into the detector. By varying the voltages in the optics, the E/q of the ions can be selected. The detector can be located such that it is not directly exposed to the Solar heat input entering the aperture. The aperture is a $5 \times 2 \text{ cm}^2$ slit at the rear of the Sun shield.

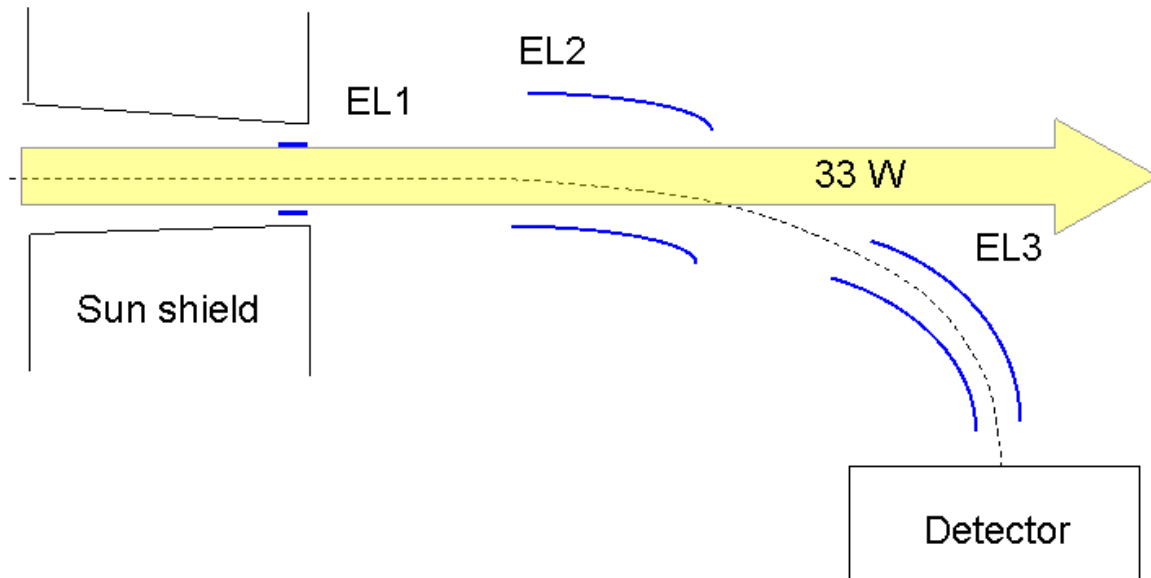


Figure 3.1.1. Functional block diagram of the SW-PAS sensor. The Sun is to the left. EL1, EL2 and EL3 are electrostatic lenses used to deflect the incident particles into the detector allowing the Solar heat input to be rejected to space.

Sensor performance requirements

The energy pass-band shall be $200 \text{ eV}/q - 20 \text{ keV}/q$ with an energy resolution of $(E/q)/(\Delta E/q) = 20$ and angular resolution of 5° by 5° . The time resolution shall be 3 s in nominal mode and 0.1 s in burst mode.

Estimated resource allocation

Parameter	Value	Remarks
Sensor mass [kg]	3	
RTC unit / DC-DC converter [kg]	0.5	
Dimensions [cm]	$40 \times 30 \times 20$	
Power average [W]	2	
Power peak [W]	2.5	
Operating temperature range [deg C]	-30 to +40	
Data rate [bps]	14,000	$(45^\circ \times 10^\circ) / 5^\circ \times 5^\circ = 72$ $\sim 90E/q$ steps $72 \times 90 = 6500$ bins 2200 bps, 7bits deep

Accommodation and pointing requirements

The SW-PAS sensor is Sun pointing. The opening area of the aperture is 10 cm^2 . The FOV is $\pm 45^\circ$ (in-orbital plane) $\times \pm 10^\circ$ (out of orbital plane). The sensor will be located behind the Sun shield. Typical requirement for pointing error is 0.5 to 1° .

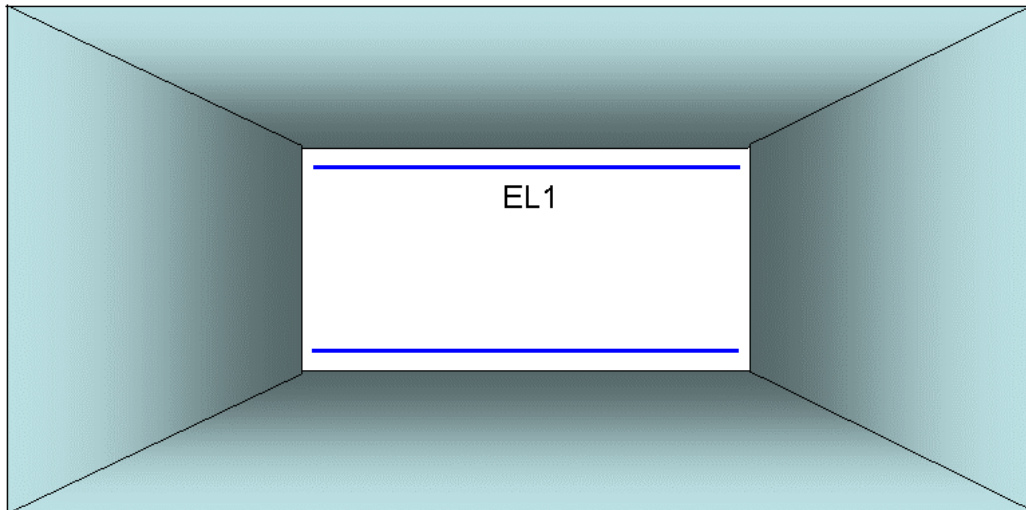


Figure 3.1.2. View of the PAS through the Sun shield as viewed from the Sun with the slit aligned along orbital plane. The slit size is $5 \times 2 \text{ cm}^2$ at the rear of the Sun shield.

Either within the sunshield or at the back of the sunshield two electrostatic deflectors are required which must be able to operate to up to 7 kV and be thermally isolated.

Cleanliness, AIV and other requirements

The sensor should reject Solar UV radiation flux to a sufficiently low level in order to ensure adequate SNR

The Multi-Channel-Plate detector is very sensitive to molecular contamination and the instrument would need continuous dry nitrogen purging before launch.

Due to internal high voltages (electro-static optics), several weeks out-gassing are needed after launch before instrument switch-on.

Open points, critical issues and Technology Development Activities

The electrostatic optics for energy/angle imaging will need development. The development of a Charge Sensitive Amplifier (CSA) and Time-of-Flight ASIC has high priority. The thermal dissipation inside the S/C depends on the aperture and will have to be carefully analyzed.

4.1.3.2 Solar Wind Heavy Ion Sensor (SW-HIS)

The SWA HIS sensor is very similar in construction to the PAS, in that it also uses electrostatic optics to separate and analyze ions. The device is shown schematically in Fig. 3.1.3. Like the PAS, the detector can be located such that it is not directly exposed to the Solar heat input entering the aperture. The aperture is $5 \times 2 \text{ cm}^2$ slit at the rear of the Sun shield.

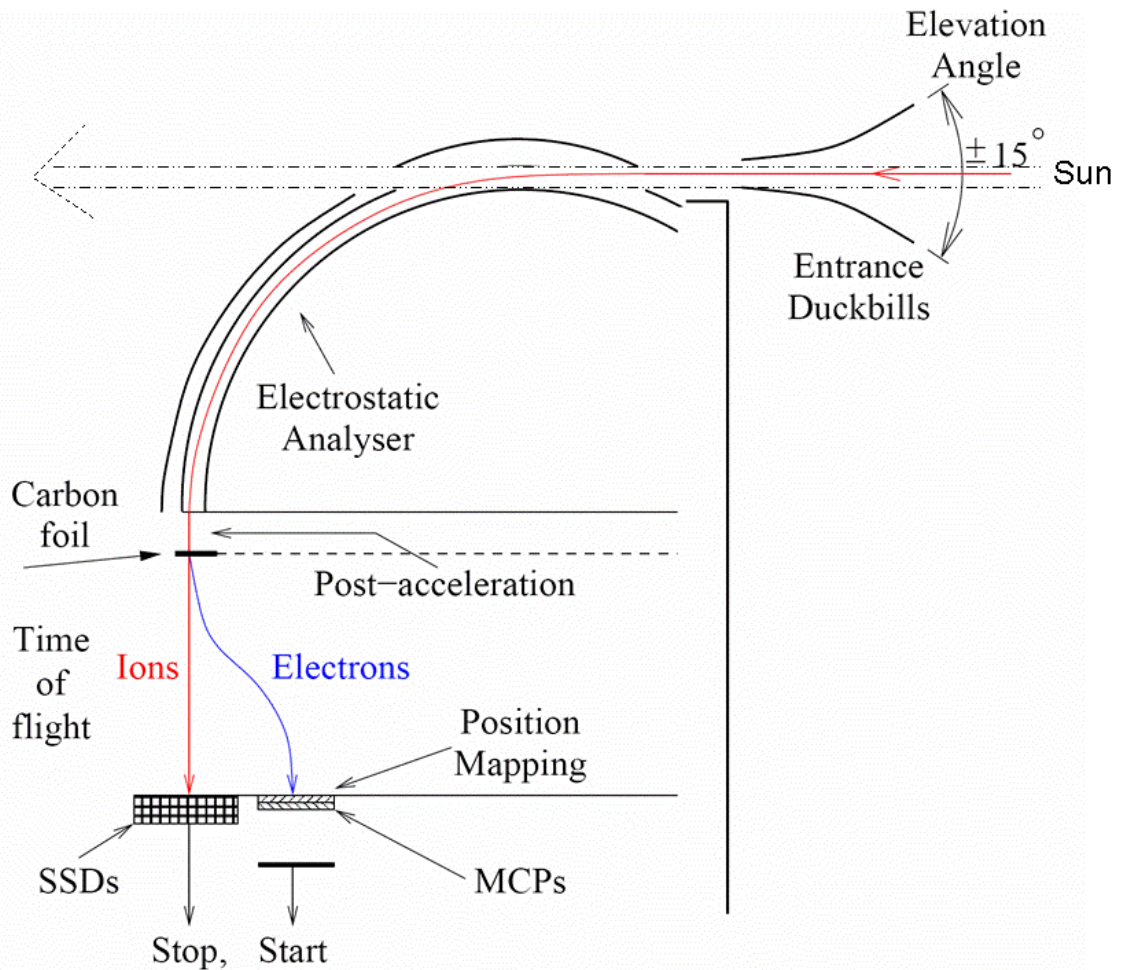


Figure 3.1.3 Schematic of the HIS sensor.

Sensor performance requirements

The pass-band shall be $500 \text{ eV}/q - 100 \text{ keV}/q$ with an energy resolution of $(E/q)/(\Delta E/q) = 20$ and angular resolution of 6° by 6° . The time resolution shall be 300 s in nominal mode and 30 s in burst mode.

Estimated resource allocation

Parameter	Value	Remarks
Sensor and RTC mass [kg]	8	
Dimensions [cm]	$40 \times 40 \times 30$	
Power average [W]	7	
Power peak [W]	9	
Operating temperature range [deg C]	-30 to +40	
Data rate [bps]	4000	Prioritised events plus counters for different ions with look-up table compression

Accommodation and pointing requirements

The SW-HIS sensor is Sun pointing. The opening area of the aperture is 10 cm². The FOV is $\pm 45^\circ$ (in orbital plane) $\times \pm 10^\circ$ (out of orbital plane). The sensor will be located behind the Sun shield (see Fig. 3.1.2). Typical requirement for pointing error is 0.5 to 1°.

Either within the sunshield or at the back of the sunshield, electrostatic deflectors are required which must be able to operate to up to 7 kV and be thermally isolated.

Cleanliness, AIV and other requirements

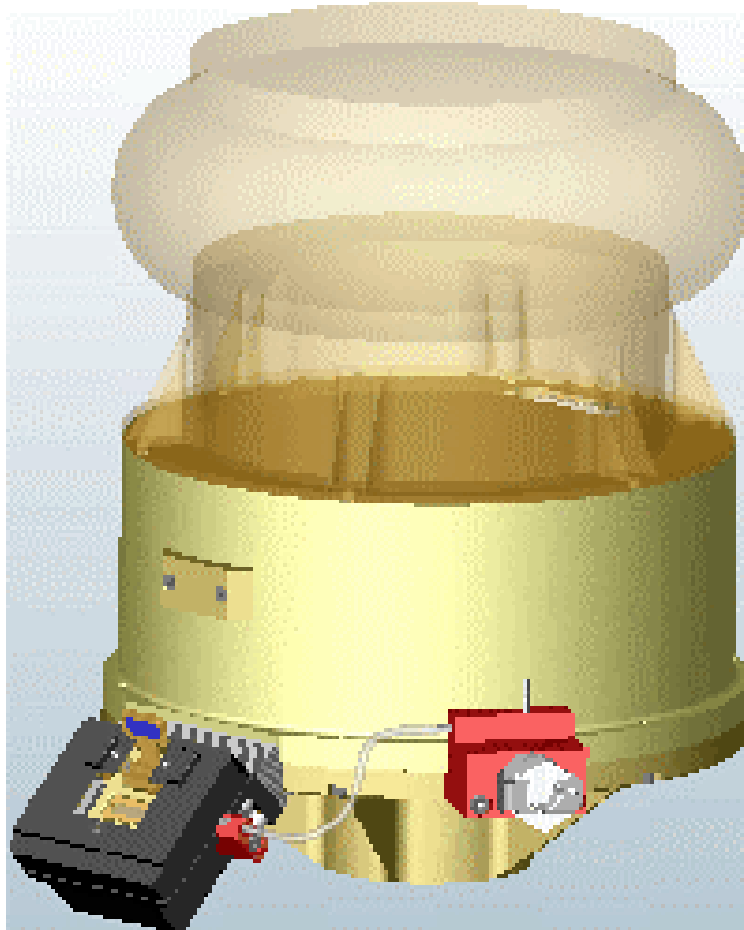
The sensor should reject Solar UV radiation flux to a sufficiently low level in order not to compromise the detection of rare particles. Class 10,000 particulate clean environment and continuous dry nitrogen purging required.

Due to internal high voltages (electro-static optics, MCPs), several weeks out-gassing are needed after launch before instrument switch-on.

Open points, critical issues and Technology Development Activities

Electrostatic sweeping optics needs development. Also, the development of integrated read-out electronics for solid-state detector pixels and a CSA and Time-of-Flight ASIC also has high priority. The thermal dissipation inside the S/C depends on the aperture and would have to be carefully analysed.

4.1.3.3 Electron Analyser Sensor (SW-EAS)



Sensor performance requirements

The energy pass-band shall be 1 eV – 5 keV with an energy resolution of $E/\Delta E = 10$ and angular resolution of 10° by 10° . The time resolution shall be 3s or better with 0.1s resolution in burst mode.

Estimated resource allocation

Parameter	Value	Remarks
Sensor mass [kg]	3	2 sensors (3 optional if resources allow, each 1.5 kg)
RTC unit / DC-DC converter [kg]	0.5	TBC
Dimensions [cm]	15 × 15 × 15	Single sensor
Power average [W]	4	
Power peak [W]	4	
Operating temp. range [deg C]	-30 to +40	
data rate, average [bps]	2,000	Histograms plus some burst data: 16 energy channels, 12 anodes, 13 elevation angles, 8 bit counters

Accommodation and pointing requirements

The Electron Analyser System (EAS) consists of two body-mounted sensors, mounted on perpendicular sides of the spacecraft, preferably on Y/Z edges. The free field-of-view for each sensor $360^\circ \times \pm 45^\circ$. An important requirement is that the 2 EAS sensors cover as much of 4π steradian of viewing space as possible. This requirement is to be taken into consideration in determining the final S/C accommodation, and specifically to maximise the un-obstructed field of view.

Absolute Pointing Error (APE)	0.5°
Absolute Measurement Accuracy (AMA)	1.0°

Cleanliness, AIV and other requirements

Special care has to be taken to ensure near-equipotential conditions in the vicinity of the EAS entrance apertures.

The sensor should reject Solar UV radiation flux to a sufficiently low level in order to ensure adequate SNR. Due to internal high voltages (electro-static optics, MCPs), several weeks outgassing are needed after launch before instrument switch-on.

Open points, critical issues and Technology Development Activities

1. HIS and PAS apertures: both HIS and PAS have entrance apertures directly exposed to the Sun radiation, thus requiring a dedicated thermal design and adequate materials.
2. Final configuration DPU / RTC: separate RTC for each sensor or common RTC / DPU.
3. Data compression: an effective data compression strategy needs to be identified and implemented.

SWA - Summary of allocated power and mass values.

Unit	Power [W]	Mass [kg]	Remarks
PAS sensor	2.0	3.0	
HIS sensor	7.0	8.0	
EAS (2 units)	2x 2	3.0	
RTC and DC/DC units	1	1.0	Detailed configuration is TBC
Total (before margin)	14	15.0	

4.2 Radio and Plasma Wave Analyser (RPW)

4.2.1 Science goals

The principal scientific goal of the Radio and Plasma Wave Analyzer (RPW) is:

- To provide measurements of both the electric field and magnetic field in a broad frequency band (typically from a fraction of a Hertz up to several tens of MHz) covering characteristic frequencies in the solar corona and interplanetary medium.

Measurements of both electrostatic and electromagnetic waves provide different diagnostics:

- Electrostatic waves provide *in-situ* information in the vicinity of the spacecraft;
- Electromagnetic waves provide extensive remote-sensing of energetic phenomena in the solar corona and interplanetary medium.

Furthermore, the RPW instrument on Solar Orbiter will enable the investigation of:

- Waves and turbulence that occur much closer to the Sun than previously measured;
- The north-south symmetry of the radio radiation in the solar corona using, for the first time, viewing angles from well out of the ecliptic plane.

4.2.2 Instrument concept

The Radio and Plasma Waves Analyser (RPW) comprises two main sub-systems: A Plasma Waves System (PWS) covering *in-situ* measurements and the Radio Astronomy Detector (RAD) for remote-sensing.

The two sub-systems share some of the sensors and have common digital signal processing. The same receivers can be used to analyse the different types of waves detected by different sensors, for instance electric antennae and magnetic coils.

PWS Concept

The PWS will identify the *in-situ* plasma waves and kinetic modes comprising the electromagnetic part of the fluctuation and turbulence spectra. A brief description of the characteristics of the plasma waves expected to be present at 0.22 AU follows.

The expected field strength may range between a few $\mu\text{V/m}$ and a mV/m , and up to about 1 V/m for the convection electric field. The magnetic field strength is expected to vary between a few nT and mT , with large differences between the longitudinal and transverse components with respect to the mean magnetic field and the solar wind flow direction (substantial Doppler shifts are to be expected).

From Helios observations one can estimate that a sensitivity equal to $10^{-6} \text{ nT/Hz}^{1/2}$ will be required at 0.22 AU to identify without ambiguity whether the observed waves are electromagnetic or electrostatic.

At and above the electron plasma frequency, intense electron plasma oscillations and solar radio waves are expected. Helios observations show that wave intensities associated with type III bursts increase very rapidly with decreasing radial distance from the Sun. Intense emission could extend up to $10^{-4} \text{ nT/Hz}^{1/2}$.

The Solar Orbiter electric antenna length is constrained by the measurement of the plasma thermal noise. This noise, which is mainly due to the electron thermal motion around the antenna, provides electron density and temperature measurements, independently of any calibration gain determination or intrinsic limitations due to the spacecraft charging. This immunity is essentially due to the fact that, close to the local plasma frequency, the antenna is sensitive to Langmuir waves with very large wavelengths. Therefore, at the plasma peak the antenna samples an average over a large plasma volume. In order to detect correctly the thermal Langmuir waves and measure correctly the electron temperature, the thermal noise spectroscopy requires an antenna whose length L is larger than the local Debye length L_D . In the heliocentric distance range between 0.2 to 0.7 AU is expected to range between roughly 0.5 and 8 meters. Moreover, for an orthogonal dipole antenna the effective length L that has to be compared to L_D is closer to half the tip-to-tip length than to the physical length of a monopole (the precise value of the effective L has to be modelled while modelling the thermal noise itself). Therefore the reasonable minimum monopole length required for Solar Orbiter is 5 meters

The Figure below shows estimated electric sensitivity requirements. The galactic non-thermal emission sets the effective background for the radio measurements between a few hundred kHz and 20 MHz. At lower frequencies, the antenna photoelectron noise dominates, while antenna resonances reduce the sensitivity above 30 MHz (for 5-6 meter antennas).

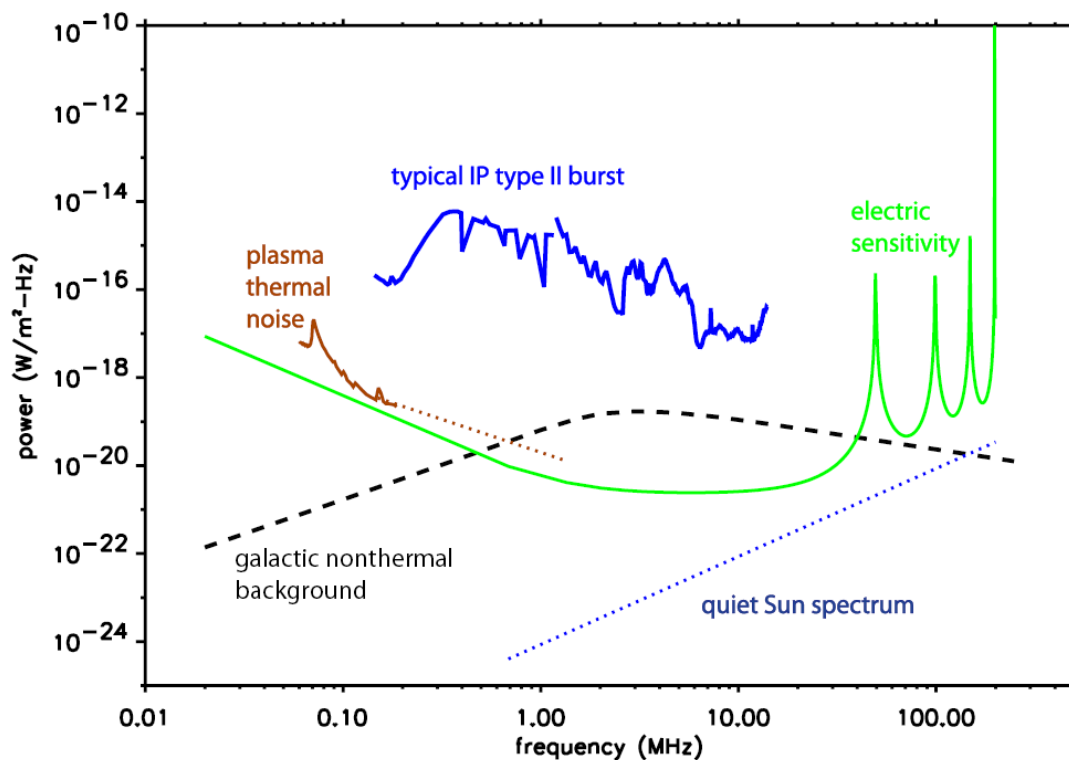


Figure 3.2.1: Electric sensitivity requirements for HFR.

The PWS will cover a broad band in frequencies, extending from about 1 Hz into the MHz range. Resolving the vector components of the electric and magnetic fields is scientifically highly desirable to determine wave modes unambiguously. Furthermore, multiple electric antennas allow for common-mode rejection of spacecraft generated noise and waves. The three components of the fluctuating magnetic field can be easily

measured with a 3-axial search coil magnetometer arranged in a compact configuration and mounted on a short boom, which should point into the anti-Sun direction. This boom (spacecraft item) is required for magnetic cleanliness reasons and could be shared with the MAG (see 3.3) as long as a minimum distance between the two sensors is respected. PWS can exchange burst triggers with other instruments in the *in-situ* payload to facilitate payload-wide burst modes.

HFR Concept

The HFR will measure the solar and interplanetary radio waves in the frequency range from 100 kHz to 20 MHz, with a sweep period between 0.1 s and 10 s and a high spectral resolution ($\Delta f/f \approx 0.07$). The HFR will observe plasma processes associated with energetic electrons from the corona up to about 0.5 AU. It will

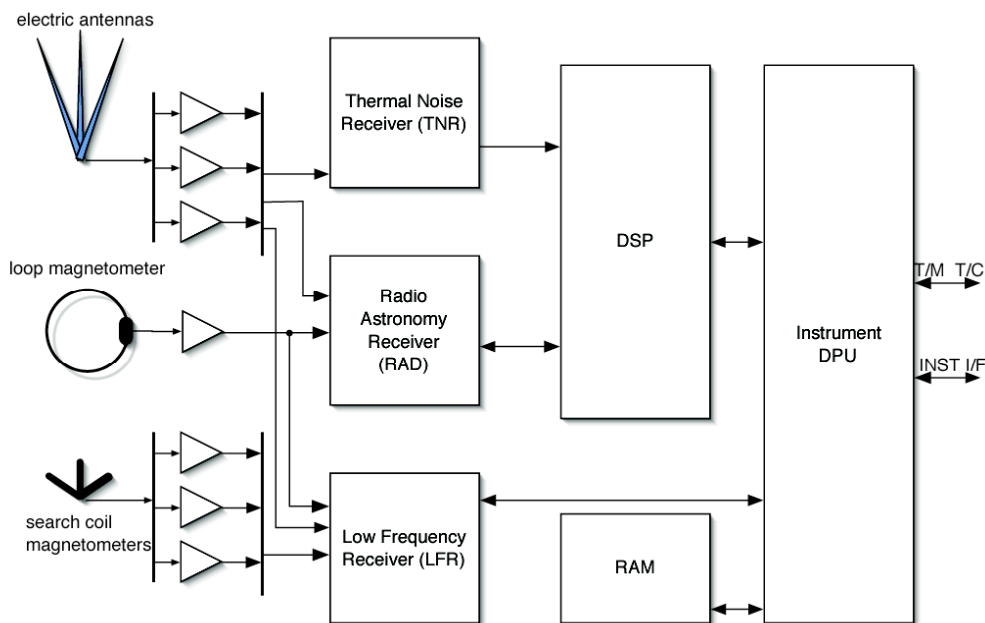


Figure 3.2.2: Solar Orbiter RPW block diagram

probe the plasma at distances ranging from near the solar surface to the spacecraft location, thereby connecting the coronal regions observed by the optical instruments with the near-Sun heliospheric conditions specified by the *in-situ* measurements. Since radio radiation is generally beamed (beam widths sometimes down to a few tens of degrees) more or less along a radial direction from the Sun, this technique is particularly relevant for different vantage points, for instance when the Solar Orbiter observes the far side of the Sun. The time history provided by the regular acquisition of the radio dynamic spectrum will help to trace the development of an active region in a synthetic manner.

The time resolution required to detect the rapidly varying solar bursts varies with the radio frequency. Typically, the duration of a type III burst (stream of energetic electrons) is $Dt(s) = 220 / f(\text{MHz})$. This points to time resolutions of the order of 0.1 s or better for the high frequencies and of 10 s for the low frequencies. Different designs are used on many space missions and the heritage goes right back to the birth of space radio astronomy at long wavelengths.

The radio astronomy receiver (HFR) can be of the classical super-heterodyne type. Frequency synthesizers will allow for a maximum flexibility in the choice of the observing frequencies (for instance to avoid

“polluted” frequencies on the spacecraft). Each sub-receiver can consist of up to 256 selectable channels. Only a selection of these channels could be transmitted to the telemetry stream. The Instrument Control Unit (DSP, RAM and Instrument DPU) will perform the front-end digital signal processing functions (waveform detection, FFT and correlations) and command the instrument subsystems.

4.2.3 Sensors

4.2.3.1 Thermal Noise Receiver (TNR)

Sensor performance requirements

The frequency band shall be 10 kHz - 1 MHz with a sensitivity of 3 nV/Hz^{1/2}.

TNR is a very sensitive, digital receiver designed specifically to measure the plasma thermal noise spectrum very accurately. TNR will provide an accurate, and high time resolution, reference for the solar wind experiments.

Estimated resource allocation

Parameter	Value	Remarks
Mass [kg]	0.5	
Dimensions [cm]	N/A	Single electronics card
Power average [W]	1	
Power peak [W]	1	
Operating temperature range [deg C]	-30 to +50	
Raw data rate, average [bps]	1630	
Raw data rate, peak [bps]	6520	
Data compression method	Log amplitude	
Data compression factor	0.3	

Accommodation and pointing requirements

Inside electronics box.

Open points, critical issues and Technology Development Activities

The length of the harness for the RPW should be < 1m, and not multiples of the target frequency.

4.2.3.2 Low Frequency Receiver (LFR)

Sensor performance requirements

The frequency band shall be 1Hz – 10 kHz with a sensitivity of 30 μV/m for electric field antennas and 0.2 pT for the loop magnetometers. Sensitivities of 1 pT/√(Hz) at 10 kHz and 0.1 pT/√(Hz) at 1 kHz for the search coils are required.

The LFR is designed to study lower frequency, more intense, plasma waves associated with heliospheric shocks, plasma radio emission, and solar wind thermalization. The LFR will perform onboard processing of

the electric and magnetic data and produce both spectra and waveforms to identify non-linear coherent structure.

Estimated resource allocation

Parameter	Value	Remarks
Mass [kg]	1.5	
Dimensions [cm]	N/A	Single electronic card
Power average [W]	1.5	
Power peak [W]	2	
Operating temperature range [deg C]	-40 to +50	
Raw data rate, average [bps]	2500	
Raw data rate, peak [bps]	TBD	
Data compression method	TBD	
Data compression factor	TBD	

Accommodation and pointing requirements

Inside electronics box.

4.2.3.3 High Frequency Receiver (HFR)

Sensor performance requirements

The frequency band shall be 100 kHz - 20 MHz with a sensitivity of 10 nV/ $\sqrt{\text{Hz}}$ for antennas and 10^{-6} nT/ $\sqrt{\text{Hz}}$ for the loop magnetometer.

Estimated resource allocation

Parameter	Value	Remarks
Mass [kg]	0.6	
Dimensions [cm]	N/A	Single electronics card
Power average [W]	0.8	
Power peak [W]		
Operating temperature range [deg C]	-40 to +50	
Raw data rate, average [bps]	800	
Raw data rate, peak [bps]	TBD	
Data compression method	Log amplitude	
Data compression factor	TBD	

4.2.3.4 Antennas

Sensor performance requirements

The frequency range for the antennas and associated pre-amplifiers shall be 1 Hz to 20 MHz.

Estimated resource allocation

Parameter	Value	Remarks
Mass [kg]	4.8	Each antenna assembly is estimated to be 1.6 kg
Dimensions [cm]	500-600 60 (diameter), 20 (height)	Length of each antenna RPW platform envelope (before deployment)
Power average [W]	0.3	Pre-amplifiers
Power peak [W]	0.3	
Operating temperature range [deg C]	TBD	

Accommodation and pointing requirements

The primary accommodation concern for RPW is the location of the three, 5-6 meter electric antennas. Ideally, the three electric antennas would be mounted orthogonal to one another, although some deviation from orthogonality can be tolerated. Since at low frequencies ($< \sim 1$ kHz) the antennas couple to the plasma resistively, their response is strongly determined by the photoelectron flux generated by sunlight. Therefore, the RPW antennas should be orientated such that they have equal exposure to the Sun. Also, a long base line dimension of the antennas will improve the sensitivity at low frequencies. Concern should be paid to the location of nearby spacecraft structure, including the high gain communications antenna. Spacecraft structure couples electrically to the RPW antennas and distorts the effective RPW antenna pattern, though this can be studied and corrected. In the figure below we show the antenna implementation on STEREO. The right hand figure shows the footprint of the stacer configuration and is expected to be contained within a cylindrical envelope of ~ 60 cm diameter and 20 cm height).

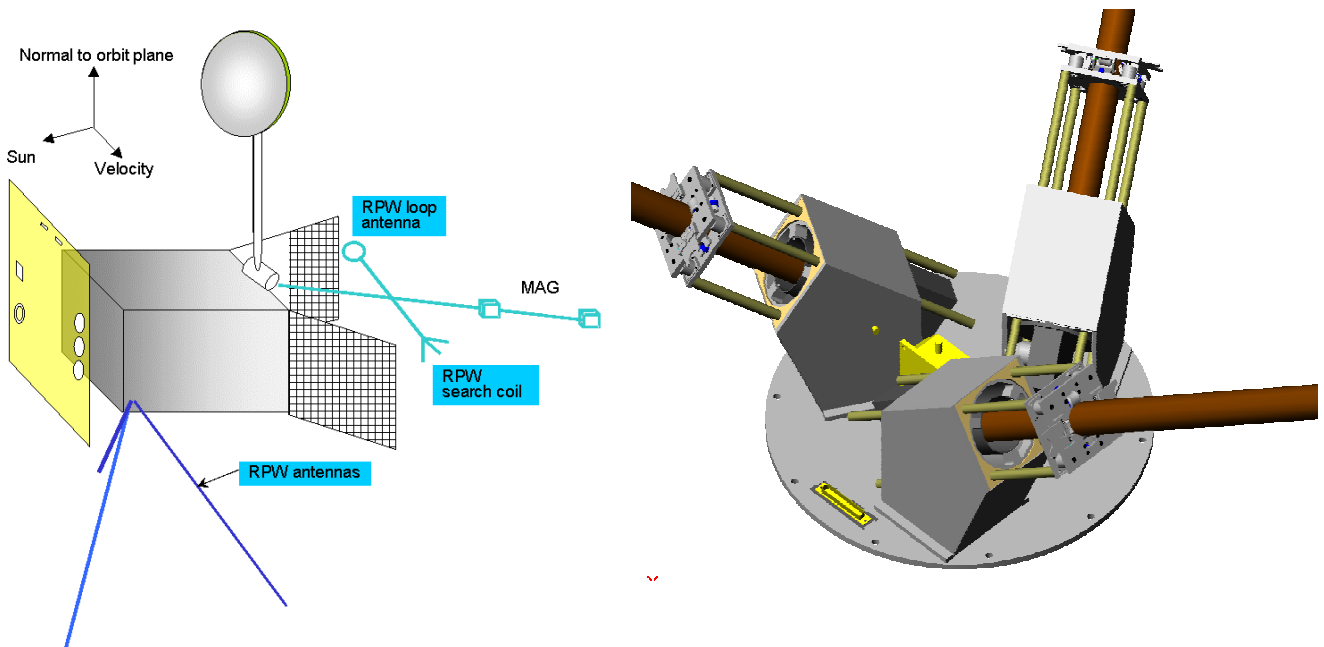


Figure 3.2.3: Left: Possible accommodation of the RPW sensors on the spacecraft. Right: 3-axis stacer footprint.

The RPW pointing requirements are not strict compared to optical/EUV instruments.

Operations requirements

Since RPW is very sensitive to spacecraft generated noise, a good strategy is to deploy the RPW antennas early and be one of the first instruments to turn on. This allows RPW to understand, and control, noise sources as other experiments begin operations.

Cleanliness, AIV and other requirements

Many of the RPW scientific objectives are based on the measurement of low-level signals for which maximum sensitivity is required. Several inexpensive measures can be taken at the spacecraft and project level to ensure that the Solar Orbiter spacecraft is clean from the point of view of both conducted and radiated electromagnetic interference. The sensitivity of the RPW instrument will be approximately 10^{-8} V/m/Hz^{1/2} in the frequency range of 1 kHz to 20 MHz and 3×10^{-7} V/m/Hz^{1/2} below 100 Hz. In addition, the waveform analyser is sensitive to impulsive interference of duration as short as a fraction of a microsecond. Although these sensitivities may appear to require an excessively "clean" spacecraft, they are not difficult to achieve if good EMC practices are incorporated in the spacecraft design.

Open points, critical issues and Technology Development Activities

Since the RPW antennas float electrically and extend into sunlight, they will also be hot and radiate back to the spacecraft. This aspect of the design is currently being studied.

4.2.3.5 Search Coil Magnetometer

Sensor performance requirements

The frequency band shall be 1Hz – 10 kHz with a sensitivity of 10^{-5} nT/Hz^{1/2} at 1 kHz.

Estimated resource allocation

Parameter	Value	Remarks
Mass [kg]	0.5	Three rods
Dimensions [cm]	18	Length each rod
Power average [W]	0.25	
Power peak [W]		
Operating temperature range [deg C]	TBD	

Accommodation and pointing requirements

The search coil magnetometers need to be mounted on a boom to be away from spacecraft noise sources. Such a boom should extend into the shadow behind the spacecraft. The coil is most easily accommodated on the MAG boom. In this case, the separation between MAG sensors and search coils should be >1 m. Separation between search coil and S/C will depend on actual EM cleanliness of the spacecraft, but a distance > 1 m is anticipated.

4.2.3.6 Loop Magnetometer

Sensor performance requirements

The frequency band shall be 10 kHz – 20 MHz with a sensitivity of 10^{-7} nT/Hz^{1/2} at 1 MHz.

Estimated resource allocation

Parameter	Value	Remarks
Mass [kg]	0.5	
Dimensions [cm]	50	Diameter
Power average [W]	0.3	
Power peak [W]		
Operating temperature range[deg C]	TBD	

Accommodation and pointing requirements

The loop magnetometer needs to be mounted on a boom to be away from spacecraft noise sources. Such a boom should extend into the shadow behind the spacecraft and is most easily accommodated on the MAG boom. In this case, the loop magnetometer should be located 1 m away from MAG. Separation between magnetometer loop and S/C will depend on actual EM cleanliness of the spacecraft, but a distance > 1 m is anticipated.

RPW calibration

Spacecraft structure will modify the RPW electric antenna pattern in unknown ways; these perturbations can be modeled, computationally and in the lab. Spacecraft rolls around the Sun pointing axis are required to understand the antenna pattern. In particular, a series of rolls early in the mission, while near Earth, would be preferred. The roll period should be longer than the RPW radio sweep period (which will be 10-20 seconds); so 1 deg/s roll would be adequate and consistent with MAG calibration requirements.

RPW - Summary of allocated power and mass values.

Unit	Power [W]	Mass [kg]	Remarks
Thermal Noise Receiver	1.0	0.5	Electronics (single card)
	---	4.8	Antenna's
Low Frequency Receiver	1.0	1.5	Electronics (single card)
	0.3	0.5	Search coil magnetometer
High Frequency Receiver electronics	0.8	0.6	Electronics (single card)
	0.3	0.5	Loop magnetometer
DPU/RTC / DC-DC / preamp	2.9	2.6	TBC
Harness	---	0.8	
Total	6.3	11.8	Before margin

4.3 Magnetometer

4.3.1 Scientific goals

The principal scientific goal of the Magnetometer (MAG) is:

To provide vector measurements of the solar wind magnetic field with high resolution (better than 1 nT) at sub-second sampling.

The MAG instrument will enable the investigation of:

- The link between coronal structures and their signatures in the solar wind;
- Kinetic effects in the solar wind plasma;
- Large-scale structures in the solar wind, *e.g.*, coronal mass ejections;
- MHD waves and turbulence.

The measurement requirements to satisfy these scientific goals are given in the table below.

Mission goal	Timescale required	Precision required
Kinetic physics	128 vectors/s (burst mode)	1 nT absolute, few degrees angular, few pT resolution
MHD waves and turbulence	16 vectors/s (normal mode)	Few pT resolution
Onboard plasma moments	Plasma instrument resolution (few s)	Angle only: to within a few deg.

4.3.2 Instrument concept

The reference MAG instrument consists of dual 3-axis fluxgate sensors mounted on a deployable boom, which is positioned in the shadow of the Orbiter body. One sensor is at the end of the boom and the other at an intermediate distance from the spacecraft body. It measures fields in several gain-ranges, which are automatically selected by the DPU according to the *in-situ* magnetic field strength. This configuration allows compensation for spacecraft generated stray fields.

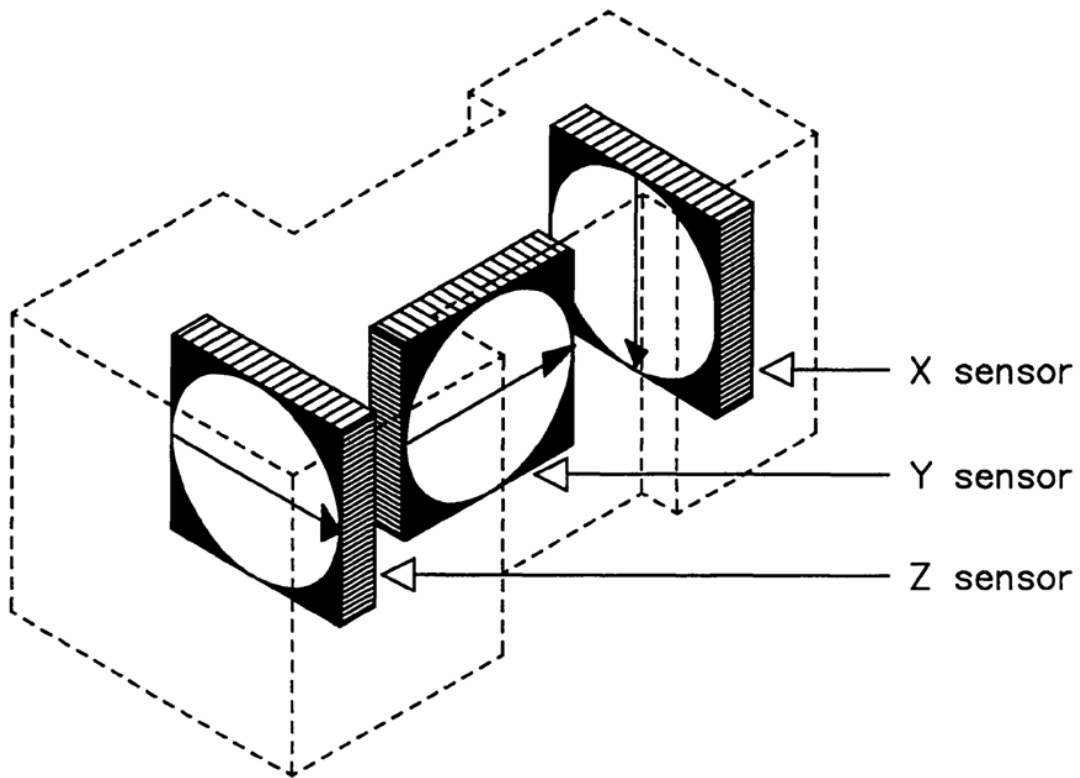


Figure 3.3.1: Functional diagram of the sensor head.

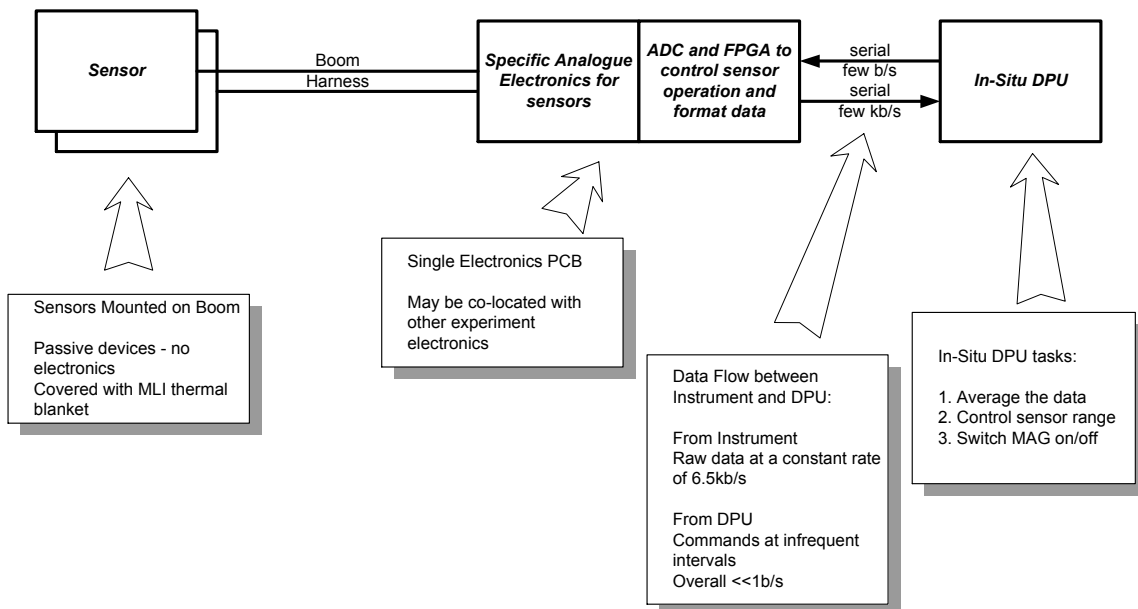


Figure 3.3.2: Block diagram of the Magnetometer

Sensor performance

The sensors operate in the frequency range from DC to 128 Hz with a sensitivity 2-5 pT and 2-5 deg angle precision.

Estimated resource allocation

Parameter	Value	Remarks
Mass [kg]	1.9	Two sensors (with related FEE), harness, MLI and I/F card, DC/DC converter and DPU (before margin).
Dimensions [cm]	11 × 7 × 5	Sensor heads
Power average [W]	1.5	Including electronics, sensor only is 0.1W
Power peak [W]	1.5	
Operating temperature range [C°]	-100 to +100	Sensor head
Raw data rate, average [bps]	800	Compressed data incl. HK, 16 vectors/s
Raw data rate, peak [bps]	6500	128 vectors/s, 16 bits
Data compression method	Loss-less	
Data compression factor	1.3	25 to 35 % reduction

Accommodation and pointing requirements

The sensors must be mounted on a boom in the permanent shadow of the spacecraft. One sensor will be mounted at the end of the boom and the other in an intermediate position. The boom should be of sufficient length to guarantee the sensors are not susceptible to magnetic interference from the spacecraft or other boom-mounted sensor units. It is also critical for the MAG sensor temperatures to be controlled with respect to short-term and long-term variations. It is expected that the sensors will therefore be thermally isolated from the boom structure, and surrounded by MLI. Even though the sensors are permanently in shade, due to the very eccentric orbit it is expected that there will be long-term temperature changes. It may even be necessary to implement a heater in the sensor to keep it warm.

The MAG has no specific requirements on orbit or pointing.

Operations requirements

The largest problem for the MAG team during flight operations will be the calibration of the fluxgate sensor offsets, which always evolve with time and temperature fluctuations. It is baselined for calibration purposes to carry out a limited number of S/C rolls (2 to 3 complete turns per manoeuvre) around the Sun pointing axis at non-critical times. Roll manoeuvres will be performed at specific times when a direct link to the S/C is available and in the absence of other critical phases. It is anticipated that such manoeuvres will be carried before entering each science phase and at an even spread of heliocentric distances. The max S/C roll rate is limited by the AOCS performance and should not exceed 1 deg/s.

Operationally, the MAG is a simple instrument. The DPU will control the MAG ON/OFF status and select the sensor gain-range according to a pre-defined 'auto-ranging' algorithm. The MAG has a built-in self-

calibration function which will be used occasionally (approximately once per week), but this will be planned in advance and executed by command. The MAG data rate is switched between:

- 1) Burst,
- 2) Normal and
- 3) Survey modes

according to the mission-plan or in response to some on-board event trigger. It is expected that MAG data will be provided to other instruments on-board and/or that some processing of the MAG data in the DPU will be performed in order to select 'events' in the magnetic field data. These may be used to trigger other experiments' burst modes.

Cleanliness, AIV and other requirements

Magnetic Cleanliness

It is most important that magnetic issues are considered in the design from day one and needs the cooperation of all concerned - spacecraft, payload and AIV. This can reduce costly workarounds at a later date. Good design practice is quite straightforward, for example minimising the use of permanent magnets and soft magnetic materials, and careful design of power distribution systems to minimise current loops.

Ground Operations

The magnetometer should have a gain-range which allows operation and functional testing to be performed in Earth magnetic field.

A system-level magnetic test is highly recommended since it allows the magnetometer to operate the flight gain-ranges and to check for compatibility with the spacecraft systems. Such a magnetic test may be performed at a large magnetic test facility such as that at IABG, Ottobrun, Germany. This test would also be used to verify the spacecraft overall magnetic compatibility versus the requirements.

An EMC board consisting of members from the project, prime and instrument representatives should identify critical platform and instrument units that could cause AC disturbances. Such critical units should be carefully characterized for different operating modes.

It is necessary to use non-magnetic tools on the spacecraft and particularly on the boom and associated units. MAG has no particular requirements for molecular or particulate cleanliness.

Open points, critical issues and Technology Development Activities

Thermal Electric Currents

Due to the extreme thermal environment, there may be a problem with currents induced in the (conducting) spacecraft surfaces and structure due to large temperature gradients. The magnetic fields generated would be a special problem close to the magnetometer sensor. Some experimental work has been done (TU-Braunschweig, GSFC) to quantify this. Thermal electric currents can be minimized by 'banding' conducting surfaces that may be subject to large thermal gradients.

Accommodation of the sensors

A boom is required for the fluxgate magnetometer sensors, in order to keep them as far away as possible from sources of magnetic interference on the spacecraft and other instruments. The boom and the sensor units must be in permanent shadow of the spacecraft.

Interference from Spacecraft Systems

The spacecraft design from the assessment study is well optimised from a thermal point-of-view, but both the solar panels and the high-gain antenna are located close to the magnetometer sensor. These are mobile structures that are likely to cause magnetic interference. For the magnetometer this would be impossible to separate from the real *in-situ* field.

Magnetometer Calibration

Fluxgate magnetometer sensor calibrations have a tendency to change with temperature in a way that is not entirely predictable or repeatable. On a spinning spacecraft this is less of a problem since the spin-axis offsets can be easily recovered. Solar Orbiter has two problems: firstly it is three-axis stabilised, secondly over an orbit one can expect large temperature changes even for a shadowed unit. The S/C should be able to perform yaw manoeuvres to allow MAG to calibrate away DC offsets. These manoeuvres would consist of 2 or 3 rotations about the sun-pointing axis, approximately twice per orbit. Roll manoeuvres will be performed at specific times, when direct link to the S/C is available (*e.g.*, HGA availability) and in absence of other critical phases. They could be planned before entering the science operations (*i.e.*, perihelion pass, max southern and max northern latitude pass). The maximum spin rate is TBD but will depend on the impact of dynamical disturbances on the AOCS and spacecraft (flexible appendages, RPW antennas, HGA, solar arrays) and liquid sloshing. A preliminary assessment, suggests a maximum roll rate of 1 degree per second (based on a reaction-wheel approach).

Summary of allocated mass values.

Unit	Mass [kg]	Remarks
Sensors	0.5	2 × units (0.25 kg each)
MLI	0.15	2 × 50 g
Harness	0.2	40 g/m, 4m boom, connectors
Sensor electronics	0.4	Including I/F to DPU
DPU/RTC	0.2	Electronics (single card)
DC/DC converter	0.2	Loop magnetometer
Electronic box	0.25	TBC
TOTAL	1.9	Before margin

4.4 Energetic Particle Detector (EPD)

4.4.1 Scientific goals

The principal scientific goals of the Energetic Particle Detector (EPD) are:

- To determine *in-situ* the generation, storage, release and propagation of different species of solar energetic particles in the inner heliosphere;
- To identify the links between magnetic activity and acceleration on the Sun of energetic particles, by virtue of combined remote-sensing of their source regions and *in-situ* measurements of their properties;
- To characterize gradual (typically CME-related) and impulsive (typically flare-related) particle events and trace their spatial and temporal evolution near the Sun.
- To measure energetic pick-up particles originating from the interaction of the Solar Wind with near-Sun dust.

In order to achieve these goals, measurements should be acquired at high time resolution (capable of up to 1 s, during high flux situations), with as complete an angular coverage as possible in order to resolve particle pitch-angle distributions.

4.4.2 Instrument concept

The EPD will determine chemical and nuclear charge composition and energy spectra of ions in a wide energy range, from about the typical solar wind energies of a few keV/ nucleon to several 100 MeV/nucleon for protons and heavy ions. Electrons should be measured from 10 keV to 10 MeV. The combination of electrostatic E/q -analysis with time-of-flight E/M -determination and subsequent direct energy measurement in a solid state detector has been employed in many EPDs in the past and is also a possible design option for the Solar Orbiter.

The specific design suggested here resembles closely the one recently selected for the IMPACT instrument on the STEREO mission. It is a multi-head sensor system using solid-state technology.

The EPD for the Solar Orbiter model payload consists of 5 separate types of detector systems with specific measurement tasks to cover the required range of particles and energies. Determination of the pitch angle distributions on a 3-axis stabilized S/C requires either multiple sensor heads at different S/C locations looking into different directions relative to the magnetic field direction.

STE (Supra-thermal Electron Detector): Electron flux and anisotropy, 2-100 keV

EPT (Electron and Proton Telescope): Flux measurements of electrons 20-400 keV, protons and He nuclei 20-7000 keV/nucleon.

SIS (Supra-thermal Ion Spectrograph): Elemental composition of He-Fe, Flux of ^3He ions 0.010-0.25 MeV/nucleon. and ions of mass 2-60 with 0.005-2 MeV/nucleon.

LET (Low Energy Telescope): Flux and angular distribution of protons 0.5-20 MeV, ^3He , ^4He 1.5-20 MeV/nucleon and ions $Z > 2$, 2.5-60 MeV/nucleon

HETn (High Energy Telescope): Flux of electrons 0.3 - 20 MeV, positrons 0.3 - 1 MeV, ions (protons - Fe) 5 - 100 MeV/nucleon, neutrons 1 - 30 MeV, and X-rays < 1 MeV.

Near sun observations require measurements of angular distributions with high time resolution of less than 12 minutes and from at least 8 sectors with an average aperture of 45°.

The pointing requirement is modest, *e.g.*, 1° for both pointing accuracy and stability.

4.4.3 Open points and critical issues

Detectors:

- Sensors field of view and actual accommodation on S/C.
- Radiation tolerance of ion-implanted detectors to be resolved.
- Front end electronics: analog ASIC with multiple CSA channels (8-16), filter amplifiers, AD converters and discriminators.
- EMC disturbances to the magnetometers and radio science instruments.

4.4.4 Sensors

4.4.4.1 Supra Thermal Electron Detector (STE)

Sensor performance requirements

The electron energy range for the sensor shall be 2 keV – 100 keV with a field of view of 60 × 60 degs.

Estimated resource allocation

Parameter	Unit Value	Remarks
Mass [kg]	0.35	Single sensor
Dimensions [cm]	9 × 6 × 11	
Power average [W]	0.2	
Power peak [W]	TBD	
Operating temperature range [deg C]	-30 to +30	
Detector count rates [sec]	100 – 2 × 10 ⁵	
Raw data rate, average [bps]	460	Data is binned with 2 × 8 discriminators, 16 bins, 4.5 read/min, 24 bit counters

Accommodation and pointing requirements

The sensor is currently assumed to be located on the S/C body in permanent shadow.

Operations requirements

Door opening mechanism, opening once.

Cleanliness, AIV and other requirements

Dry-N₂ purge required for detector safety throughout ground operation period.

Acids, organic liquids except ethanol, and cleaning agents should be avoided in presence of STE EPD detector systems.

4.4.4.2 Electron and Proton Telescope (EPT)

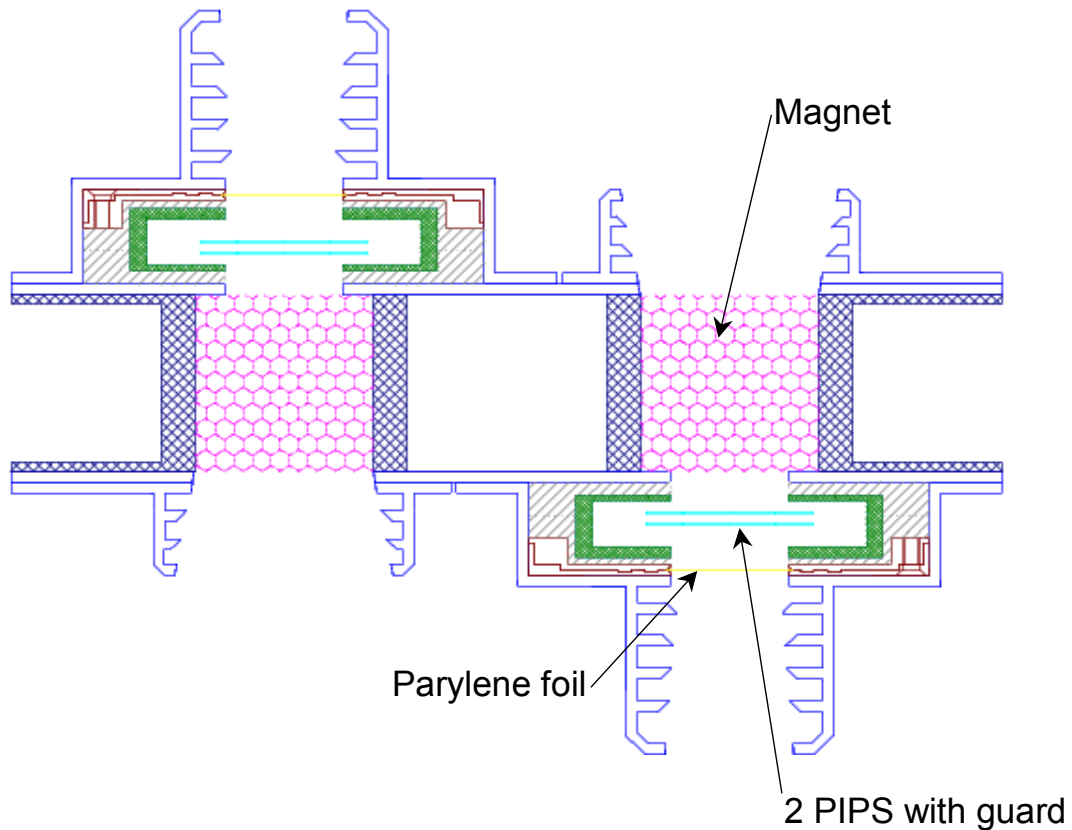


Figure 3.4.1: Cross section of the EPT Sensor

Sensor performance requirements

The Electron and Proton Telescope reference instrument is similar to the STEREO Solar Electron Proton Telescope (SEPT). The sensor telescope is constructed as an open cylinder with two solid-state detectors. One detector aperture (electron side) is covered by a thin organic foil and the other detector aperture is surrounded by a magnet. The thin foil leaves the electron spectrum essentially unchanged but stops low energy protons (*i.e.*, it is essentially only sensitive to electrons in the energy range 20 keV – 400 keV). The magnet sweeps away electrons on the other side of the cylinder but lets ions pass to that detector. Ions within an energy band from 400 keV/nucleon to 7 MeV/nucleon will be measured in this detector. The electron detector also detects ions with an energy high enough to enter through the thin foil - this flux can be computed and subtracted from the electron flux.

The sensor includes 2 telescopes mounted in parallel, but with the electron/proton detectors facing opposite directions. These form a compact unit since the magnetic yokes are shared between the telescopes. The complete telescope FOV consists of four 56° cones (two parallel and two antiparallel). The external magnetic field can be kept to low levels by exact matching of the individual magnets.

Estimated resource allocation

Parameter	Unit Value	Remarks
Mass [kg]	0.7	2 units, 1.4 kg
Dimensions [cm]	16 × 15 × 10	
Power average [W]	0.7	
Power peak [W]	0.7	
Operating temperature range [deg C]	-30 to +40	
Detector count rates [sec]	$10 - 2 \times 10^5$	
Raw data rate, average [bps]	700	4 × 8 discriminators, 32 bins, 2 read/min

Accommodation and pointing requirements

The sensor is currently assumed to be located on the S/C body in permanent shadow.

Operations requirements

Door opening mechanism, opening once.

Cleanliness, AIV and other requirements

Dry-N₂ purge required for detector safety throughout ground operation period.

Acids, organic liquids except ethanol, and cleaning agents should be avoided in presence of EPT EPD detector systems.

Open points, critical issues and Technology Development Activities

Magnetic disturbance to magnetometer.

4.4.4.3 Supra-thermal Ion Spectrograph (SIS)

Sensor performance requirements

The energy range for the SIS shall be 5 keV/nucleon – 2 MeV/nucleon for He to Fe ions. The sensor shall also be able to separate ³He from ⁴He above 10 keV/n.

Suprathermal Ion Spectrograph (SIS)

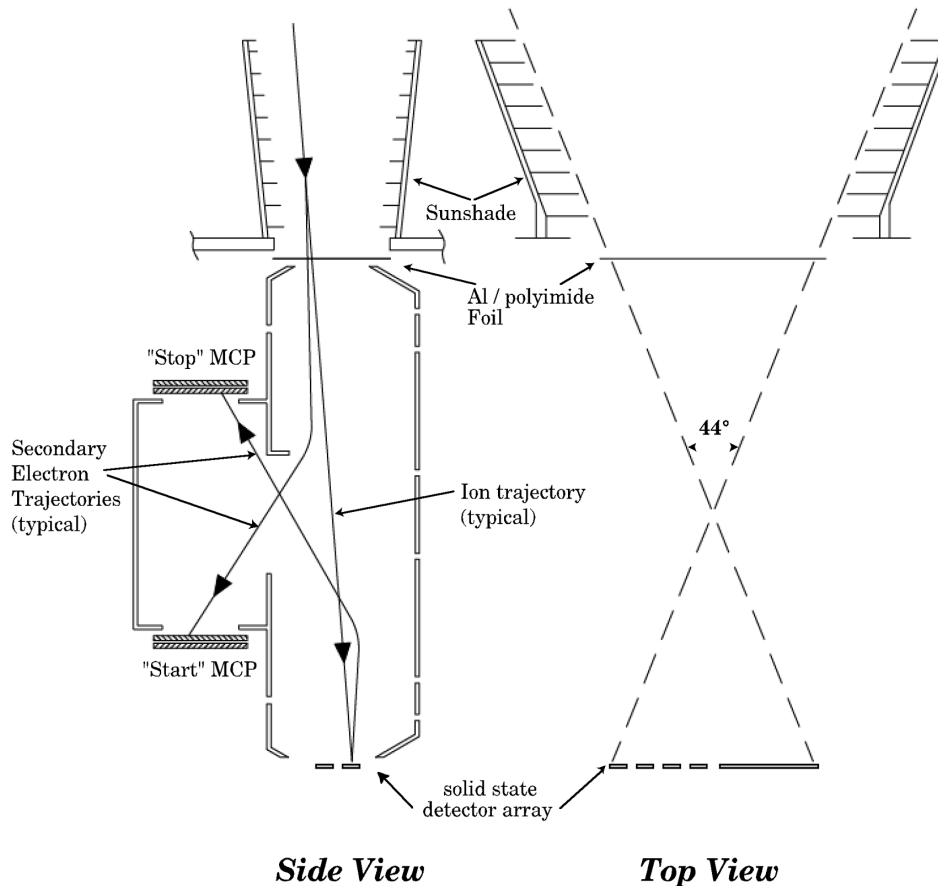


Figure 3.4.2: Cross section of the SIS Sensor

SIS is a time-of-flight mass spectrometer whose telescope cross section is shown in Fig. 3.4.2. The FOV is $16^\circ \times 44^\circ$, with the 44° angle in the orbital plane. Referring to the figure, the telescope analyses ions that enter the telescope through a thin entrance foil (200Å Al on 1000Å polyimide) and stop in an array of 9 solid state detectors. Secondary electrons from the entrance foil and solid state detector are accelerated and deflected, then strike chevron microchannel plates (MCPs), providing START and STOP signals for the time-of-flight measurement. The solid state detector signal provides a measurement of the kinetic energy of the ion. The time-of-flight T , the energy E , and the 8 cm path length in the telescope (L) are then combined to derive the mass of the ion: $M = 2E(T/L)^2$. The incident energy is obtained by correcting for the energy losses in the entrance foil and detector window.

The SIS geometry factor is $0.20 \text{ cm}^2 \text{ sr}$, large enough to allow study of even small impulsive solar particle events. SIS is optimized for detection of He and heavy ions: the triggering efficiency for protons is $\ll 1\%$, ensuring the ability to measure heavy ions even in very large intensity events in the inner solar system. For each ion triggering the telescope, time-of-flight and energy information is obtained. Full information on selected events is telemetered, and all events are classified into mass & energy bins which are summed on-board to allow rapid accumulation of flux and spectra. SIS uses a common low-voltage power supply, and detector bias, and generates its own high voltage ($\sim 4 \text{ kV}$) for the microchannel plate/secondary electron assembly. The only commanding is occasional (every few months) adjustment of MCP bias.

Estimated resource allocation

Parameter	Unit Value	Remarks
Mass [kg]	1.5	2 units – 3 kg total
Dimensions [cm]	10 × 20 × 13	
Power average [W]	1.4	
Power peak [W]		
Operating temperature range [deg C]	-30 to +30	
Detector Count Rate	$10 - 2 \times 10^5$	
Raw data rate, average [bps]	420	Classification in mass and energy bins, selected sample events transmitted as PHA words

Accommodation and pointing requirements

The sensor is currently assumed to be located on the S/C body in permanent shadow. The estimated field-of-view is $16^\circ \times 44^\circ$; the 44° view being 26° off the orbital plane.

Operations requirements

Door opening mechanism, opening once.

Cleanliness, AIV and other requirements

Dry-N₂ purge required for detector safety throughout ground operation period.

Acids, organic liquids except ethanol, and cleaning agents should be avoided in presence of SIS EPD detector systems.

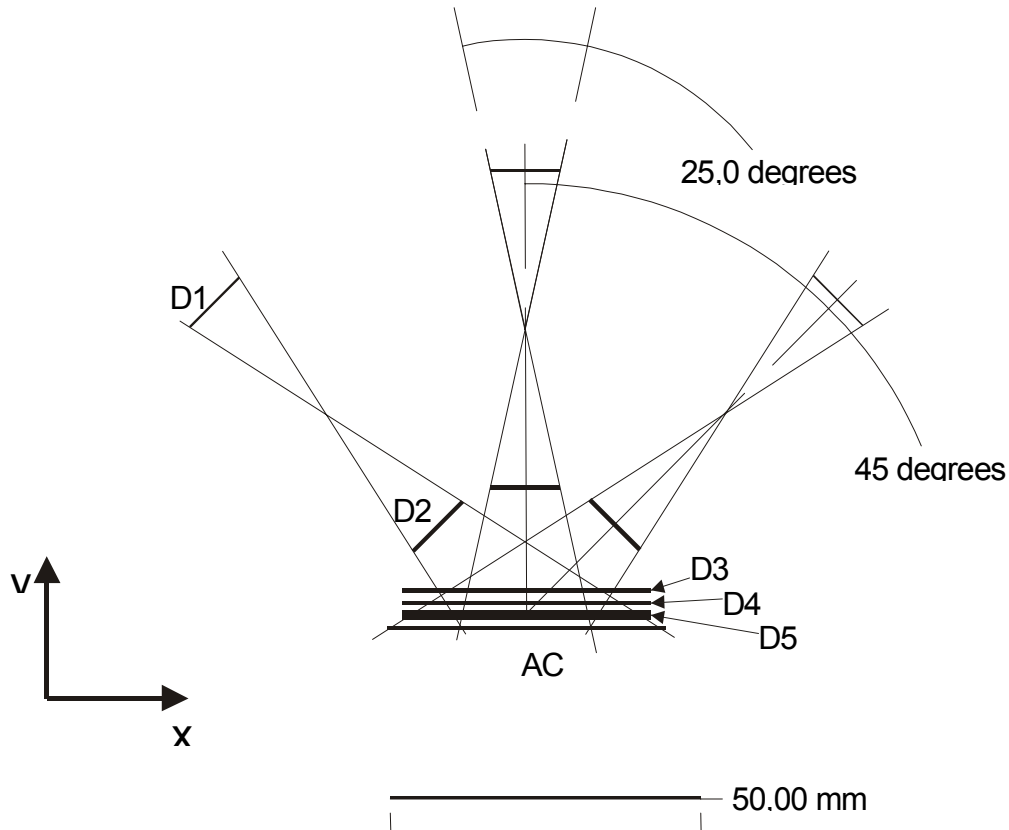
4.4.4.4 Low Energy Telescope (LET)

The Low Energy Telescope (LET) measures the elemental composition of H-Fe and angular distribution of protons and helium. The energy range of protons and helium is 0.5 - 20 MeV/nucleon. In the energy range 1.5 - 20 MeV/nucleon ³He is resolved from ⁴He. Heavier ions are measured from 2.5 MeV/nucleon (O) and reach up to 60 MeV/nucleon (Fe). Thus, LET covers the gap between EPT and HET for protons and helium, and between SIS and HET for heavier ions.

In precise identification of ions, LET relies on the well-proven dE/dx-E technique with pulse height measurements. Most abundant species are identified and tabulated in energy by on-board algorithms in order to limit the telemetry requirements. Thus only a sample of pulse height data is linked down. In addition, classification in mass and energy based on a hardware implementation without pulse height analysis is required for high flux conditions. All data are collected with a time resolution of the order of seconds and with a wide angular coverage.

LET has three front telescopes each consisting of two silicon detectors (D1 and D2 in Fig. 3.4.4), and sharing a common stack of larger silicon detectors extending the energy range up to 20 MeV for protons. The view cone of each telescope is 25×25 degrees, with a total angular coverage of 115 degrees. The total geometric factor of LET is $0.11 \text{ cm}^2\text{sr}$, approximately independent on energy. In the ideal case, LET should be

accommodated such that the axis of the view cone of the centre telescope is in the orbital plane, the other two telescopes looking at North and South of the orbital plane.



- D1: circular 100 mm.² 20 microns
- D2: circular 100 mm.² 300 microns
- D3, D4: 40x30 mm.² 500 microns
- D5: 40x30 mm.² 1000 microns
- AC: 45x35 mm.² 500 microns

Figure 3.4.3: LET design principle showing the three front telescopes each consisting of a pair of silicon detectors (D1, D2), and the common stack of large-area detectors (D3-D5, AC).

Sensor performance requirements

The energy range for the LET shall be:

- 0.5 MeV/nucleon to 20 MeV/nucleon for protons and Helium
- 1.5 MeV/nucleon to 60 MeV/nucleon for other ions

The sensor shall also be able to separate ³He from ⁴He between 1.5 – 20 MeV/nucl.

Estimated resource allocation

Parameter	Unit Value	Remarks
Mass [kg]	0.65	3 sensors = 2 kg
Dimensions [cm]	15 × 8 × 11	
Power average [W]	0.75	
Power peak [W]		
Operating temperature [°C]	-30 to +30	
Detector Count Rate	10 – 2 × 10 ⁵	
Data rate, average [bps]	1,000	Classification in mass and energy bins every minute plus selected sample events transmitted as PHA words

Accommodation and pointing requirements

In the ideal case, LET should be accommodated such that the axis of the view cone of the centre telescope is in the orbital plane, the other two telescopes looking at North and South of the orbital plane. In addition, for full directional measurements, LET should be mounted such that they have an unobstructed view in the range 20-340 degrees towards West of sun in permanent shadow. Estimated field-of-view is TBD.

Cleanliness, AIV and other requirements

Dry-N₂ purge required for detector safety throughout ground operation period.

Acids, organic liquids except ethanol, and cleaning agents should be avoided in presence of LET EPD detector systems.

Open points, critical issues and Technology Development Activities

Radiation damage to the silicon sensors should be assessed in view of the probable inverse square scaling of particle fluxes.

4.4.4.5 High Energy Telescope with Neutron Detection (HETn)

Sensor performance requirements

The energy range for the HETn shall be:

- 0.3 to 20 MeV for electrons
- 0.3 to 1 MeV for positrons
- 5 to 100 MeV/nucleon for protons and ions (He – Fe)
- 1 to 10 MeV for neutrons
- 100 keV to 5 MeV for X-rays and Gamma-rays

Several identical telescopes define the fields of view by sharing a CsI scintillator calorimeter in an efficient, weight saving geometry and allowing for substantial anisotropy information. The telescopes each contain three circular PIPS SSDs (thickness of 0.15 mm, 1 mm and 1 mm) with a total geometric factor of ~0.5 cm² sr. The FOV limits ion path length differences in all detectors so individual elements from protons to iron can be resolved. The particle type (e, p, heavy nuclei) is identified by measurement of energy loss (dE/dx) versus total energy via pulse height analysis. Penetrating particle signatures will be pulse height analysed as well in order to provide additional channels for adjacent higher energies and minimally ionizing particles. The whole detector system is wrapped in active anti-coincidence shielding. The CsI light output is detected with photodiodes, and so is the light from the plastic scintillator. For the anti-coincidence shielding readout a photomultiplier tube is foreseen. A >30g plastic scintillator is mounted on the sun-facing side of the sensor,

embedded in the anti-coincidence shield and adjacent to the CsI, with the aim to provide the minimum-weight fast neutron spectroscopy capabilities by measuring the energy loss of recoil protons. The plastic scintillator does not interfere in any way with the instruments' scope to measure highly energetic ions. Without any extra sensor mass, the detector can be used for X-ray and positron observations. The high-Z CsI scintillator material is extremely sensitive to X-rays, providing even vital information of the time-dependent background for the neutron spectroscopy. Positrons are identified by an electron energy loss signal in two front SSDs of any of the telescopes, with no signal in the third SSD, in coincidence with the observation of the annihilation X-ray energy of 511 keV in the CsI scintillator.

Estimated resource allocation

Parameter	Unit Value	Remarks
Mass [kg]	1.7 kg	2 sensors = 3.4 kg total
Dimensions [cm]	17 × 15 × 8	
Power average [W]	1.4	
Power peak [W]		
Operating temperature range [C°]	-30 to +40	
Detector Count Rate	10 – 2×10 ⁵	
Data rate, average [bps]	500	Classification in type, mass and energy bins every minute plus selected sample events transmitted as PHA words (13 × 16 bins × 24 bits)

Accommodation and pointing requirements

The sensor is currently assumed to be located on the S/C body in permanent shadow. The estimated FOV is split between three cones, each ± 15 deg wide.

Operations requirements

TBD

Cleanliness, AIV and other requirements

Continuous dry nitrogen purge.

Open points, critical issues and Technology Development Activities

TBD

EPD - Summary of allocated mass values.

Unit	Power [W]	Units	Mass [kg]	Remarks
STE sensor	0.2	1	0.4	Including I/F card
EPT sensor	1.4	2	1.4	Including I/F card
SIS sensor	2.8	2	3.0	Including I/F card
LET sensor	2.3	3	2.0	Including I/F card
HETn sensor	2.8	2	3.4	Including I/F card
DPU/RTC / DC-DC / box	5	1	3.0	TBC
Harness	---	TBD	0.5	Depends on sensor location
Total	14.5	11	13.7	Before margin

4.5 Dust Particle Detector (DPD)

4.5.1 Scientific goals

The principal scientific goal of the Dust Particle Detector (DPD) is:

To determine *in-situ* the spatial distribution, mass and dynamics of dust particles in the near-Sun heliosphere, in and out of the ecliptic.

Measurements obtained by the DPD instrument will enable the study of:

- The extent of the dust-free zone around the Sun;
- The sources of dust, *e.g.*, from Sun-grazing comets;
- The role played by near-Sun dust for pick-up ions;
- Proto-planetary discs.

4.5.2 Instrument concept

The science objectives can be met with an instrument of for instance Nozomi heritage. Such a dust experiment may consist of a twin sensor assembly, with one sensor looking in the ram direction and the other sensor with FOV out of plane direction to resolve incidence angles.

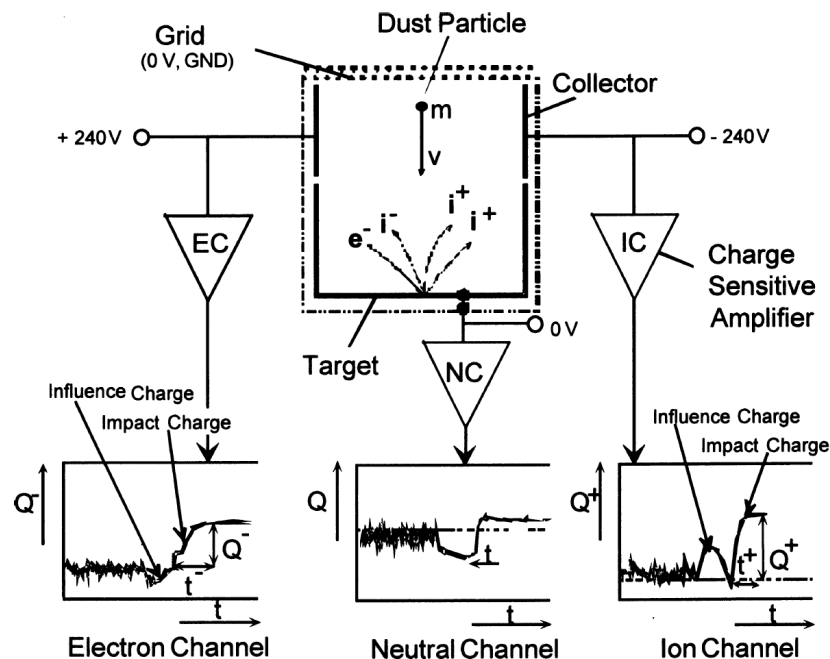


Figure 3.5.1: Block diagram of the Dust Particle Detector

For this model instrument (based on Mars Dust Counter on Nozomi), the dust particles will enter the detector through a highly transparent metal wire grid. When the dust particle impacts a target plate (*e.g.* Au), the impact plasma generated will be separated in an electric field and collected on a negatively charged (ions channel) and positively charged (electron channel) collector plates. The impact charges from both collector

plates are detected by charge amplifiers and recorded as short time sequences in the instrument. By analysing the rise time and total charge collected can the mass and velocity of the impacting particle be determined. A third collector plate with neutral potential can also be added to provide the time difference between the impact and the arrival of ions and electrons on the biased plates. The measurement principle is shown in figure 3.5.1.

4.5.3 Dust sensor

Sensor performance requirements

The dust sensor shall be able to detect particles with mass in the range in the range 10^{-15} g to 10^{-6} g and determine the speed and possible the size of the particle.

Estimated resource allocation

Parameter	Value	Remarks
Mass [kg]	1.5	2× sensors, each 0.75 kg including electronics
Dimensions [cm]	20 × 15 × 15	Envelope
Power average [W]	6	
Power peak [W]	6	Each sensor 3 W
Operating temperature range [C°]	-30 to +40	
Raw data rate, average [bps]	50	
Raw data rate, peak [bps]	TBD	
Data compression method	TBD	
Data compression factor	TBD	

Accommodation and pointing requirements

Two identical detector units should be located on the sides of the spacecraft body in permanent shadow, one looking 90° off the spacecraft-Sun line (ram direction) in the orbital plane to measure the near-ecliptic dust particles, the other one in the direction perpendicular to the orbital plane in order to measure dust particles in orbits highly inclined to the ecliptic. The field of view of each sensor is $\pm 45^\circ$.

No special pointing accuracy is required.

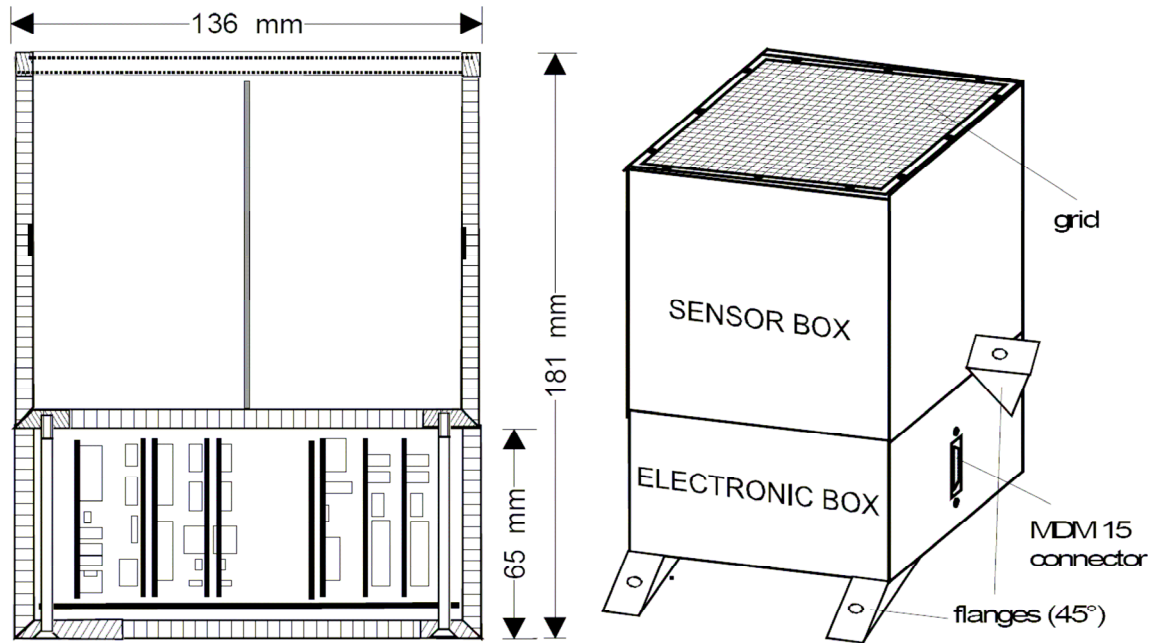


Fig. 3.5.2: Possible physical implementation for a DPD sensor and electronics unit. Two identical detector units should be located on the sides of the spacecraft body in permanent shadow.

Operations requirements

Operations will be performed continuously and modest telemetry allocation is required.

Cleanliness, AIV and other requirements

Continuous dry N₂ purging may be required.

Open points, critical issues and Technology Development Activities

No actual input from the community. Reference design only based on ESA experience (Nozomi heritage).

4.6 Neutron and Gamma-Ray Detector (NGD)

The interaction of flare accelerated ions with the solar atmosphere produces gamma-rays in the energy range 100 keV to 10 MeV and neutrons in the range 1 MeV to 1 GeV. The gamma-rays can be detected in Earth orbit, but because of the finite neutron lifetime, only high energy neutrons (> 100 MeV) have a high probability of being detected at Earth. Solar Orbiter measurements, close to the Sun, will allow us to uniquely probe low the energy MeV neutrons produced by energetic ion reactions with thresholds around 1 MeV/nucleon. These data will provide information on the accelerated ion spectrum in the energy range between ~ 1 MeV and 100 MeV/nucleon when used in conjunction with the information obtained from γ -ray line measurements. The lines originate from the interactions of protons and energetic ions with the thermal plasma and are our primary tracer of ion acceleration in flares.

Low-energy neutrons from small events on the Sun could even be measured almost continuously by Solar Orbiter during its closest approach to the Sun, giving new insights to the problem of coronal heating by nano-flares. These neutron measurements, when combined with optical or EUV remote-sensing observations, will provide valuable information not only on solar acceleration processes but also on coronal heating.

4.6.1 Scientific Goals

The principal scientific goals of the Neutron and Gamma-ray Detector (NGD) are:

- To measure low-energy (above ~ 1 MeV) solar neutrons that are produced by interaction of flare-accelerated ions with the solar atmosphere.
- To measure temporal and spectral distributions of gamma-ray flare events.

Furthermore, the NGD instrument will study:

- The link between interacting and escaping ions, while removing most of the transport effects.
- The problem of coronal heating by nanoflares (low-energy neutrons from small events on the Sun).

4.6.2 Instrument Concept

The instrument described here is a combined neutron and gamma-ray detector designed to achieve the scientific goals of the Solar Orbiter mission. Restrictions on mass, power and mission duration preclude the use of the type of detector used on Mars Odyssey – a cryogenically cooled, high purity Ge detector. In addition, in view of the pointing stability requirements dictated by the remote-sensing units, a mechanical cooler cannot not be considered.

The design concept described here is based on an evolution of earlier instruments (e.g. Lunar Prospector). The configuration consists of three components - an actively shielded LaBr_3 gamma-ray detector, a boron doped plastic active anti-coincidence shield and neutron detector, and an electronics and data processing unit. The NGD is illustrated in figure 3.6.1 and consists of an actively shielded cerium doped lanthanum bromide ($\text{LaBr}_3:\text{Ce}$) spherical crystal of diameter 8 cm with a total geometric factor of 201 cm^2 . LaBr_3 was chosen for the principal detection element because of its high density (1.5 times that of $\text{NaI}(\text{Tl})$, *i.e.*, 5.3 g cm^{-3}) and its extremely high light output (61,000 photons per MeV (50% higher than that of $\text{NaI}(\text{Tl})$). An alternative material would be LaCl_3 or $\text{CsI}(\text{Tl})$. An active shield surrounds the LaBr_3 detector and consists of a boron-doped plastic scintillator, BC454, which serves as the NGD fast and slow neutron detector as well as

reducing charged particles and the Compton and pair production contributions in the primary crystal. The shield is segmented into 5 optically cemented pieces, each viewed by a silicon photodiode. The central detector is viewed by a small photomultiplier tube (PMT). Pulses from each photodiode are buffered with a unity gain head amplifier and passed to high gain shaping amplifiers and then to discriminators. The discriminated output signals are fed to a digital logic unit, which determines the hierarchy for pulse height conversion. A flash ADC is used for pulse height conversion and so all events, (central detector and shield) are processed and passed to a DPU. An FPGA then sorts events into valid gamma ray interactions in the central detector (*i.e.*, those which did not produce a coincident signal in the shield).

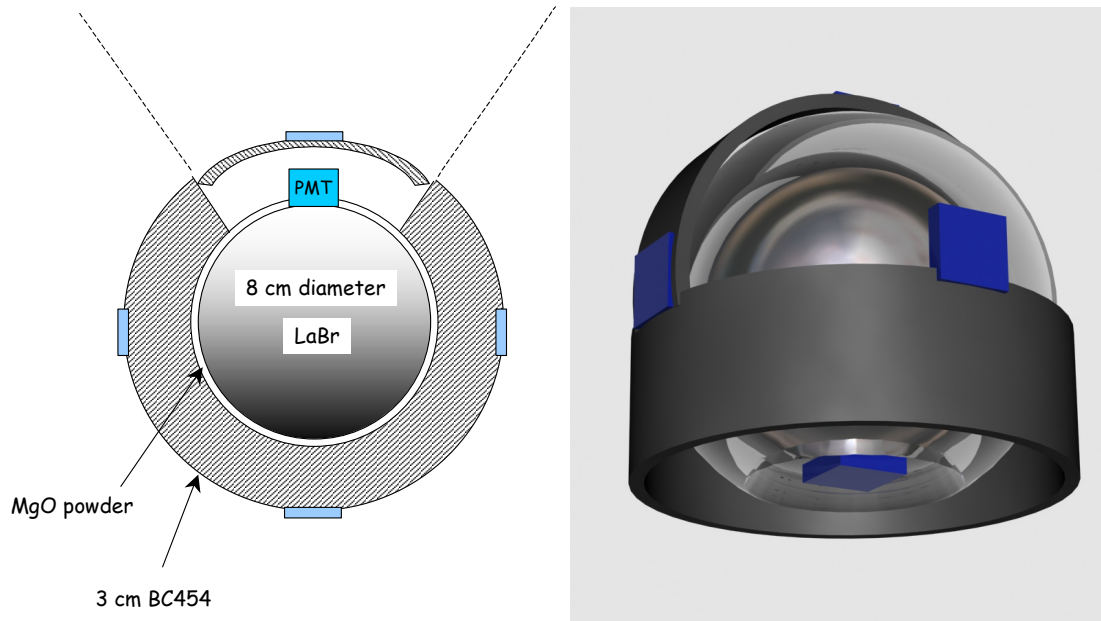


Figure 4.6.1: Cross sectional and schematic views of the NGD instrument.

The electronics also tests for fast neutron and slow neutron signatures as follows. Fast neutrons ($0.5 < E_n < 8$ MeV) are identified by looking for time-correlated events in the plastic scintillator. Fast neutrons interact in the shield *via* in-elastic n,p scattering followed by neutron capture ($^{10}\text{B}(n,\alpha)^7\text{Li}^*$) and the emission of an alpha particle some $2.2 \mu\text{s}$ later after thermalization of the incident neutron. In 94% of cases, the Li nucleus is left in its 1st excited state and de-excited to the ground state by the emission of a 478 keV gamma-ray after 10^{-13} s. The Q value for this reaction is 2.3 MeV which is shared between the alpha (1.47 MeV) and the $^7\text{Li}^*$ recoil nucleus (840 keV). Thus, a fast neutron signature is an initial energy deposit in the shield, which is proportional to the incident neutron energy, followed by second pulse height in the shield within $25 \mu\text{s}$ (*i.e.*, $\sim 10 \times$ the thermalization half-life), from the alpha particle and recoil nucleus plus in a fraction of cases a simultaneous 478 keV signal in the central LaBr_3 detector.

Slow or moderated neutrons (*i.e.*, a composite of thermal/epithermal and slow neutrons ($0 < E_n < 500$ keV)) are recognized by a pulse height signature consistent with a 2.3 MeV alpha particle plus Li recoil in the shield and a coincident 478 keV photon signal in the central gamma-ray detector.

Thermal

There are no difficulties with the P/L thermal accommodation within the spacecraft, since the instrument can operate within a wide temperature range 253 K to 293 K. Unlike other scintillation materials, such as BGO,

both LaBr_3 and plastic scintillator are insensitive to thermal changes over a wide range of temperatures (-60 °C to +60 °C). The relevant temperatures ranges are as follows:

- Operations: 0°C to +20 C
- Storage long term: -40 °C to +60 °C (long term ~2 years)
- Stability assumed ± 1 °C during science operations within the range 0°C to +20 C.

Estimated resource allocation

Parameter	Value	Remarks
Mass [kg], before margin	5	Including DPU/RTC unit
Dimensions [cm]	15 × 15 × 25	
Power average [W]	5	Including DPU/RTC
Power peak [W]	5	
Operating temperature range [C°]	-20 to +30	
Raw data rate, average [bps]	400	Before compression
Raw data rate, peak [bps]	TBD	
Data compression method	TBD	
Data compression factor	TBD	

4.6.3 Accommodation

Mechanically, the NGD consists of a single box, constructed of composite material in order to reduce unwanted backgrounds, with dimensions of approximately $15 \times 15 \times 25 \text{ cm}^3$. The box is mounted directly behind the spacecraft (S/C) thermal shield and contains the scintillators, PMT and some electronics. Care will have to be given to the design of the thermal shield (or at least to the design of an appropriate “window” in the shield) so that the type and amount of material between the NGD and the Sun will not significantly attenuate the flux of neutrons and gamma-rays. A general guideline is that the shield window should be no thicker than $\sim 3 \text{ g cm}^{-2}$ and high Z materials should be avoided. The angle that the window should subtend, when viewed from the NGD scintillators, should be at least 5° greater than the central detectors FOV assuming the spacecraft +X axis remains within 2° of the center of the Sun. Similarly, the NGD should not be located directly adjacent to large amounts of hydrogenous material (e.g., hydrazine, blocks of polyethylene) as these materials will efficiently moderate high-energy neutrons to lower energy particles that can scatter back to the sensor and be detected.

The electronics consist of a high-voltage power supply (HVPS), bleeder-board and preamp/line-drivers for the PMT and photodiodes. Although the NGD has its own DPU, it may be possible to share a DPU with other *in-situ* instruments should resource reduction be necessary. In this case, a power/signal cable connects the NGD box to the shared, in-situ payload DPU. The NGD experiment would supply two electronics cards to the DPU and these would be used for NGD processing.

4.6.4 Orbit, Operations and Pointing Requirements

For maximum science return, it is desirable that the NGD experiment be operated over all orbits and at all solar radial distances. The instrument is self-calibrating during operation using known background lines. The largely autonomous operation of the sensor and the low power and data rates required should not present significant impediments to this operational goal. The only ground commanding necessary would be to switch

the sensor on, off or to standby (sleep) mode as special S/C operations dictate. It may additionally be desirable to adjust detector gains and thresholds from the ground at infrequent intervals during the course of the mission. NGD will likely have a background and a burst mode that will be internally triggered and there will probably be provision for autonomously reducing PMT high-voltage (to reduce detector gain) in case of severe solar energetic particle events. There are no NGD requirements for S/C pointing other than that the sensor should always remain shaded by the thermal shield and that the Sun should normally be viewable through a thinned section of the thermal shield (see above).

4.6.5 Cleanliness, Ground Operations and Other Requirements

Standard cleanroom practices should be adhered to when integrating, testing and storing NGD. There are no critical particulate requirements as the unit will be sealed and no critical surfaces exposed. The PMT is susceptible to degradation if exposed to elevated concentrations of helium gas for extended periods and this should be avoided.

The LaBr₃ scintillator is hygroscopic and could be damaged if exposed to high levels of water vapour or liquid water. The crystal will be packaged in an hermetically sealed enclosure allowing normal levels of clean-room humidity control during storage or handling operations.

There are no pyrotechnic or other hazardous items associated with NGD. As the instrument has no mechanisms or deployables, no special provisions/fixtures are needed for mechanical testing during ground processing. No sensor purge is required.

It will probably be necessary to use low-activity neutron- and gamma-ray-producing radioactive sources during ground processing to demonstrate aliveness, recheck calibration, etc., subsequent to integration, environmental testing, and other launch preparations. Alternately, if radioactive sources present unacceptable difficulties at the S/C contractor facilities, NGD could be returned to the home institution after integrated testing, tested and recalibrated, and subsequently reintegrated to the S/C prior to launch.

4.6.6 Open Points, Critical Issues and technology development activities

Technology development activities will be required to produce large volume (~300 cm³) LaBr₃ crystals. However, viable alternative scintillators already exist such as LaCl₃:Ce and CsI(Tl), albeit with reduced sensitivities, but still adequate for the science objectives. All of the other technologies associated with NGD have been successfully demonstrated in flight and will require no significant development.

It is possible to simplify the design and use a silicon photodiode to readout the LaBr₃ crystal. This would however, degrade the energy resolution.

5 HIGH PRIORITY AUGMENTATION UNITS

High Priority Augmentation Units are described in Annex 1.

Part 3 Annexes

ANNEX I HIGH PRIORITY AUGMENTATIONS TO BASELINE MISSION

In the event that additional resources become available, the SDT recommended a number of so-called High Priority Augmentations to the Solar Orbiter Baseline Mission. These are:

- Higher-resolution remote-sensing measurements (*e.g.*, 0.25 arc-sec pixels for imaging).
- High-resolution EUV imaging in 3 wavelength bands and an additional band.
- Dust particle composition measurements (*i.e.*, chemical analysis and mass resolution of carbonaceous materials like H, C, N, O, and metals like Na, Mg, Al, Si, Ca, Fe)
- Neutral particle measurements (*i.e.*, energetic neutral atoms in the solar wind / supra-thermal velocity range between ~350 and 5000 km/s)
- Coronal Radio Sounding experiment
- Total solar irradiance measurements

Where available, summary parameters for these high priority augmentations are given in Tables 1, 2 and 3 of this annex.

Table 1 – Solar Orbiter High Priority Augmentation payload: summary of main characteristics.

Instrument	Acronym	Science goals	Spectral band – Particle range	Nom. Mass (^) [kg]	Mass margin (%)	Total Mass [kg]	Physical size of main units (^^) [cm]	Power (*) [W]	TM (#) [kbps]
Neutral Particle Detector	NPD	Investigation of density and velocity distribution of neutral atoms (H, He, O) in the solar wind	0.05 – 5 keV/nucleon	1.6	20	1.9	40 × 10 × 10	2	0.3
Coronal Radio Sounder	CRS	Sounding the solar corona (electron density, faraday rotation, scintillation) using S/C radio link	X and K α bands	0.2	20	0.25	Ant.: 500-600	3	0.01
Dust Composition Analyzer	DCA	Augmentation of the Dust Particle Detector performance, including elements analysis	1-600 amu	2.7	20	3.0	20 × 17 × 19	7.5	0.01
TOTAL						4.75	---	12.5	0.32

Table 2 – Solar Orbiter High Priority Augmentation payload: summary of pointing and accommodation aspects.

Instrument	Acronym	Pointing direction & FOV	LOS pointing stability (RPE)	Instrument accommodation
Neutral Particle Detector	NPD	7.5 ⁰ off the S/C-Sun axis, on the orbital plane, FOV = 7 ⁰	Relaxed accuracy and stability < 0.1 ⁰	1 sensor mounted on the S/C body behind the heat shield. Possible addition to the rear of the +Y panel
Coronal Radio Sounder	CRS	NA (HGA pointing)	NA	The instrument uses the TT&C subsystem, with an added USO. No real accommodation issues.
Dust Composition Analyzer	DCA	Pointed to RAM direction, Half-cone angle = 60 ⁰	NA	Located behind shield, 1 aperture (<11 cm diameter)

Table 3 – Solar Orbiter High Priority Augmentation payload: summary of instrument design maturity and related development activities.

Instrument	Acronym	Instrument concept	Critical issues	Maturity Level	Technology Development Activity
Neutral Particle Detector	NPD	Time Of Flight detection chain – direct Sun radiation blocked via a collimator and UV filters	UV suppressing filter, improved efficiency detectors	3	NA
Coronal Radio Sounder	CRS	Passive radio science experiment, based on coherent, dual frequency down-links (X. K α)	Availability of dual-frequency phase coherent downlink without affecting TM rate	1	NA
Dust Composition Analyzer	DCA	Impact ionization – electro-optics and MCP	High voltage, detector development	3	NA

⁽¹⁾Maturity levels:

1 Existing hardware	4 New, Detailed design level
2 Existing +minor modifications	5 New, Preliminary design level
3 Existing +major modifications	6 Concept only

1 HIGH PRIORITY AUGMENTATION INSTRUMENTS

1.1 Neutral Particle Detector (NPD)

1.1.1 Instrument Description

1.1.2 Scientific drivers

Neutral hydrogen is indicative of the behaviour of the main solar wind component formed by protons out to at least 2-3 solar radii. In fact, beyond this distance the characteristic time for charge exchange between hydrogen atoms and protons becomes comparable to the coronal expansion time scale causing the neutrals to decouple from the charged solar wind. However they retain information on the three-dimensional coronal distribution of hydrogen at the level where they are generated.

In the solar corona up to 2-3 solar radii, neutral atoms are closely coupled to the emerging solar wind plasma and give rise to the prominent solar Ly α corona mainly by resonant scattering of chromospheric HI Ly α photons. From the measurement of the Ly α spectral line profile, the hydrogen velocity distributions in the solar corona have been deduced. These distributions generally reflect the proton one up to about 2-3 solar radii. Above this altitude, because of the low coronal density, the neutral solar wind (NSW) decouples from the ionised component and escapes towards space. Contrary to charged particles, they can cover long distances on ballistic trajectories through space, undisturbed by magnetic field. However they constitute an in situ trace particle population of the solar wind plasma within a few solar radii where it is generated. The understanding of the corona and hydrogen plasma interaction beyond 3 solar radii derives from the comparison between the neutral and the proton component of the solar wind. In fact, the former carries the coronal information while the latter carries information on the wind evolution after decoupling from the neutrals.

The in situ measurements of the NSW velocity distribution performed far from 3 solar radii (e.g. at the Solar Orbiter position) allow remote sensing of the three-dimensional coronal distribution of hydrogen at the level where the neutral and charged component decouple and where we find the peak of the hydrogen kinetic temperature. Hence, such observations represent a powerful diagnostic technique enabling to infer the degree of anisotropy, if any, in the neutral and charged coronal hydrogen close to 3 solar radii. This diagnostics would then provide an extremely valuable test for deciding whether the ion cyclotron process is indeed acting on protons, since this would result in a broader velocity distribution, indicative of more effective heating, across the magnetic field than along the field direction, corresponding to the radial direction in polar coronal holes. Moreover, the proposed NSW measurements would also represent a unique remote diagnostics to infer the velocity distribution along the magnetic field direction, information that is not accessible via spectroscopic measurements of the coronal hydrogen emission, being the field direction approximately perpendicular to the UV Coronagraph line-of-sight, but that is essential to establish the degree of anisotropy of the hydrogen velocity distribution in the corona.

The neutral atom flux is expected to be about 100-1000 atoms cm⁻² s⁻¹ at 0.21 AU, but it could be up to 10⁶ atoms cm⁻² s⁻¹ in a CME. The NPD might also measure energetic neutral atoms emitted from various coronal sources, and thus enable images of these coronal emission regions to be constructed from rays of neutral atoms with different velocities. Nevertheless the neutral instrument candidate entrance system must block radiation emerging from the solar disc. The UV scattered in the solar corona, i.e. Ly α , must be suppressed by a factor of more than 10⁻¹². The entrance system must reduce ions and electrons of the solar wind plasma by a

factor of about 10^{-9} whilst transmitting neutral atoms. Neutral atom detectors have been flown on SOHO, Cassini and IMAGE. Time-of-flight instruments are for example flown on Ulysses, SOHO and ACE.

1.1.3 Instrument concept

The neutral sensor concept is based on micro-valve choppers, which can gate the incoming neutral particles impinging on the detector entrance with a definite timing. Thanks to this approach neutral atoms can be processed and discriminated from ions without interacting at all with any impacting surface thus preserving a high directional information up to the stop detector. This technique developed for the neutral atom camera ELENA in the frame of the BepiColombo can allow an angular resolution better than 1.8° within a large 1-D FOV (e.g. 76°) and cover an energy range from 5keV down to a few eV (Figure 1.1.1-left).

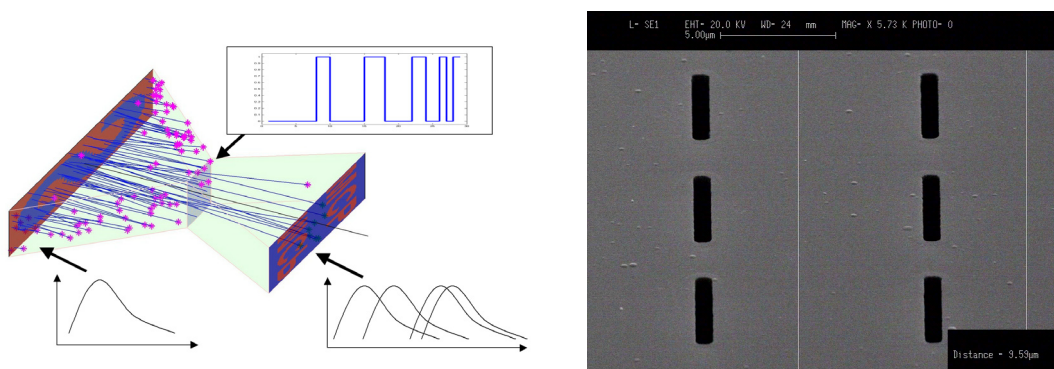


Figure 1.1.1: (Left) NPD Sensor concept. (Right) ELENA prototype grid sample. Narrow slots (dark lines) are etched on a suspended $4\text{mm} \times 4\text{mm}$ Si_3N_4 membrane.

The timing performances of the micro-valve choppers, which in last extent determine the Time-of-Flight (TOF) of the particles, are optimized basing the design on the state-of-the art of ultra-sonic oscillator (operated at frequencies up to a 100 kHz) and high resolution gating nano-grids (figure-right).

The collimated particles released by the entry chopper are then flown in a TOF chamber, and finally detected by a 2-dimesional array (based on Micro Channel Plates - MCPs - and discrete anodes sets), allowing reconstructing both velocity and direction of the incoming particles.

The MCPs “see” a sequence of pulses generated by the oscillation of the mask with respect to a fixed collimator. Randomization of the mask pattern could be also considered to improve the duty cycle, associating the “opening/closing” state to pseudo-random sequences (PRS) of ones and zeros, according to the technique described in Wilhelmi and Gompf, 1970. With PRS mode the chopper gate can be considered open up to $\sim 50\%$ of the time.

As a reference, such a NPD instrument on the Solar Orbiter could have the following parameters: Energy range: 0.05 to 5 keV, velocity resolution about 0.05, being mass resolution a secondary objective. The field of view of the NPD should be centred at about 7.5° off the spacecraft-Sun-centre line, the field of view half-cone measures 4° . Thanks to such limited extension of the FOV a small primary deflector can be housed in front of the gating chopper thus contributing in a first raw removal of the charged particles background. Then the TOF section within the sensor body can provide a longer fine discrimination path in which charge particles gated together with neutral can be rejected to the requested 10^{-9} ratio, deflecting and trapping the ion and the electrons out of the FOV neutral path. The collimator plate length, distance and potential would determine the cut-off of the charged-particle transmission (at about $100\text{ keV}/q$). It can be achieved by means of high voltage biased plates within the instrument itself without protruding large external collimators. In this respect sensor could be confined in a simple parallel piped box with about 1 cm^2 hole entrance. The first compartment can also accommodate the baffle plates keeping out solar UV. The direct solar radiation is

blocked by the sunshield (making use of the aberration of particles up to 8° , see Figure 1.1.2. For the suppression of scattered light within the collimator, the plates could be covered with sawtooth-like structures.

In this respect, one of the major merits of the nano-grids shuttering geometry is the capability to block the UV light by default, thanks to the minimal width of the slit apertures (goal width $<100\text{nm}$) which may stop photons Lyman α in a ratio better than 10^{-7} . The residual photons, even though transmitted and not distinguishable from neutrals, remain accumulated when detected (in a ratio of the order of 10^{-2}) in the first slot of the measured velocity distribution and therefore can be used as “marker” and easily stripped out from the statistics.

As far as heat flow due to irradiation, an external mesh overlaid on the hole entrance can be foreseen for protecting and minimising the IR transmission. Various types of metallic meshes may be used as IR semi-reflectors with almost any Γ reflectivity in the range $|\Gamma| \approx 0-1$ while residual trapped heat can be conducted by the mesh to the housing box.

1.1.4 Orbit, Operations and Pointing Requirements

The instrument points 7.5° off the S/C-Sun axis in the plane of the orbit. The field of view is a half cone of 3.5° .

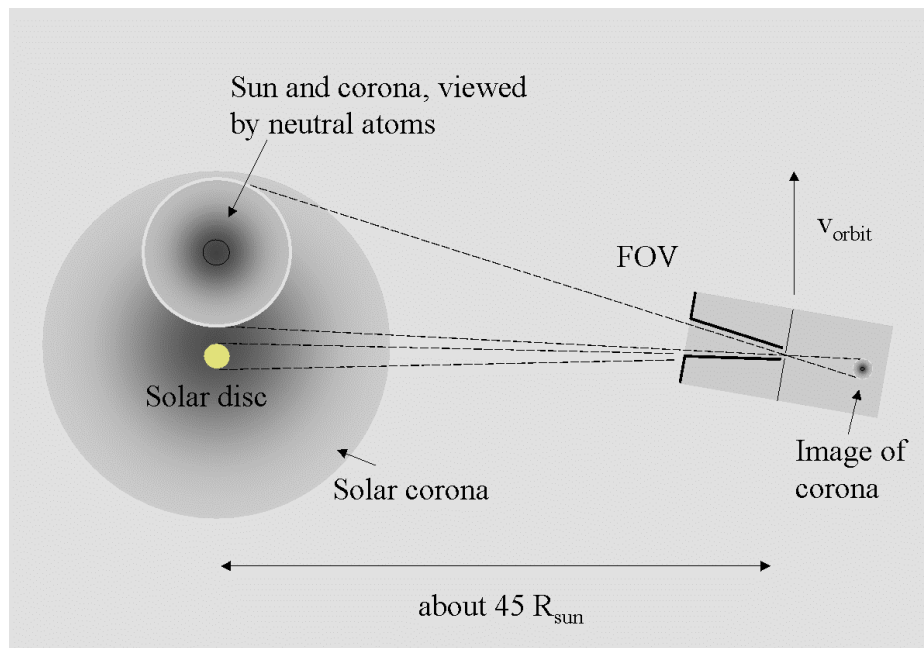


Figure 1.1.2: Instrument schematics and field of view of the Neutral Particle Detector. Imaging the solar corona via neutral atoms. The aberration causes the shift of the “neutral solar wind” image of the corona of the Ly- α corona (plotted for $v_{sw} = 400\text{ km/s}$, $v_{orbit} = 65\text{ km/s}$).

1.1.5 Accommodation

The instrument should point 7.5° off the S/C - Sun axis in the plane of the orbit. A possible accommodation would be the +Z panel, in a position behind the sunshield and with an unobstructed field of view of $\pm 4^\circ$, 7.5° off the S/C - Sun axis.

1.1.6 Interface and Physical Resource Requirements

The NPD can be built for a mass of 1.6 kg. The power consumption would be about 2 W. The required telemetry rate is less than 0.32 kb/s. The FOV has to be 7.5° off the spacecraft-Sun line because of the typical 5° to 10° aberration at 0.21 AU for the fast and slow solar wind velocities.

Unit	Mass (kg)	Power (W)	Volume (cm ³)	Data rate (b/s)
Structure	0.33			
Electronics	0.43	2		
Harness	0.04			
Connectors	0.02			
Sensor (MCP+collimator)	0.28			
DPU	0.50			
Total	1.6	2	2560	320 b/s

Table 1.1.1: NPD resource requirements.

1.1.7 Cleanliness, Ground Operations and Other Requirements

At S/C level a class-100000 clean room shall be enough. The instrument is envisaged to operate autonomously and commanding is only required to update lookup table for voltage settings and data classification schemes.

1.1.8 Open Points and Critical Issues

- 1) The possible UV-suppression system via nano-shuttering system is being studied.
- 2) Increasing the detection efficiency is being studied.

Reference:

G.Wilhelmi, F.Gompf, Nucl.Instrum. Methods, 81 (1970) 36.

1.2 Coronal Radio Sounding (CRS)

1.2.1 Scientific goals

A passive radio science experiment can be carried out using the available S/C radio links when the spacecraft passes behind the Sun (superior solar conjunction). In this configuration it is possible to investigate the solar corona by radio sounding down to at least 2 solar radii. Integrated line-of-sight parameters such as electron content (densities), Faraday rotation, scintillations and angular broadening can be recorded.

1.2.2 Instrument concept

The CRS investigation with a two-way radio link via the spacecraft high-gain antenna (ranging capability) would require a radio subsystem with dual-frequency phase coherent downlinks at X-band and K α -band. Linear polarisation of the downlink signals would enable Faraday rotation measurements as an option. The RF power for both radio links (X and K α) planned for this mission is sufficient for this investigation. A two-way dual-frequency coherent radio link (X-band uplink; X-band and K α -band simultaneous coherent downlinks) is considered as the optimal configuration for a sufficiently stable link and for detecting signatures of CME events traversing the radio ray path.

Sensor performance requirements

Estimated resource allocation

Without a USO, no spacecraft resources are required. However accommodation issues and constraints on the temperature control of the communication system are expected.

The use of a USO would require the following:

Parameter	Value
Mass [kg]	0.2
Dimensions [cm]	TBD
Power average [W]	3
Power peak [W]	3

Accommodation and pointing requirements

If a USO is required, it should be thermally stable and not effected by magnetic sources.

Operations requirements

To be operated during Solar superior conjunction for which, based on the S/C present trajectory, the following candidate operations periods are described:

Sun-S/C-Earth Angle (degrees)	Month	S/C – Earth Distance (AU)	Comment
1.46	Feb 2015	1.8	During Thrust 4
2.3	June 2015	1.5	
4.7	Sep 2016	1.22	During 0.22AU perihelion so communications probably not possible.
5.7	Jan 2018	1.7	During GAM V4
5.6	Feb 2020	1.7	

The spacecraft communication system would need to be warmed and at a stable temperature prior to radio sounding.

Cleanliness, AIV and other requirements

None.

Open points, critical issues and Technology Development Activities

The impact of any required CRS equipment on the S/C is presently under evaluation. It is presently unclear whether or not an ultra-stable oscillator would be necessary to guarantee the frequency stability of the downlinks. The practicality of using linear polarised signals for Faraday rotation measurements is another trade-off to be explored. The final decision depends critically on the geometry and mission operation plan. Considerable interaction between the radio scientists and the spacecraft's radio subsystem contractor is a prerequisite for conducting a successful coronal sounding experiment. The occultation geometry during the solar conjunctions is another aspect that needs to be studied in detail.

The design of the high-gain antenna by the S/C contractor should take into account the following requirements:

- radio subsystem with dual-frequency phase coherent downlinks at X-band and Ka-band.
- linear polarisation of the downlink signals as an option.

1.3 Dust Composition Analyser (DCA)

1.3.1 Scientific goals

The principal scientific goal of the Dust Composition Analyser (DCA), being an augmentation to the performance of the baseline Dust Particle Detector (DPD), is:

- To measure dust elemental composition.

The augmented instrument would acquire measurements of the dust elemental composition, as well as preferably the mass and velocity distributions of dust particles.

1.3.2 Instrument concept

The model instrument concept would detect dust particles through the process of impact ionisation when the in-falling particles hit a target plate. The produced ions are then reflected and deflected with electro-optics to a Multi-channel-plate (MCP) detector. Recording the time-of-flight for the different ion species to reach the MCP allows the separation of elemental composition of the dust particle.

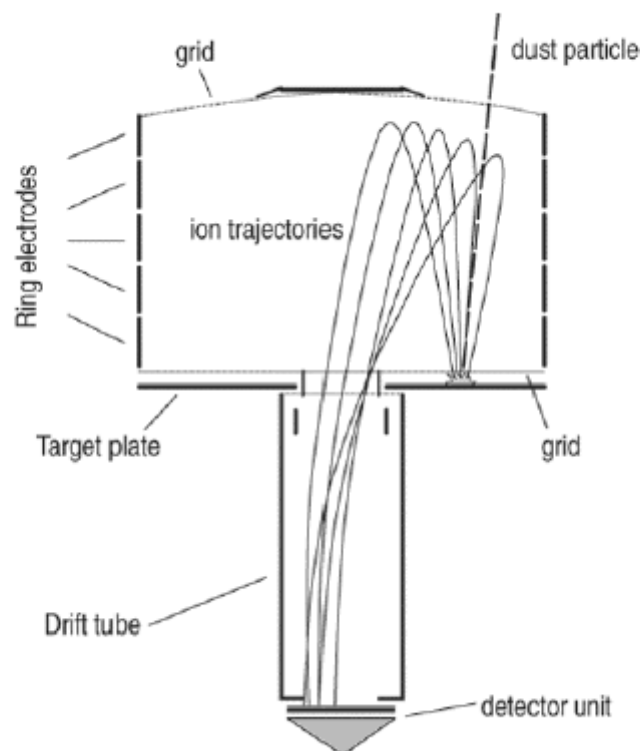


Figure 1.3.1: DCA Sensor concept

The proposed instrument (see figure above) consists of a detector cup covered with an entrance grid and with a basic annular target plate that is covered with an acceleration grid, the ring electrodes with voltages from a few 100 V to 4 kV are mounted around the side walls of the cup and form the reflectron field configuration.

Ions that are formed upon dust impacts are accelerated and deflected into the central region of the annulus and enter a drift tube of approximately 10 cm length. The ions are measured with a Multi Channel Plate at the end of the drift tube. Using the reflectron configuration also reduces the risk of ions escaping the sensor and secondary ions to reaching the ion detector. The target area amounts to 65 cm². Measuring the mass of infalling particles is feasible but still needs further experimental studies and may lead to minor modifications of the design. Test time-of-flight measurements have reached typical resolutions $m/\Delta m = 50-150$ for light elements ($m = 1-30$ amu), $m/\Delta m = 150-300$ for medium elements ($m = 30-100$ amu), and $m/\Delta m = 200-600$ for elements with $m > 100$ amu.

1.3.3 Dust composition sensor

Sensor performance requirements

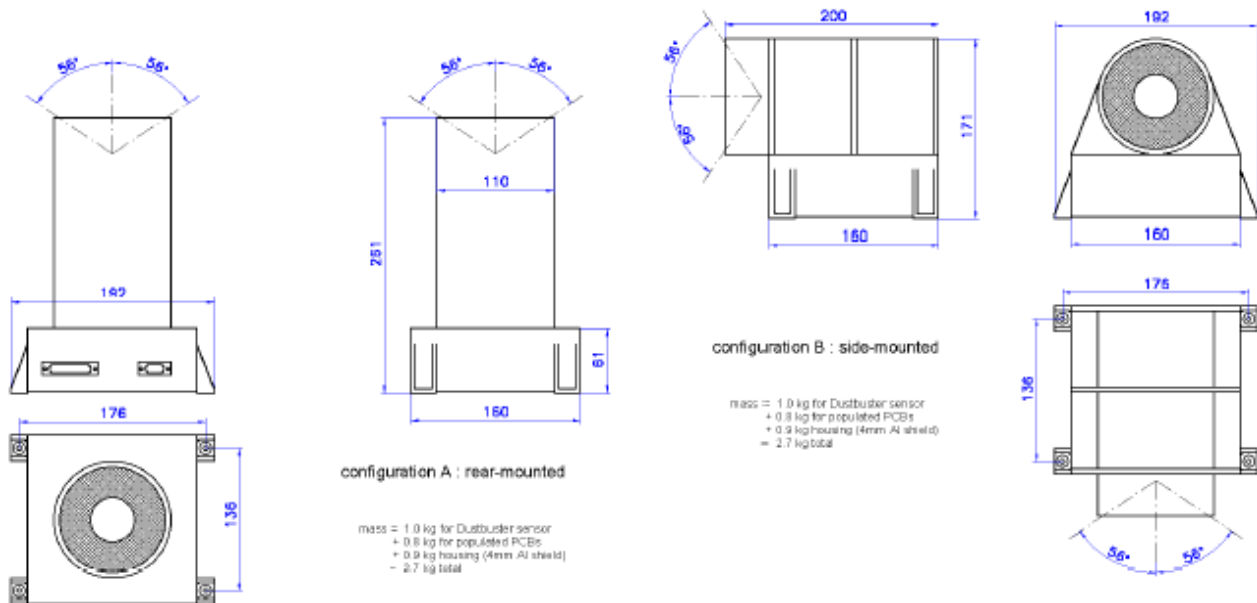
The sensor should be able to measure dust particles with mass between 10^{-15} to 10^{-6} g. The Dust composition sensor should be able to clearly distinguish organic or possibly organic compounds that consist of the elements C, H, O, N compared to silicate compounds with the major elements Mg, Si, and Fe. The instrument should be able to distinguish between different mineralogical species.

Estimated resource allocation

Parameter	Value	Remark
Mass [kg]	2.7	1 kg for sensor tube and 1.7 kg for read-out and HV electronics.
Dimensions [cm]	20 × 17 × 19	Side mounted option including electronics box
Power average [W]	3	
Power peak [W]	TBD	
Operating temperature range [C°]	TBD	
Raw data rate, average [bps]	100	
Raw data rate, peak [bps]	TBD	
Data compression method	TBD	
Data compression factor	TBD	

Accommodation and pointing requirements

The dust instrument should be located in permanent shadow behind Sun shield, pointing to the ram direction of the spacecraft with the field of view tilted from the solar direction, possibly with a baffle. The unobstructed field of view in ram direction should be a 60° half-cone angle. The instrument should have an external cover to be removed once after launch. The instrument is housed in a tube of 110 mm diameter and 200 mm length with an additional electronic box of 160 mm × 160 mm × 61 mm mounted either to the side or at the end of the cylinder shaped detection unit as shown in figure below.



Operations requirements

After opening the cover, the DCA instrument should be operated continuously.

Cleanliness, AIV and other requirements

N₂ purging should be considered during AIV operations.

Open points, critical issues and Technology Development Activities

1. Detector Development: The basic instrumental concept of impact ionization was shown to be feasible and worked successfully for other missions. The time-of-flight mass spectrometry was demonstrated in a lab model and further tests and developments are needed. Issues to be addressed are the high voltage parts, the influence of the radiation environment and of outgassing from the heat shield on the measurements; an external baffle needs to be considered. Measurement of the particle mass are standard for impact ionisation detectors but were not demonstrated for the suggested instrument yet.
2. Laboratory Studies: The detected species stem from a complex ionization; expansion and recombination process that takes place in the dust-plasma cloud that is formed at the high velocity impact. The interpretation in terms of the elemental compositions of the impacting dust particles is not unambiguous and requires a detailed analysis of the impact ionization process.